AN EXPERIMENTAL INVESTIGATION AND MODELLING INTO VISCOSITY OF NANOFLUIDS

A

THESIS

Submitted in partial fulfillment of the requirement for the award of degree

of

Master of Engineering

In

Thermal Engineering

Submitted by

NIKHILESH

(ROLL NO: 801183024)

Under the Guidance of

Dr. S. S. MALLICK

(ASSISTANT PROFESSOR)

Department of Mechanical Engineering

Thapar University, Patiala

July, 2013

CERTIFICATION

I, Nikhilesh, declare that this thesis report, submitted toward fulfillment of the requirements for the award of Master's degree in Thermal engineering in the Mechanical Department, Thapar University, Patiala, is wholly my own work. This document has not been submitted for any degree at any other institution.

Nikhilesh

Date: 8th July 2013
Place: Patiala

Nikhilesh
801183024
Thermal Engineering
Thapar University, Patiala

This is to certify that the above statement made by the candidate is correct and true to the best of my knowledge.

8/7/13

Guide
Dr. S.S. Mallick
Assistant Professor
Mechanical Engineering Department
Thapar University, Patiala

Countersigned by

Dr. Ajay Batish
Professor and Head
Mechanical Engineering Department
Thapar University, Patiala

Dr. S.K. Mohapatra
Senior Professor and
Dean of Academic Affairs
Thapar University, Patiala

ACKNOWLEDGEMENT

No volume of words is enough to express my gratitude towards my guide**,** Dr. S.S. Mallick, Department of Mechanical Engineering, Thapar University, Patiala, who has been very concerned and has aided for all the material essential for the preparation of this report. He has helped me explore this vast topic in an organized manner and provided me with all the ideas on how to work towards a research-oriented venture.

I would also like to thanks, Dr. Bonamali Pal, School of Chemistry and Biochemistry, Thapar University, Patiala, and Mr. Bhupinder Pal, Research Scholar, School of Chemistry and Biochemistry, Thapar University, Patiala, who were always there at the need of the hour and provided with all the help and facilities, which I required, for the completion of my report work.

I would also like to thank Thapar University, Patiala for providing me funds which I used for my thesis work.

Most importantly, I would like to thank my parents and the almighty for showing me the right direction out of the blue, to help me stay calm in the oddest of the times and keep moving even at times when there was no hope.

Nikhilesh

801183024

Thermal Engineering

Thapar University, Patiala.

ABSTRACT

Nanofluid is the suspension of nanoparticles (1 – 100 nm) in traditional heat transfer fluids called base fluids. Nanofluids are supposed to have better heat transfer properties than traditional heat transfer fluids which make it useful in cooling application. The coolant is circulated by pump in most of the cooling systems. Thus pumping power requirement is an important issue in the selection of coolant. This pumping power requirement is based on the viscosity of fluid. Moreover the heat transfer coefficient of a fluid is also influenced by the viscosity of the fluid. In the present work, the accuracy of existing theoretical models and empirical models has been evaluated by using them to predict the experimental values of viscosity. It has been found that none of the model could predict the exact value of viscosity. The error in predicting the experimental values comes out to be in the range of 8.27 to 71.87%. The effects of various parameters like sonication time, settling time and temperature on the viscosity of ZnO-water, ZnO- ethylene glycol, SWCNT – water and aqueous silver-water nanofluid is evaluated. It has been found that the viscosity of nanofluid decreases with the increase in the sonication time. The viscosity of ZnO-EG nanofluid decreases by 7% for a sonication of 6 hours. The viscosity of nanofluid is found to be increasing with the increase in settling time. The viscosity of SWCNT – water nanofluid for a volume fraction of 1% increases by 8% for a settling time of 6 hours. The viscosity of nanofluid is found to be decreasing with the increase in temperature. An empirical model has been prepared for the viscosity measurement of nanofluid by using the experimental data of ZnO-water and ZnO-EG. This empirical model has been validated for different experimental values of viscosity and it has been found that the error in predicting the experimental values of viscosity is in the range of 1.561 to 8.28%.

CONTENT **PAGE NO.**

Chapter 1: Introduction and Objectives

1.1 Introduction

Suspension of fine nanoparticles in the size range of 1-100 nm with the traditional heat transfer fluids like water, ethylene glycol, oil etc. is called nanofluid. These traditional heat transfer fluids are called base fluids. The term nanofluid was given by Choi (1995) to describe new class of nanotechnology based heat transfer fluids that exhibit thermal properties superior to those of traditional heat transfer fluids. The goal of nanofluid technology is to achieve the highest possible thermal properties at smallest possible concentration by uniform dispersion and stable suspension of nanoparticles (Das et al. 2008). It is found that addition of small amount of nanoparticles to the basefluid leads to the change in the thermal properties like viscosity, thermal conductivity etc. of basefluid. Moreover addition of different nanoparticles lead to change in the properties of nanofluid to a different range e.g. for an addition of 1% of aluminum oxide by volume in water leads to an increase in viscosity by 12% (Nguyen et al. 2008) and an addition of 1% of titanium oxide by volume in water leads to an increase in viscosity by 25% (Murshed et al.2007).

There are various types of nanoparticles used to prepare nanofluids (Das et al. 2008), which are as follows:

1) Metal nanopowder, such as silver, aluminum, gold.
2) Non metal nanopowder, such as diamond, carbon nanotubes (CNT).
3) Oxide nanopowder, such as aluminum oxide (Al_2O_3), copper oxide (CuO)

Advantages

The conventional way to increase heat transfer in thermal systems is to increase the surface area of cooling devices (Das et al. 2008). Increase in surface area is constrained by the space

available for the thermal systems. So increase in heat transfer is limited by this method. Another method to increase heat transfer is to disperse solid particles in heat transfer fluid. Generally the solid particles were in the range of millimeters or micrometers. There are certain disadvantages with these particle sizes which are overcome by using nanotechnology which are as follows:

(1) The micrometer or millimeter size particle suspension settles rapidly, but nanoparticles stay suspended much longer time comparatively (Das et al. 2008).
(2) Micro particles are found to clog the micro channels made for cooling the system whereas no such problem occurs with nanoparticles (Das et al. 2008).
(3) Flow of micro particles suspension leads to increase in pressure drop in microchannels as the diameter of flow passage decreases, which leads to increase in pumping power, but this problem is eliminated by using nanofluids (Choi et al. 1992).
(4) Continuous circulation of conventional solid liquid suspensions causes erosion of system but nanoparticles finishes this problem (Das et al. 2008).

Applications

Nanofluids are used in following fields (Wong et al. 2009):

(1) Industrial cooling applications.
(2) Nuclear reactors
(3) Extraction of geothermal power and other energy sources.
(4) Automotive applications
(5) Brake and other vehicular nanofluids.
(6) Cooling in microchips.

The use of nanofluids is advantageous as compared to traditional heat transfer fluids, but still these are commercially viable because it is difficult to fundamentally model some key design factors like viscosity, conductivity, coefficient of heat transfer because many parameters like particles size distribution, shape of particles, temperature, volume fraction of nanoparticles, sonication time, settling time etc. are involved with it. Since the term nanofluid given by Choi (1995), work has been done on the conductivity of nanofluids such as Wang et al. (1999), Das et al. (2003), Choi et al. (2004), but little work has been done on the viscosity of nanofluids. A classical expression for calculating the heat transfer coefficient in a smooth circular tube can be given by Colburn analogy (Incropera et al. 2012) which is as follows:

$$Nu = 0.023 Re^{4/5} Pr^{1/3} \tag{1.1}$$

where

$$Nu = \frac{hl}{k} \tag{1.2}$$

$$Re = \frac{\rho V d}{\mu} \tag{1.3}$$

$$Pr = \frac{\mu c_p}{k} \tag{1.4}$$

Replacing equation 1.2, 1.3 and 1.4 in equation 1.1, it is found that the heat transfer coefficient depends upon the viscosity. The equation 1.1 is given for single phase fluid. In the similar way, the heat transfer coefficient for nanofluid also depends upon the viscosity of nanofluid. A coolant is made to flow in the system by a pumping system. A less viscous fluid requires less pumping power as compared to the highly viscous fluid, which further increase the efficiency of the system. Thus a nanofluid to be used as a coolant and for the measurement of heat transfer coefficient, viscosity of nanofluid needs to be measured. Few researchers like Nguyen et al. (2008), Prasher et al. (2006) have studied the effect of certain parameters like temperature and volume fraction on the viscosity of nanofluids, but the effect of these parameters needs to be evaluated for different nanofluids. The available data is

random and is not reproducible (Kulkarni et al.2009). There exist certain models to evaluate the viscosity of nanofluids like Einstein (1906) model, Brinkman (1950) model. The accuracy of these models needs to be evaluated. Because of above limitation, further work needs to be done to evaluate the effects of different parameters on viscosity of nanofluid and a model needs to be built for better and accurate measurement of viscosity.

1.2 Objectives

Specific objectives include:

(1) Investigating the viscosity of nanofluid with different nanoparticles such as ZnO, SWCNT, CuO, Aqueous silver.

(2) Investigating the viscosity of nanofluid with different base fluids such as water, EG.

(3) Development of a model for viscosity of nanofluid and investigating its accuracy against experimental data.

Chapter 2: Literature Review

This chapter consist the comprehensive review of nanofluids, method of preparation of nanofluids, surfactants, characterization of nanofluids and an extensive literature review of several research papers of viscosity of nanofluids. Although the theoretical and empirical models of viscosity of nanofluids are the part of literature review, these models are discussed in Chapter 3.

2.1 Nanofluids

Nanofluids are composed of solid nanoparticles dispersed in base fluid such as water, ethylene glycol, propylene glycol etc. There are two methods of formation of nanofluids as reported by Yu et al. (2011) which are as follows:

1) Two Step method
2) One Step method

Two step method:

According to Yu et al. (2011), nanoparticles are first produced as dry powders by chemical or physical methods. Then the nanosized particles are dispersed into a fluid called base fluid (Garg et al. 2008). Two step method is a relatively economic method to produce nanofluids in large scale because nanopowder synthesis techniques have already been scaled up to industrial production levels, but the nanofluids prepared from this method agglomerates very rapidly. In order to avoid agglomeration, surfactants may be added to the nanoparticles. However, the working of surfactant is a matter of concern at high temperature.

One step method

In order to reduce the agglomeration of nanoparticles, one step physical vapour condensation

method was developed by Akoh et al. (1978). This method consists of simultaneously making and dispersing the particles in the fluid. In this method, the processes of drying, storage transportation and dispersion of nanoparticles are avoided which leads to decrease in agglomeration of nanoparticles and hence increase in stability. One step physical method cannot produce nanoparticles in large scale (Yu et al. 2011). Therefore, one step chemical method is used to produce nanofluids (Zhu et al. 2004) in which nanofluid is prepared by chemical reaction of two reactants and a well dispersed nanofluid is generated.

2.2 Surfactant

When nanoparticles are mixed in base fluids, they come close to each other and agglomerates. In order to avoid agglomeration, the surfactants are added to nanoparticles. These surfactants can affect the surface characteristics of a system in small quantity. Surfactants are employed to increase the contact of two materials. In two phase system, a dispersant tends to stick to the interface of the two phases where it introduces a degree of continuity between nanoparticles and fluid (Yu et al. 2011). This continuity does not let the particles to agglomerate. Oleic acid is one of the surfactant used in the nanofluids to avoid agglomeration.

2.3 Characterization Techniques

Characterization of nanoparticles is necessary to establish understanding and control of nanoparticles synthesis and application. Characterization may be carried out by a variety of techniques. Commonly used techniques for the characterization of nanoparticles are as follows:

1) Transmission Electron Microscopy (TEM)
2) Dynamic Light Scattering (DLS)
3) X- Ray Diffraction (XRD)
4) Zeta Potential
5) Scattering Electron Microscopy (SEM)

Transmission Electron Microscopy

The transmission electron microscope is used to characterize the microstructure of materials with high spatial resolution. Information about the morphology, crystal structure and defects, crystal phases, composition and magnetic microstructure for nanoparticles can be obtained by a combination of electro-optical imaging, electron diffraction, and small probe capabilities. The transmission electron microscope uses a high energy electron beam transmitted through a very thin sample to image and analyze the microstructure of particles with atomic scale resolution (Cullity and Stock, 2001). The electrons are focused with electromagnetic lenses and the image is observed on a fluorescent screen, or recorded on film or digital camera. The entire arrangement, including the specimen has to be placed in high vacuum to avoid scattering and absorption of electrons by air. Generally the pressure maintained in the chamber is of the order of 10^{-4} to 10^{-8} kPa (Shah et al. 2010).

Dynamic Light Scattering

Dynamic light scattering is used to determine the size distribution profile of small particles in suspension (Ghadimi et al. 2011). When light hits small particles, the light scatters in all directions (Rayleigh scattering) as long as the particles are small compared to the wavelength (below 250 nm). If the light source is a laser, then one observes a time-dependent fluctuation in the scattering intensity. These fluctuations are due to the fact that the small molecules in

solutions are undergoing Brownian motion and so the distance between the scatterers in the solution is constantly changing with time. With this scattered light, information about the suspension is calculated. DLS is used to characterize size of various particles including proteins, polymers, micelles, carbohydrates, and nanoparticles. The mean effective diameter of the particles can also be determined.

X-Ray Diffraction

X-ray powder diffraction (XRD) is a rapid analytical technique primarily used for phase identification of a crystalline material. The analyzed material is finely ground, homogenized, and average bulk composition is determined. X-ray diffraction is based on constructive interference of monochromatic X-rays and a crystalline sample. X rays are passed through the sample and the diffracted rays are then detected, processed and counted (Cullity and Stock 2001). By scanning the sample through a range of 2θ angles, all possible diffraction directions of the lattice should be attained due to the random orientation of the powdered material. Conversion of the diffraction peaks to d-spacing allows identification of the mineral because each mineral has a set of unique d-spacing. Typically, this is achieved by comparison of d-spacing with standard reference patterns.

Zeta potential

Uniform dispersion and stable suspension of nanoparticles in liquids is the key to most applications of nanofluids since the final properties of nanofluids are determined by the quality of the dispersion and suspension. Zeta potential is the potential difference between the dispersion medium and the stationary layer of fluid attached to the dispersed particle. Measurement of Zeta potential is critical for stability of dispersion (Muller 1996). It is found that a suspension with zeta potential above 30 mV are physically stable and above 60 mV

show excellent stability while a suspension below 20 mV has limited stability and below 5 mV undergoes pronounced aggregation.

Scanning Electron Microscopy

The scanning electron microscope is used for the examination and analysis of the microstructure morphology and chemical composition for nanoparticles. The scanning electron microscope uses a focused beam of high- energy electrons to generate a variety of signals at the surface of solid specimens (Shah et al. 2010). The signals that derive from electron-sample interactions reveal information about the sample including external morphology, chemical composition, crystalline structure and orientation of material making up the sample. The scanning electron microscope produces an electronic map of the specimen that is displayed on a cathode ray tube. The scanning electron microscope is also capable of performing analyses of the selected point locations on the sample. This approach is especially useful in qualitatively or semi-quantitatively determining chemical composition.

2.4 Experimental Investigation by Previous Researchers

Kwak et al. (2005) investigated the rheological properties of ethylene glycol (EG) based Copper Oxide (CuO) nanofluid. He investigated the effect of sonication on the aggregation of particles in nanofluid. He varied the sonication time from 1 hour to 30 hours and found that particles remained aggregated even after prolonged sonication and 9 hour sonication was the time at which minimum aggregation was found in the nanofluid. Also the viscosity of nanofluid showed shear thinning behavior, which indicated that the viscosity of nanofluid was continuously decreasing with the increase in shear rate.

Prasher et al. (2006) studied the viscosity behavior of propylene glycol based alumina nanofluid. He studied the effect of shear rate, diameter, volume fraction of nanoparticles in base fluid and temperature on the viscosity of nanofluid. He found that viscosity of the nanofluid did not change with the shear rate, which showed the Newtonian behavior of the nanofluid. He determined that viscosity was not changing with diameter that indicated that the viscosity was not strongly dependent on diameter. Viscosity of nanofluid was increasing with the increase in volume fraction. Viscosity of nanofluid was not varying with the increase in temperature which indicated that viscosity was not a strong function of temperature.

Jang et al. (2007) investigated the viscosity of aluminum oxide nanoparticles dispersed in water for a volume fraction range of 0.01 - 0.3%. The nanofluid was prepared by the two step method and no surfactant was added in the fluid for stabilization of nanoparticles. The average diameter of nanoparticles was found to be 30 ± 5 nm by the TEM microscopy. He investigated the variation of viscosity of nanofluid with volume fraction and temperature. Temperature of the nanofluid was varied from 21 to 39˚C. He found that with the increase in the volume fraction of nanoparticles in the base fluid, the viscosity of nanofluid increased and with the increase in temperature of fluid, there was a continuous decrease in the viscosity. He noted an increase of 2.9% in viscosity for a volume fraction of 0.3%.

Namburu et al. (2007) did experiments for viscosity measurement of copper oxide nanoparticles in ethylene glycol and water mixture (base fluids are in a ratio of 60:40 by weight) for a volume fraction range of 0 to 6.12% of nanoparticles. The average diameter of nanoparticles was found to be 29 nm. The viscosity of nanofluid was measured with LVDV II Brookfield viscometer. In order to find the behavior of nanofluid, the effect of shear rate on shear stress was measured and he found a linear relation between shear stress and shear rate

that indicated the Newtonian behavior of nanofluid. He investigated the effect of volume fraction and temperature for a range of -35 to 50˚C. He found that with the increase in volume fraction, viscosity of nanofluid is increasing. The results also indicated that with the increase in temperature, viscosity of nanofluid was decreasing. At low volume fraction (Φ = 1%), relative viscosity remains almost unchanged with the increase in temperature. He also proposed a model for the viscosity of copper oxide with R^2 more than 0.99.

Schmidt et al. (2008) studied the shear viscosity behavior of alumina in Decane ($C_{10}H_{20}$) and isoparaffinic polyalphaolefin (PAO). He found that with increase in volume fraction, the relative viscosity values were increasing. Also viscosity of PAO based nanofluid is less than the viscosity of Decane based nanofluid.

Garg et al. (2008) investigated the viscosity of copper nanoparticles dispersed in ethylene glycol. The diameter of nanoparticles was measured by transmission electron microscopy and the average particle diameter was found to be 200 nm. Nanofluid was prepared up to a volume fraction of 2%. He studied the variation of viscosity of nanofluid with shear rate and volume fraction. He found that the viscosity of nanofluid did not vary with shear rate in the range of 3-3000 s^{-1}. Hence the nanofluid showed Newtonian behavior. Also he found that the viscosity of nanofluid increases with the increase in volume fraction of nanoparticles.

Nguyen et al. (2008) investigated the viscosity of aluminum oxide nanoparticles dispersed in distilled water. The diameter of nanoparticles was 36 nm and 47 nm. He studied the variation of viscosity with particle volume fraction, temperature and diameter. He reported that with the increase in volume fraction, relative viscosity of nanofluid increased. He found that with the increase in temperature, viscosity of the nanofluid was decreasing. His results also

indicated that the viscosity of nanofluid increases with the increase in diameter. Based on his experimental work, he proposed two models for viscosity measurement of aluminum oxide. He showed that there exists a critical temperature beyond which the particle suspension properties drastically altered, which in turn produced a hysteresis phenomenon. This temperature found to be strongly dependent on the particle concentration and size. He commented that this hysteresis phenomenon might affect the reliability on the nanofluids for heat transfer enhancement purposes seriously.

Murshed et al. (2008) investigated the viscosity of distilled water based aluminum oxide and titanium oxide nanofluid. The diameter of titanium oxide and aluminum oxide nanoparticles were 15 nm and 80 nm respectively. The sample nanofluids were prepared with a volume fraction of 1 to 5%. He found that the viscosity of nanofluid increases with the increase in volume fraction. Viscosity of nanofluid was found to be higher than that of base fluid. He also found that the viscosity of titanium oxide based nanofluid was more than that of aluminum oxide based nanofluid. Also the relative viscosity of aluminum oxide based nanofluid increases by 82% for a volume fraction of 5%. He commented that this amount of increase in viscosity might diminish the potential use of nanofluids.

Lee et al. (2008) investigated the viscosity behavior of aluminum oxide based nanofluid for a volume fraction of 0.01 to 0.3%. The average diameter of nanoparticles was 30 ± 5 nm. These nanoparticles were dispersed in DI water. Thus two step method was used to prepare the nanofluid. No surfactant was added in the nanofluid for the stability of nanoparticles in fluid. He studied the effect of sonication on zeta potential. He found that the value of zeta potential increased for first 5 hours of sonication and then it started decreasing. Thus the optimum time for sonication was 5 hours. He investigated the effect of temperature and

volume fraction on the viscosity of nanofluid. He found that relative viscosity of nanofluid decreases significantly with the increase in temperature and increases with the increase in volume fraction. He noted an increase of 2.9% in the viscosity of nanofluid for a volume fraction of 0.3%

Duangthongsuk et al. (2009) investigated the viscosity of titanium oxide nanoparticles dispersed in water. The size of nanoparticles was approximately spherical with an average diameter of 21 nm. He investigated the variation of viscosity with temperature and volume fraction for a volume fraction range of 0.2 to 2% and temperature range of 15 to 35˚C. He found that the viscosity of nanofluid decreased with the increase in the temperature and the viscosity of nanofluid increased with the increase in volume fraction. Also the viscosity of nanofluid was found to be more than the viscosity of basefluid.

Yu et al. (2009) investigated the viscosity of zinc oxide (ZnO) nanoparticles dispersed in ethylene glycol nanofluid for a volume fraction range of 0.2 to 5%. The average diameter and density of nanoparticles was found to be 10 to 20 nm and 5.6 g/cm^3 respectively. He investigated the effect of sonication time on the particle size distribution. He noted that the average particle size decreased rapidly for the first 3 hours of sonication and after 3 hours of sonication the average particle size did not vary with the sonication time. Hence the optimum time for the sonication of nanofluid was found to be 3 hours and the average particle size was found to be 210 nm. He found that the shear stress acting on the fluid varies linearly with the shear rate. Hence the nanofluid acted like a Newtonian fluid. He also examined the variation of viscosity of nanofluid with the temperature in the range of 20 to 60˚C under steady state conditions. He found that the viscosity of nanofluid decreased with the increase in the temperature. He also investigated the variation of viscosity with shear rate and found that for

a volume fraction less than 2%, viscosity remained independent of shear rate even if the temperature of nanofluid was increased. But for higher volume fraction of nanoparticles in the base fluids, the nanofluid showed shear shining behavior.

Abu-Nada (2010) studied the effect of variable viscosity of copper oxide-water nanofluid on heat transfer enhancement. He calculated the viscosity variation by simulation method. It was observed that for $Ra \geq 10^4$, the average Nusselt number deteriorated by increasing the volume fraction of nanoparticles. However, for $Ra = 10^3$, the average Nusselt number enhancement depended on aspect ratio of the annulus as well as volume fraction of nanoparticles. For $Ra = 10^3$, the average Nusselt number was less sensitive to volume fraction of nanoparticles at high aspect ratio and the average Nusselt number increased by increasing the volume fraction of nanoparticles for aspect ratios less than 0.4.

Chandrasekar et al. (2010) investigated the variation in viscosity of aluminum oxide (Al_2O_3) dispersed in water for a volume fraction range of 1 to 5%. The average diameter of nanoparticles was found to be 43 nm. The viscosity of nanofluid was measured by Brookfield cone and plate viscometer. He examined the variation in the shear stress acting on the nanofluid with the change in shear rate and found that the shear stress varies linearly with shear rate. Hence the nanofluid behaved like a Newtonian fluid. He also investigated the viscosity of nanofluid with volume fraction. He found that the viscosity of nanofluid increased with increase in the volume fraction of nanoparticles in the basefluid. Viscosity of nanofluid was found to be 2.36 times the viscosity of basefluid for a volume fraction of 5%. He also proposed a theoretical model for the measurement of viscosity of nanofluid and the viscosity of nanofluid predicted with this model was in good agreement with his experimental values.

Pastoriza-Gallego et al. (2011) investigated viscosity of aluminum oxide nanoparticles dispersed in ethylene glycol and water separately. Nanoparticles taken for experimentation were of two sizes. First nanoparticles size was 40 to 50 nm and was dispersed in ethylene glycol and the other nanoparticles size was less than 20 nm and this sample was dispersed in DI water. No surfactant was added for stabilization. The variation in the viscosity of nanofluids with volume fraction and temperature was measured for a temperature range of 283 to 323 K. An increase in the viscosity of nanofluid was noted with the increase in volume fraction. The viscosity of nanofluid started decreasing with the increase in temperature. He found that with decrease in diameter, viscosity of the nanofluid was increasing, e.g. at a volume fraction of 10%, viscosity enhancement of 46% and 96% were obtained for samples of nanofluids having sizes 43 ± 23 nm and 8 ± 3 nm, respectively.

Duan et al. (2011) investigated the viscosity of aluminum oxide-water nanofluid after providing a settling time of 2 weeks to the nanoparticles. The diameter of nanoparticles was 25 nm. He found that with the increase in shear rate, viscosity kept on decreasing which indicated that the nanofluid was behaving like a non-Newtonian fluid. After resonication, viscosity of nanofluid increased first linearly with shear rate and then it became constant and achieved Newtonian behavior. He found that after 2 weeks of sonication, the nanoparticles had come in a range of micron size by aggregating. He reported that with an increase in volume concentration, relative viscosity was increasing. He noted that with the increase in the volume fraction, the viscosity of nanofluid was increasing.

Fedele et al. (2012) investigated the viscosity of titanium oxide nanoparticles dispersed in bi distilled water for a concentration of 1 to 35% by mass. Acetic acid was used as a dispersant at 1 to 5 wt%. He analyzed the settling of nanoparticles in fluid for 35 days and measured the

size distribution. He found that the mean diameter of nanoparticles had decreased from 73 nm to 51 nm after 35 days. The mean diameter of 73 nm was again noted after 1 hour of sonication. Further, the behavior of viscosity as a function of temperature and composition was evaluated by AR-G2 rheometer for a temperature range of 283 to 343 K. He found that the increase in temperature had no effect on the relative viscosity. However, the viscosity of nanofluid increased with the increase in the concentration of nanoparticles in the base fluid. The effect of shear stress as a function of shear rate was also noted and he found that shear stress was varying linearly with shear rate which indicated the Newtonian behavior of nanofluid.

Chapter 3: Evaluation of Theoretical and Empirical Models of Nanofluid Viscosity

The accuracy of the existing theoretical and empirical models of viscosity has been evaluated in this chapter against a wide range of experimental data for copper oxide based nanofluids.

3.1 Experimental Data of Copper Oxide based Nanofluids

For the purpose of evaluating the existing models for the viscosity of nanofluids, the following data on CuO - water (DI) nanofluids and CuO - ethylene glycol and water nanofluids (Table 3.1) have been used.

Table 3.1: Physical Properties of CuO Based Nanofluids

Reference	**Particle Average Diameter (nm)**	**Volume Fraction (%)**	**Temperature (˚C)**
Namburu et al. (2007)	29	1 to 6.12	-35 to 50
Nguyen et al. (2007)	29	0 to 12	21 to 70
Kulkarni et al. (2009)	30	1 to 6	-30 to 55

3.2 Theoretical and Empirical Models for Viscosity of Nanofluids

In this section, classical models, models derived from classical models and empirical models are discussed. Classical models like Einstein (1906) model, Krieger and Dougherty (1952) models**,** Nielson (1970) model, Batchelor (1977) model and models derived from classical models like Saito (1950) model, Brinkman (1952) model, Lundgren (1972) model and empirical models like Maiga et al. (2004) model, Nguyen et al. (2007) models have been used

in the present study for comparing the experimental results with the predicted values.

Einstein (1906) Model

Einstein (1906) was the first researcher who developed a theoretical model to calculate the viscosity of solid liquid suspension. He assumed a viscous fluid that contains dilute suspended spherical particles (for a volume fraction of 0.02). He calculated the energy dissipated by fluid flow around a single particle and then by associating the energy with the work done for moving this particle relatively to surrounding fluid, he proposed:

$$\mu_r = \mu_{nf} / \mu_{bf} = (1+2.5\Phi) \quad (3.1)$$

Saito (1950) Model

Saito (1950) developed a model based on a theory for spherical solute molecules in which a single solute molecule is placed in the field of flow, obtained by averaging over all the possible positions of a second solute molecule. Saito model is given as:

$$\mu_{nf} = [1+ (2.5\Phi/ (1-\Phi))] \mu_{bf} = [1+2.5\Phi+2.5\Phi^2+----] \mu_{bf} \quad (3.2)$$

Brinkman (1952) Model

Brinkman (1952) model is a theoretical model and is an extension of Einstein model to concentrated suspensions (Φ < 4%). The expression is derived for viscosity of solutions and suspensions of finite concentration (Φ < 4%) by considering the effect of the addition of one solute molecule to an existing solution, which is considered as a continuous medium. The model is given as

$$\mu_r = \mu_{nf} / \mu_{bf} = 1/ (1-\Phi)^{2.5} \quad (3.3)$$

Krieger and Dougherty (1959) Model

I.M. Krieger and T.J. Dougherty (1959) developed a semi empirical equation for calculating the relative viscosity which can be expressed as

$$\mu_{nf} = \mu_{bf} [1 - (\Phi/ \Phi m)]^{-[\square] \Phi m}$$

(3.4)

Where Φ_m is the maximum packing fraction which varies from 0.495 to 0.54 under quiescent conditions and is approximately 0.605 at high shear rate and for randomly mono dispersed spheres, the maximum close packing fraction is approximately 0.64. Maximum packing fraction is the volume fraction of aggregates in closest packing at which the relative viscosity becomes infinite (Zhou et al. 1995). This model reduces to Einstein model if a monomial expansion is performed, whereas a binomial expansion will lead to another famous model named Batchelor Model (Chandrasekar et al. 2010).

Nielson (1970) Model

Nielson in 1970 proposed a theoretical model and his model is given as:

$$\mu_{nf} = \mu_{bf} (1+1.5\Phi) e^{\Phi/(1-\Phi m)} \quad (3.5)$$

Lundgren (1972) Model

T.S. Lundgren in 1972 proposed the following equation under the form of the Taylor series in

Φ

$$\mu_{nf}/\mu_{bf} = [1+2.5\Phi +6.25\Phi^2 + O(\Phi^3)] \quad (3.6)$$

It is obvious that when the terms of second or higher order of Φ are neglected, this model reduces to Einstein (1905) model.

Batchelor (1977) Model

For $\Phi > 0.01$, hydrodynamic interaction between particles became dominant as the disturbance of fluid around individual particles interacts with that around other particles. The viscosity in such a case was derived by Batchelor, which is

$$\mu_r = \mu_{nf}/\mu_{bf} = [1+2.5\Phi+6.5\Phi^2] \quad (3.7)$$

Brownian motion of nanoparticles and the interaction between them was taken into account in this model and it is an extension of Einstein Model. This model is valid up to a particle volume fraction of $\Phi \leq 0.1$, where motion of single particle and pair particle interaction become dominant.

Maiga et al. (2004) Model

Maiga et al. (2004) proposed a model to calculate the viscosity of nanofluid as follows:

$$\mu_{nf} = \mu_{bf} (1+7.3\Phi+123\Phi^2) \quad (3.8)$$

Nguyen et al. (2007) Model

Nguyen et al. (2007) has proposed a correlation for computing the CuO-water viscosity, which is as follows:

$$\mu_r = \mu_{nf}/\mu_{bf} = (1.475\text{-}0.319\Phi+0.051\Phi^2+0.009\Phi^3) \quad (3.9)$$

Maiga et al. (2004) and Nguyen et al. (2007) models are for the viscosity of nanofluids only and rest of the models are for the viscosity of solid liquid suspensions. These models have not been evaluated before for a wide range of nanofluids are to be evaluated for their accuracy. Hence, the accuracy of these models needs to be evaluated.

3.3 Evaluation of Theoretical Models for Copper Oxide based Nanofluid

Models listed in section 3.2 are evaluated by using them to predict absolute viscosity for a range of experimental conditions and compared the predicted results with experimental data given in Table 3.1 in same range of temperature and volume fraction. The following parameters have been considered here for the purpose of calculation.

1) Viscosity of EG and water basefluid is 92 cP at 35°C and 1 cP at 50°C (Namburu et al. 2007).
2) Viscosity of distilled water basefluid is varying from 1 cP at 20°C to 0.4 cP at 70°C (Nguyen et al. 2007).

In Figure 3.1, the experimental values of absolute viscosity taken from Namburu et al. (2007) for 29 nm CuO particles with EG and Water (60:40 in weight) base fluid at a volume fraction

of 2% in the given range of temperature are compared with the viscosity values predicted from theoretical and empirical models.

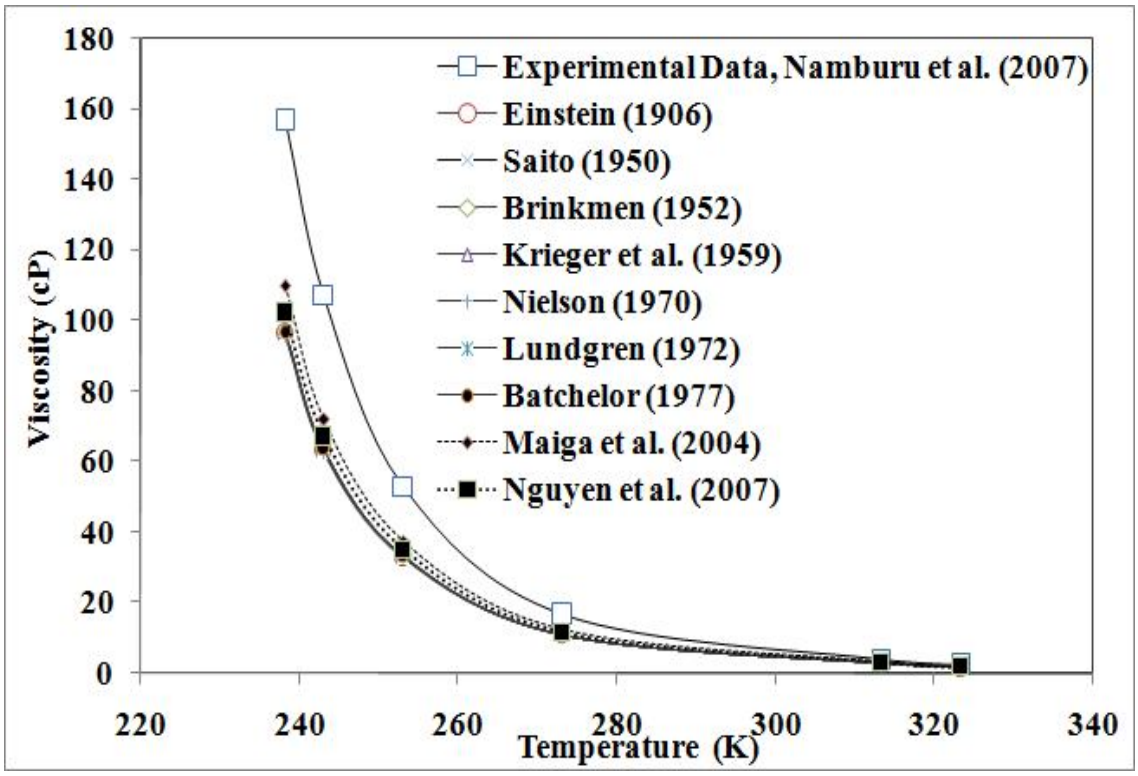

Figure 3.1: Experimental versus predicted values of absolute viscosity with increase in temperature at 2% volume fraction for 29 nm CuO particles.

Figure 3.1 show that no model could predict the experimental values exactly. At low temperature, all the models are highly under predicting the experimental values of viscosity even at a volume fraction of 2%. It is also found that the viscosity values predicted from Einstein (1906), Brinkman (1952), Krieger et al. (1959), Lundgren (1972), Batchelor (1977), Nielson (1970) and Saito (1950) models are almost overlapping with each other. With the increase in temperature, viscosity of the nanofluid is decreasing. At high temperature conditions, the viscosity predicted by the models and the experimental values comes close to each other.

In Figure 3.2, the experimental values of absolute viscosity obtained from Namburu et al. (2007) for 29 nm CuO particles at a volume fraction of 3% in given range of temperature are compared with the theoretical and empirical models.

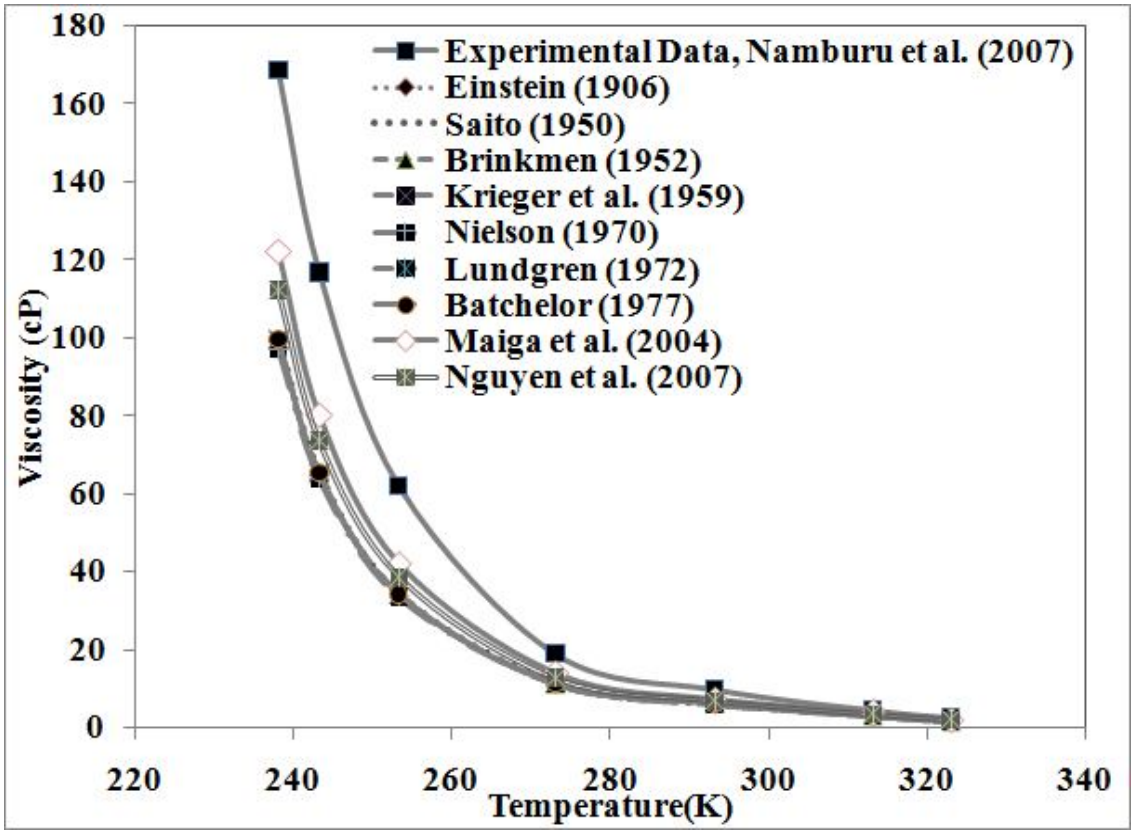

Figure 3.2: Experimental versus predicted values of absolute viscosity with increase in temperature at 3% volume fraction for 29 nm CuO particles.

In Figure 3.2, all the models are highly under predicting the experimental values of viscosity at low temperature. As the volume fraction increased to 3%, the error in predicting the viscosity values is also increased. Maiga et al. (2004) gives the highest value of prediction with an average error of 25%. Predicted values of Einstein (1906), Brinkman (1952), Krieger et al. (1959), Lundgren (1972), Batchelor (1977), Nielson (1970) and Saito (1950) models are overlapping with each other. As the temperature increases, experimental and predicted

values come close to each other.

In Figure 3.3, the experimental values of absolute viscosity obtained from Namburu et al. (2007) for 29 nm CuO at a volume fraction of 6.12% are compared with theoretical and empirical values.

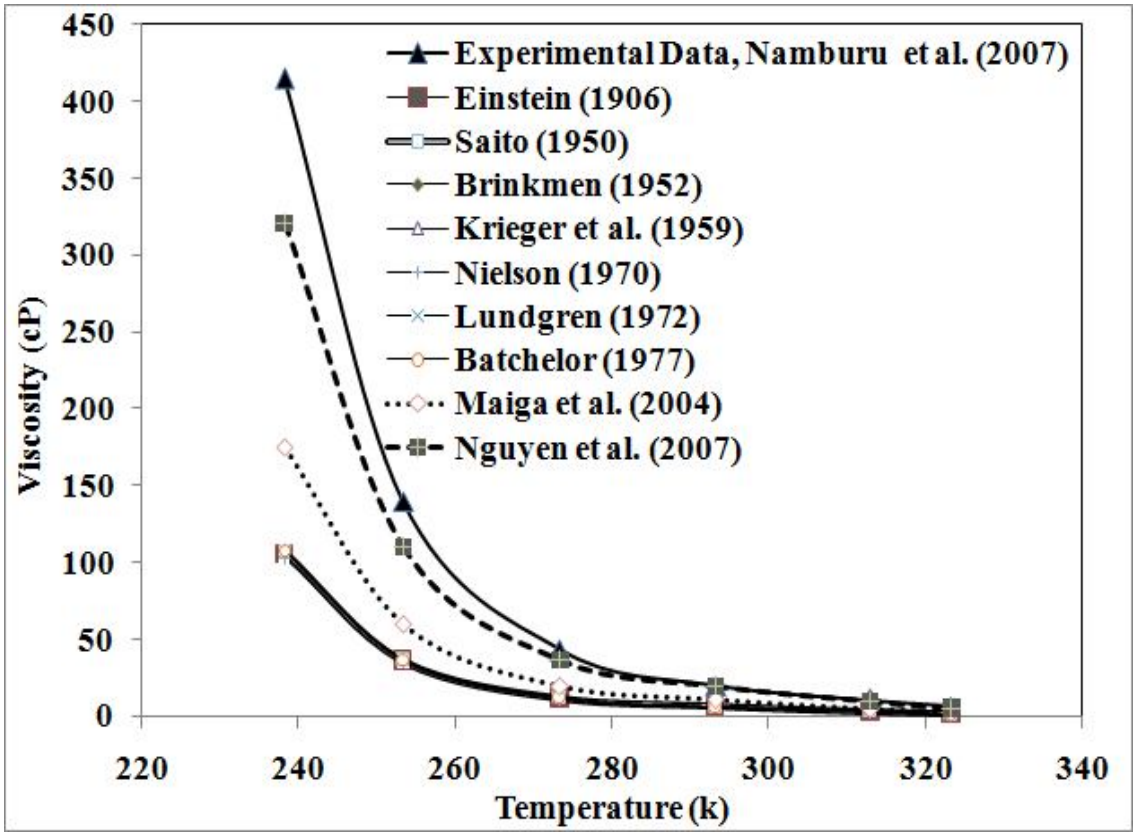

Figure 3.3: Experimental versus predicted values of absolute viscosity with increase in temperature at 6.12% volume fraction for 29 nm CuO particles

In Figure 3.3, all the theoretical and empirical models are under predicting the experimental data to a great extent. Nguyen et al. (2007) gives the highest value of prediction whereas Einstein (1906), Brinkman (1952), Krieger et al. (1959), Lundgren (1972), Batchelor (1977), Nielson (1970) and Saito (1950) gives least values of prediction. As the temperature

increases, viscosity value starts decreasing and near 320 K temperature, experimental and predicted values overlap with each other.

In Figure 3.4, the experimental values obtained from Nguyen et al. (2007) for 29 nm CuO particles with water base fluid at a volume fraction of 1% in given range of temperature are compared with theoretical and empirical models.

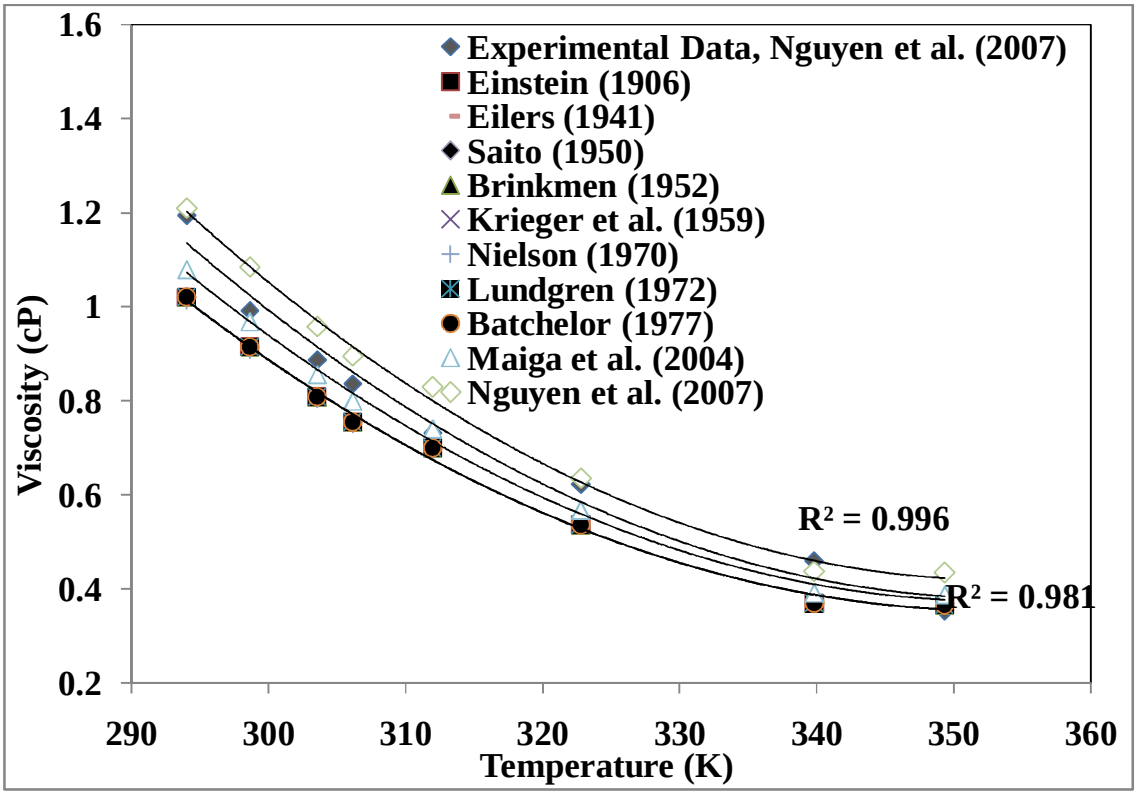

Figure 3.4: Experimental versus predicted values of absolute viscosity with increase in temperature at 1% volume fraction for 29 nm CuO particles.

In Figure 3.4, since the volume fraction is low, values of all the models come close to each other. Maiga et al. (2004) predicts viscosity values very close to the experimental values. Viscosity calculated from Nguyen et al. (2007) model over predicts its own experimental values. Einstein (1906), Brinkman (1952), Krieger et al. (1959), Lundgren (1972), Batchelor

(1977), Nielson (1970) and Saito (1950) models are predicting values very close to each other.

In Figure 3.5, the experimental values obtained from Nguyen et al. (2007) for 29 nm CuO particles, with water base fluid at a volume fraction of 4.5% in given range of temperature are compared with theoretical and empirical models.

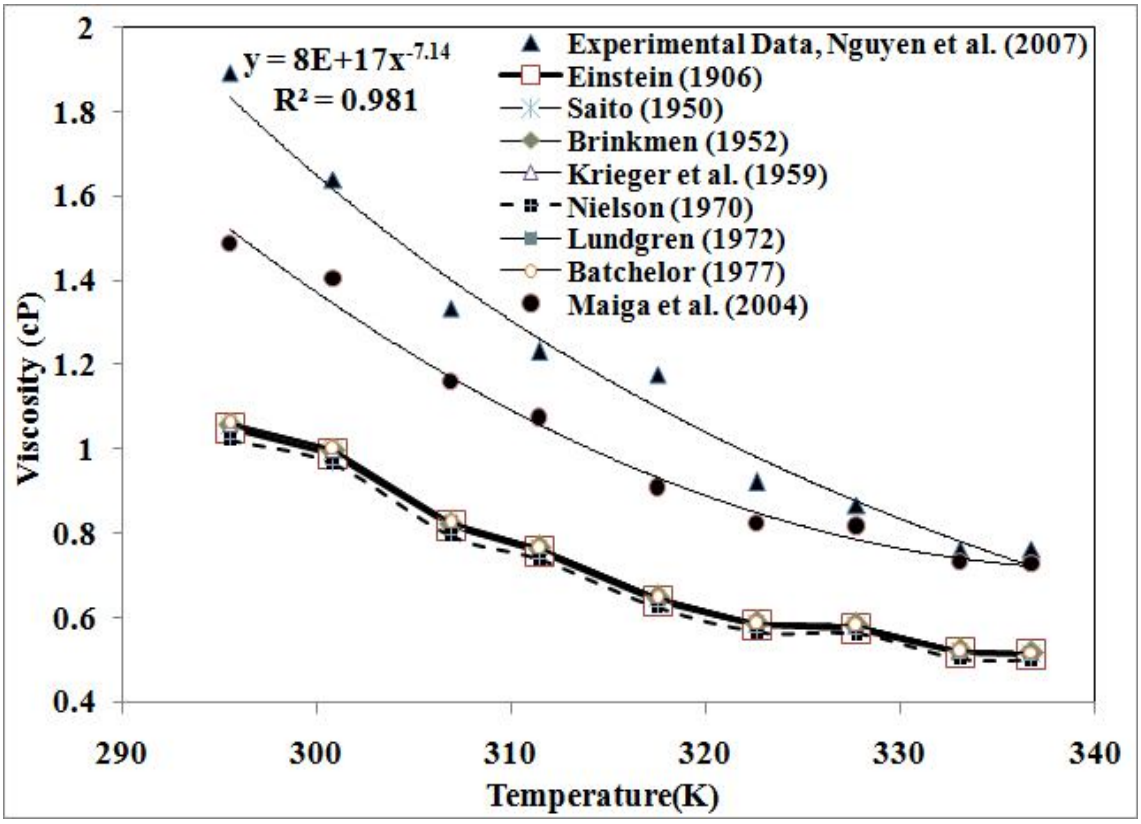

Figure 3.5: Experimental versus predicted values of absolute viscosity with increase in temperature at 4.5% volume fraction for 29 nm CuO particles.

In Figure 3.5, a trend line is made to pass through experimental values with $R^2 = 0.9814$. None of the model could predict the experimental value of viscosity. Einstein (1906), Brinkman (1952), Krieger et al. (1959), Lundgren (1972), Batchelor (1977) and Saito (1950) are highly under predicting viscosity values. Maiga et al. (2004) and Nielson (1970) gives the highest

and lowest values of prediction respectively. Even at high temperature, models are under predicting the experimental values.

In Figure 3.6, the experimental values obtained from Nguyen et al. (2007) for 29 nm CuO particles, with water base fluid at a volume fraction of 7% in given range of temperature are compared with theoretical and empirical models.

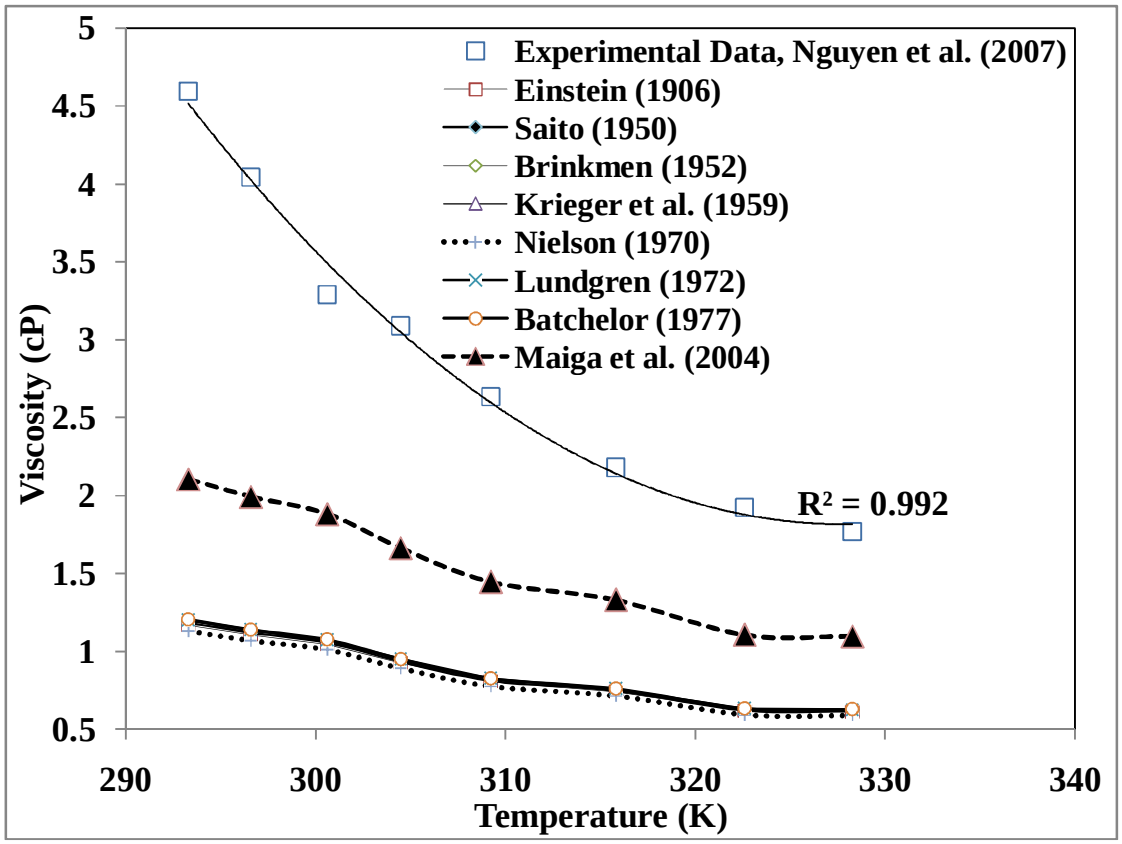

Figure 3.6: Experimental versus predicted values of absolute viscosity with increase in temperature at 7% volume fraction for 29 nm CuO particles.

In Figure 3.6, a trend line is made to pass through the experimental values with R^2 equal to 0.99. All the theoretical and empirical models are highly under predicting the experimental values even at high temperature. Maiga et al. (2004) model gives the highest value of prediction. Values of all the other models are almost overlapping. As the temperature

increases, the viscosity values decreases.

In Figure 3.7, the experimental values obtained from Nguyen et al. (2007) for 29 nm CuO particles with water base fluid at a temperature between 22 to 25°C in given range of volume fraction are compared with theoretical and empirical models.

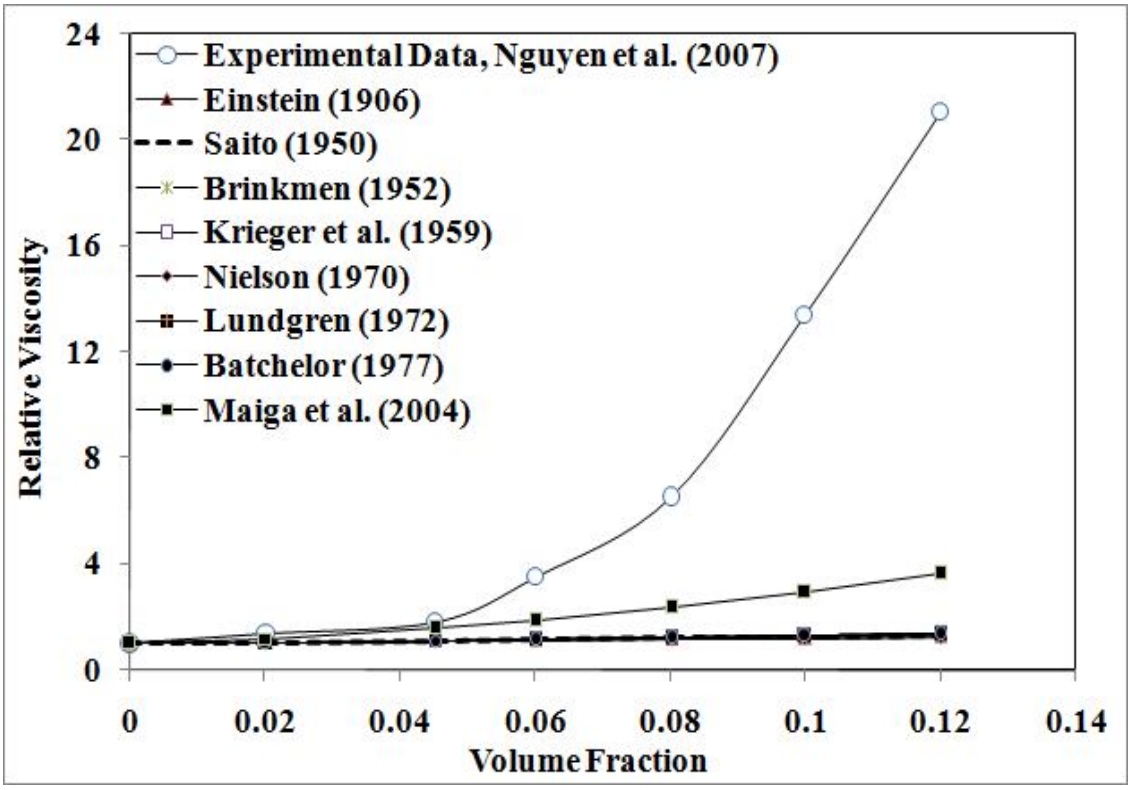

Figure 3.7: Experimental versus predicted values of absolute viscosity with increase in volume fraction at temperature between 22 to 25°C for 29 nm CuO particles.

From Figure 3.7, it is found that at a very low particle volume fraction (less than 1%) the values predicted from models comes close to the experimental values. As the volume fraction increases, difference between the predicted and experimental values increases. Maiga et al. (2004) gives the highest value of prediction. Einstein (1906), Saito (1950),

Brinkman (1952), Krieger et al. (1959), Nielson (1970), Lundgren (1972), and Batchelor (1977) models are overlapping.

In Figure 3.8, the experimental values obtained from Kulkarni et al. (2009) for 30 nm CuO particles with ethylene glycol and water (60:40 by weight) base fluid at a volume fraction of 6% are compared with theoretical and empirical models in given range of temperature.

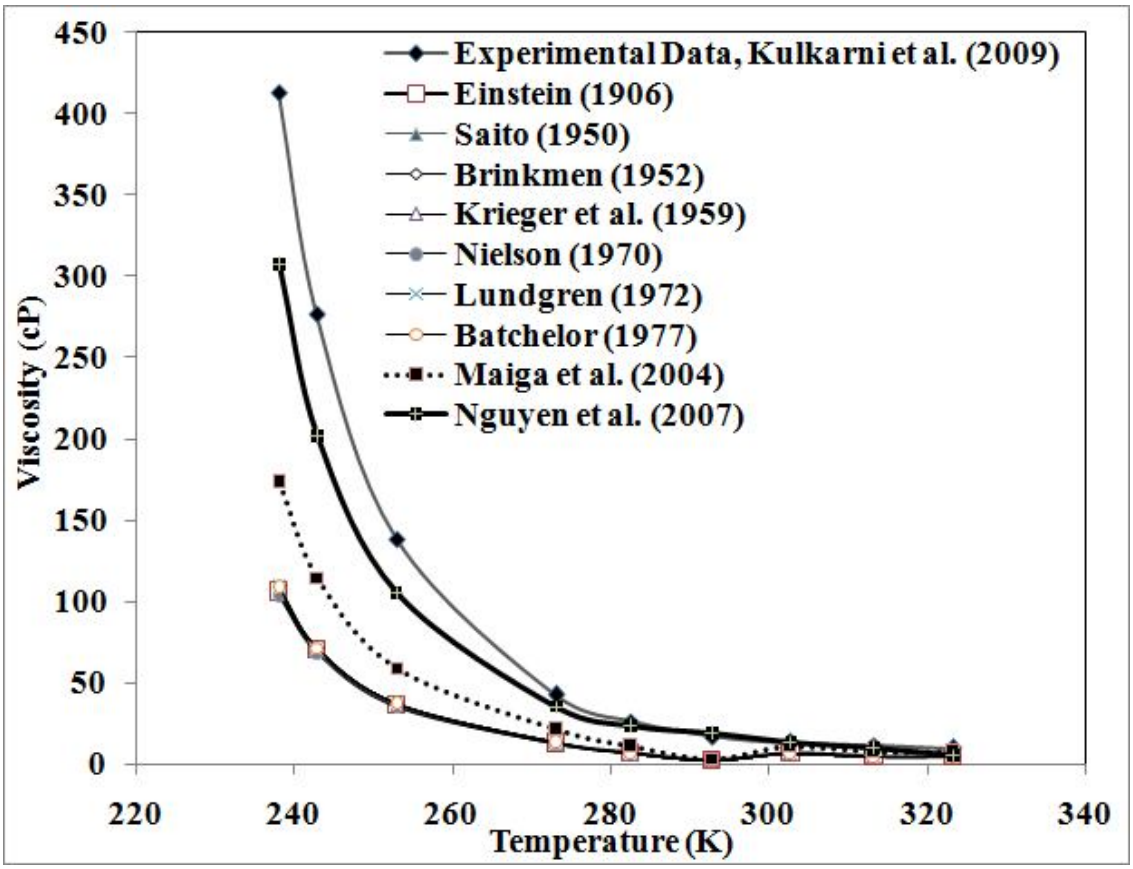

Figure 3.8: Experimental versus predicted values of absolute viscosity with increase in temperature at 6% volume fraction for 30 nm CuO particles

In Figure 3.8, neither of the models could predict the experimental viscosity values. All the models are under predicting the values. It is difficult to distinguish Einstein (1906),

Brinkman (1952), Krieger et al. (1959), Lundgren (1972), Batchelor (1977), Nielson (1970) and Saito (1950) models as these are overlapping each other. As temperature increases, predicted values are close to experimental values and at about 310 K temperature, predicted values overlap experimental values.

Table 3.2 provides average sum of absolute values of relative error for viscosity (using the formula given below) to indicate the prediction accuracies of the different models (Figure 3.1 to 3.8).

$$\text{Relative error} = \sum_{n} \left| \frac{\text{experimental value - predicted value}}{\text{experimental value}} \right| \times 100\%$$

Table 3.2: Relative Error of Model Prediction (%)

Figure Data base	Einstein (1905) Model	Saito (1950) Model	Brinkman (1952) Model	Krieger (1959) Model	Nielson (1970) Model	Lundgren (1972) Model	Batchelor (1977) Model	Maiga et al.(2004) Model	Nguyen et al. (2007) Model
3.1	33.9956	33.9327	33.8822	33.8629	34.7849	33.8384	33.8321	24.8681	30.0353
3.2	39.5067	39.3801	39.2748	39.2343	40.5564	39.1902	39.1775	25.174	31.3472
3.3	71.878	71.6496	71.4383	71.3543	72.7775	71.3071	71.2842	53.4768	14.7345
3.4	69.1013	68.8595	68.6366	68.5482	70.0739	68.4968	68.4726	49.4659	19.9142
3.5	38.0377	37.7558	37.5088	37.4124	39.573	37.3328	37.3046	12.1347	8.267
3.6	69.3162	68.9963	68.6913	68.5689	70.4077	68.5164	68.4844	44.803	26.078
3.7	66.193	65.992	65.7977	65.7187	67.0125	65.6904	65.6703	49.7862	8.6874
3.8	69.1013	68.8595	68.6366	68.5482	70.0739	68.4968	68.4726	49.4659	15.7195

Chapter 4: Experimental Evaluation of Viscosity

In order to evaluate the viscosity behavior of nanofluid, experiments have been carried out for different nanofluids. In this chapter, the experimental procedure and its results have been discussed.

4.1 Different Nanoparticles-Basefluid Combination for Measurement of Viscosity

Based upon the literature review, certain nanoparticles have been selected on which less research has been carried out. The base fluids used for the experiments are the traditional heat transfer fluid. These base fluids are most commonly used in various applications.

Nanoparticles used for the experimentation are:

1) Zinc oxide nanoparticles
2) Single walled carbon nanotube
3) Aqueous silver nanoparticles

Basefluids used in the experimentation are:

1) Distilled water basefluid (H_2O).
2) Ethylene Glycol basefluid (EG).

These nanoparticles and basefluids are used to prepare nanofluid. The different combinations of nanoparticles and basefluids are tabled in Figure 4.1

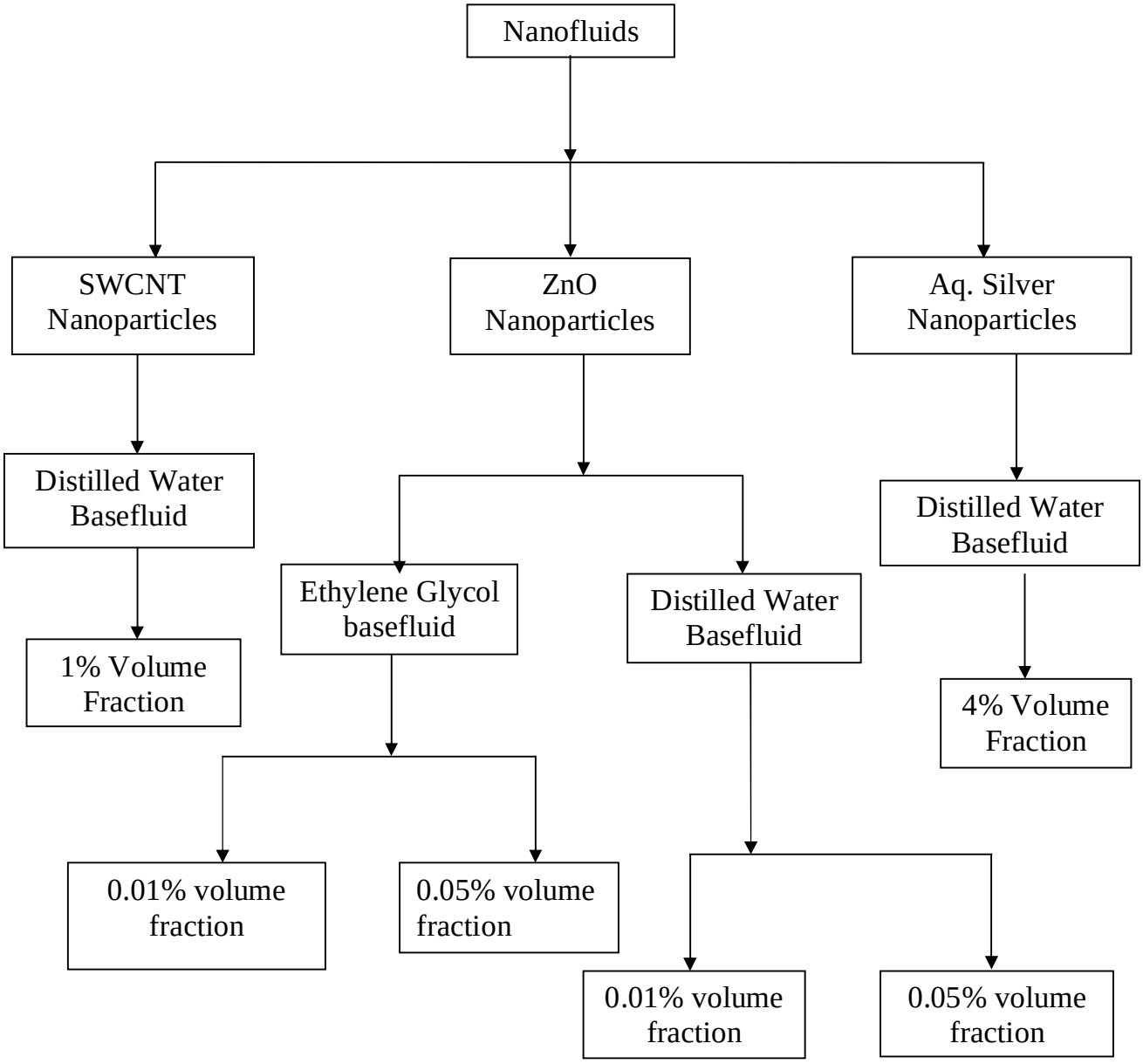

Figure 4.1: Various combinations of nanoparticles and basefluid to prepare nanofluids for experimentation.

4.2 Preparation of Nanofluids

Preparation of ZnO-H_2O nanofluid

In order to study the effect of various parameters on the viscosity of nanofluid, two samples of 14 nm and 25 nm sized zinc oxide (ZnO) nanoparticles have been purchased from Rainste Nano Ventures Pvt. Ltd, Noida. There is a coating of 1 nm oleic acid on the nanoparticles. This coating of surfactant limits the use of nanofluid at high temperature because at high temperature, the bond between the nanoparticles and surfactant become weak and the coating of surfactant dissolves in the basefluid. Nanofluid has been prepared with two different volume fractions for each size. These volume fractions are 0.01% and 0.05%. In order to prepare nanofluid, firstly the amount of nanoparticles for the sample has been calculated by using equation 5.1. 20 ml sample of nanofluid has been prepared for each volume fraction. By using the following formula of volume fraction, the amount of nanoparticles has been calculated.

$$volume\ fraction = \frac{volume\ of\ nanoparticles}{(volume\ of\ nanoparticles + volume\ of\ basefluid)} \quad (5.1)$$

It comes out to be 56 mg and 11.2 mg for 0.05% and 0.01% volume fraction respectively. Then this amount of particles has been dispersed in de ionized water. Then the nanofluid is sonicated in 3510 Granson Ultrasonicator. This ultrasonicator is a type of water bath sonicator in which the samples of nanofluids are filled in the tubes and these tubes are dipped in the DI water filled in the sonicator. Ultrasonic radiations are made to pass through the sample and sonicate the samples for the required time. The samples prepared are sonicated

for 4 different timing. First sample of each concentration was sonicated for 2, 4, 6 and 8 hours.

Preparation of ZnO-EG Nanofluid

Ethylene glycol based zinc oxide nanofluid is prepared for two different volume fractions for each size of nanoparticles. The volume fractions prepared for ZnO-EG nanofluid are 0.01% and 0.05%. The amount of nanoparticles for each volume fraction is calculated by the equation 5.1. After that these nanoparticles are dispersed in the basefluid and sonicated for the 2, 4, 6 and 8 hours. Different timing of sonication may have different effect on the viscosity of nanofluid. The nanofluid is sonicated for different timing so as to study the effect of sonication on the viscosity of nanofluid.

Preparation of SWCNT- H_2O nanofluid

Viscosity of single walled carbon nanotube has also been evaluated for water basefluid. Single walled carbon nanotube (SWCNT) has been purchased from Rainste Nano Ventures Pvt. Ltd., Noida. The SEM and TEM images of SWCNT are shown in Figure 4.2 and 4.3 respectively.

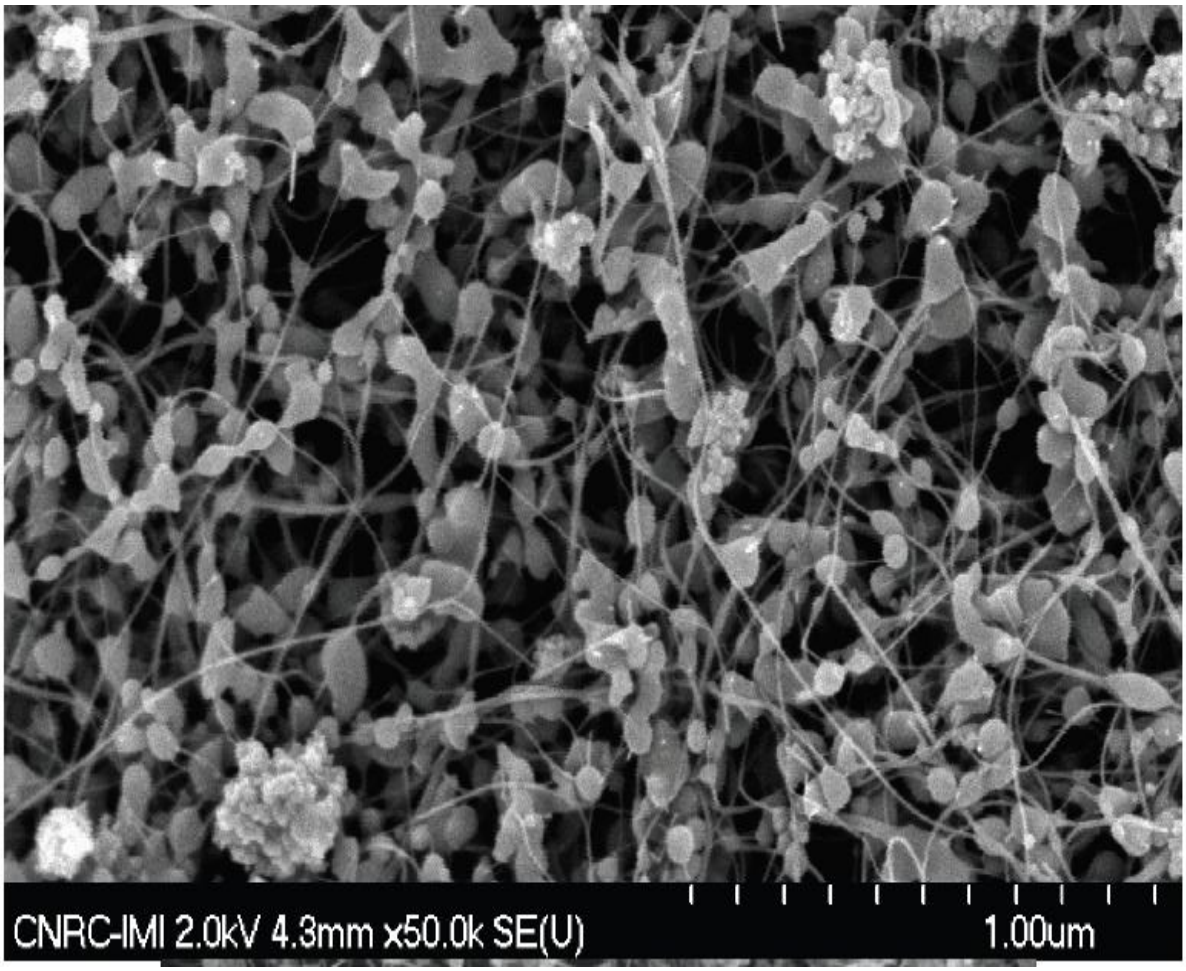

Figure 4.2: Scanning Electron Microscope image of SWCNT.

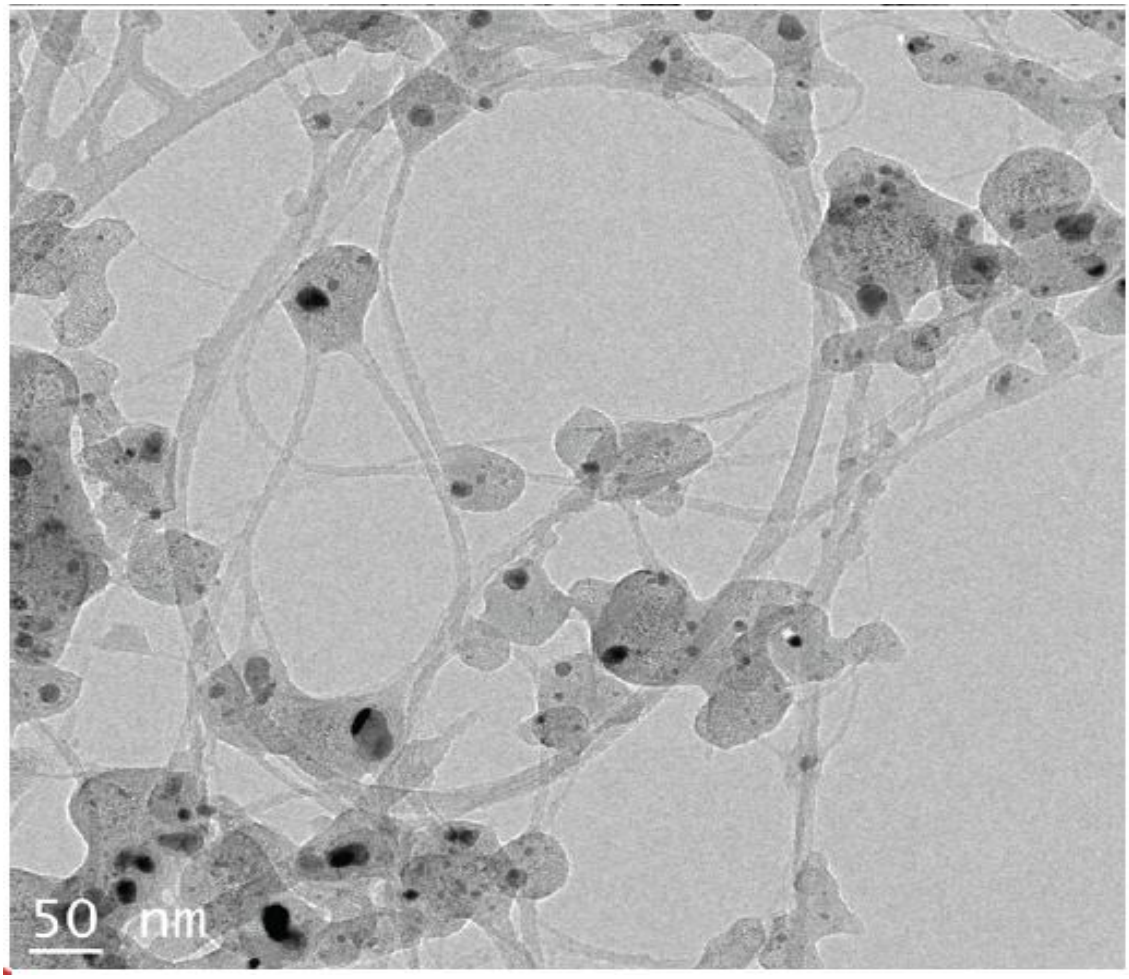

Figure 4.3: Transmission Electron Microscope image of SWCNT.

The nanoparticles received from the company were loosely agglomerated. These particles were firstly crushed manually. Then the amount of nanoparticles is calculated from equation 4.1 for a volume fraction of 1%. The amount comes out to be 25 mg for 20 ml of basefluid. Then the calculated amount of nanoparticles is dispersed in distilled water basefluid by Digital Magnetic Stirrer with hot plate firstly and then by Ultrasonicator. The Magnetic Stirrer and Ultrasonicator are shown in Appendix A1 and A2 respectively. The nanofluid has been sonicated for 2, 4 and 6 hours.

Preparation of Aqueous Silver–H_20 Nanofluid

Viscosity of water based aqueous silver nanofluid is evaluated. The size of silver nanoparticles is 10 nm and the concentration of aqueous silver nanoparticles is 0.1 mg/ml. The aqueous silver nanoparticles are dispersed in distilled water for a volume fraction of 4% and the nanofluid is sonicated for 2, 4 and 6 hours. Then the nanofluid is used for the measurement of viscosity for different parameters.

4.3 Measurement Technique of Viscosity

Viscosity of the sample is measured by the instrument named Brookfield DV III Rheometer (Brookfield DV III Ultra Manual). This rheometer is a cone plate viscometer which is a precise torque meter. The operating principle of rheometer is shown in Figure 4.4.

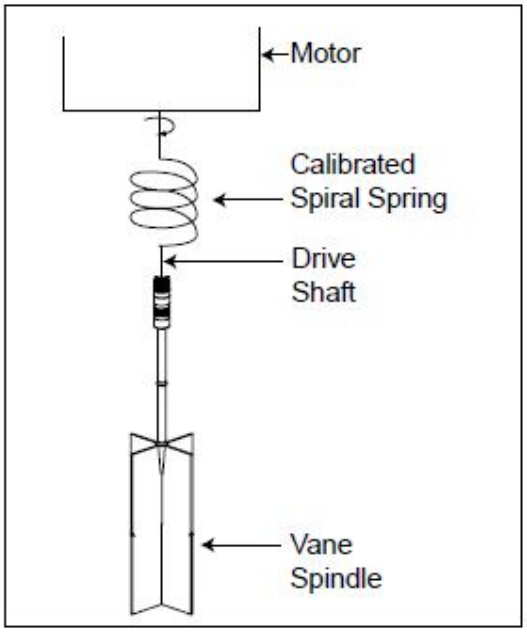

Figure 4.4: Operating principle of Brookfield Viscometer.

This rheometer is driven at discrete rotational speeds. The torque measuring system, which consists of a calibrated beryllium-copper spring connecting the drive mechanism to a rotating cone, senses the resistance to rotation caused by the presence of sample fluid between the cone and a stationary flat plate. The resistance to the rotation of the cone produces a torque that is proportional to the shear stress in the fluid. This reading is easily converted to absolute centipoise units (mPa·s) from precalculated range charts. The stationary plate forms the bottom of a sample cup which can be removed, filled with 0.5 ml to 2.0 ml of sample fluid (depending on cone in use) and remounted without disturbing the calibration. The cone available for the experiments is CPE - 42. The completer set up is shown in Appendix A3 and the cup and cone arrangement is shown in Appendix A4. This cone works with 1 ml of sample fluid. The sample cup is jacketed and has tube fittings in order to connect it to a constant temperature circulating bath. Circulating water bath is used to maintain the temperature of sample in cup. The system is accurate to within ± 1.0% of full scale range. Reproducibility is to within ± 0.2%. Working temperature range is from 0 to 100°C.

4.4 Calibration

In order to check the accuracy of the instrument, it was calibrated by measuring the viscosity of de ionized water at 6 temperature points (15, 20, 25, 30, 35 and 40°C). Standard data of viscosity of de ionized water is taken from Kestin (1978) and a calibration curve is drawn between measured viscosity and expected viscosity. The calibration curve is shown in Figure 4.5. From the calibration curve, a calibration equation is developed. This calibration equation is used in calculating the actual viscosity in further all the experiments.

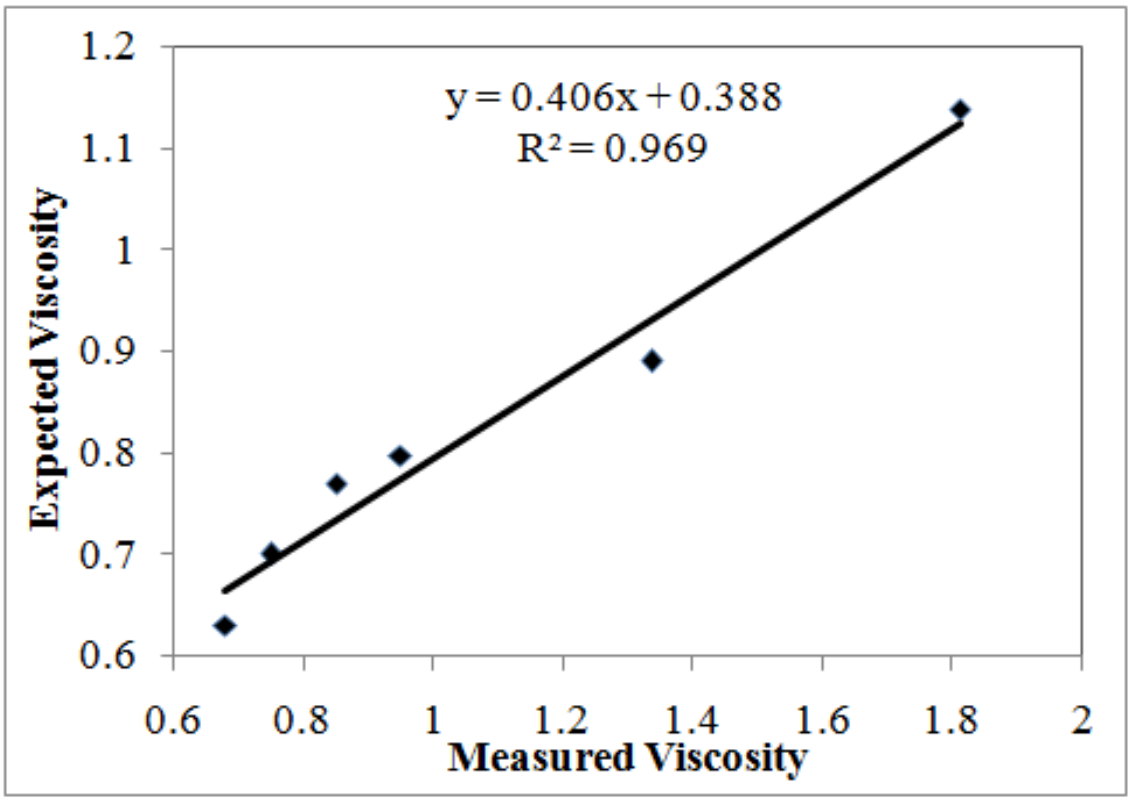

Figure 4.5: Calibration curve for DI water.

4.5 Testing Parameters

Viscosity behavior of the nanofluids has been evaluated by varying certain parameters. These parameters are as follows:

1) Variation of viscosity with temperature
2) Variation of viscosity with sonication time
3) Variation of viscosity with settling time

A nanofluid has to be used at different temperature conditions. Nanofluid has to be operated at high temperature. On the same time, it can be used at low temperature. These operating conditions affect the viscosity of nanofluid. Thus it becomes important to study the effect of

temperature on viscosity of nanofluid. From literature review, it has been found that few researchers have worked on sonication time. The effect of sonication time on viscosity of nanofluid is not evaluated by any researcher. Sonication time may have different effect on the viscosity of different nanofluids. This parameter may become important for the selection of nanofluid for a specific application. Thus the effect of sonication time on viscosity of nanofluid needs to be evaluated. Settling time is another important parameter effecting the viscosity of nanofluid. It may be impossible to use a nanofluid by preparing it on the spot. A nanofluid once prepared may be used after few days. If the viscosity of nanofluid gets affected during that time, then it may affect the use of nanofluid in any application. So it becomes important to study the effect of nanofluid on the viscosity of nanofluid as it is also associated with stability of nanofluid.

For every nanofluid, the temperature of sample is varied by the rheometer and the viscosity of the sample is measured. Sonication time is the time given to the sample in the sonicator so that it may disperse properly. The effect of different sonication times on the viscosity of nanofluid is measured. Settling time is the time given to nanofluid after sonication so as to study the behavior of nanoparticles. After sonication, the nanoparticles are dispersed in basefluid, but slowly the particles starts coming close to each other and start to agglomerate because of their cohesive forces. The size of particle increases because of this agglomeration. This increase in size makes the particle to settle down. The viscosity of this nanofluid is measured after giving it a specific time to settle down. The time for which the particles are allowed to settle down is called settling time. During settling time, the nanofluid is kept idle and no reading is taken in between that duration. After a specific time, the viscosity of nanofluid is measured and the effect of settling is evaluated.

4.6 Experimental Results

Experimental results of the variation of viscosity for different nanofluid with different parameters are discussed here. The results are as follows:

1) ZnO-H_2O Nanofluid

In Figure 4.6, the variation of viscosity with temperature for ZnO nanoparticles dispersed in distilled water is presented. The variation of viscosity is shown for the two sizes (14 and 25 nm) and 0.01% volume fraction. Figure 4.6 shows that the viscosity of nanofluid decreases with the increase in temperature. Viscosity in a fluid is because of cohesive forces and momentum transfer. In liquid, the cohesive forces of particles are more than that of momentum transfer. When the temperature of nanofluid is increased, the cohesive force of particles decreases and hence the viscosity of nanofluid decreases.

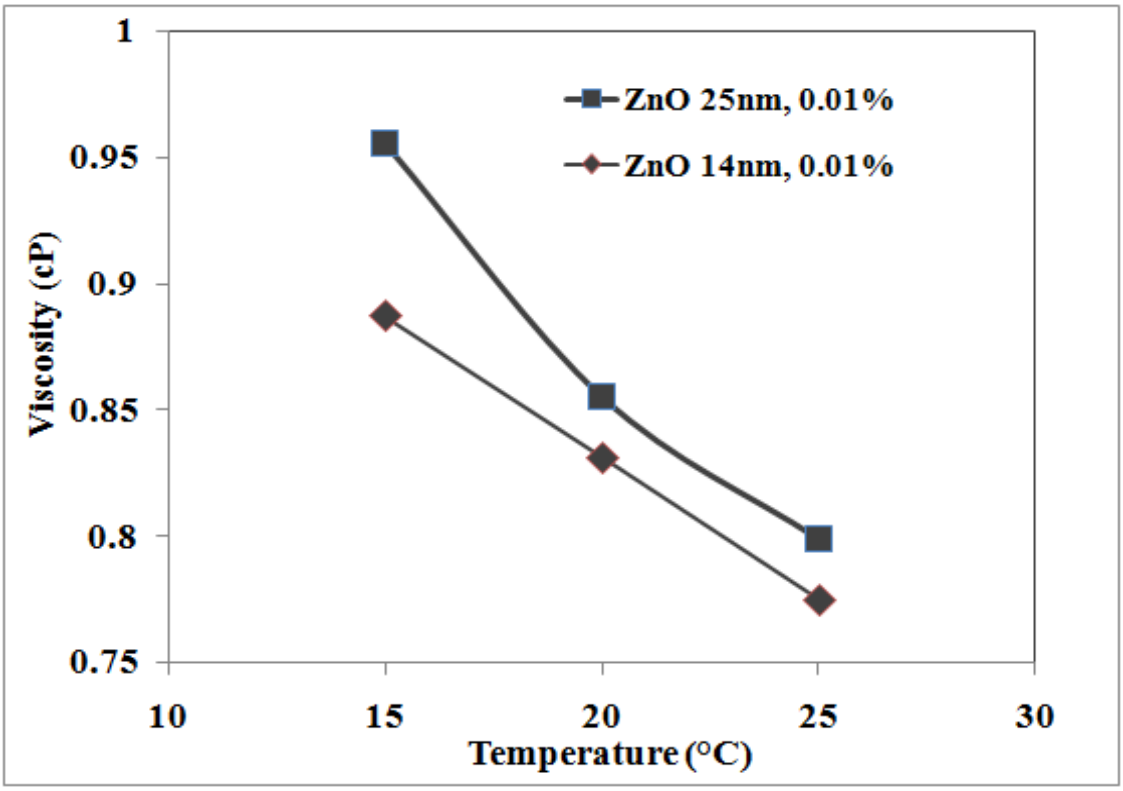

Figure 4.6: Variation of viscosity with temperature for ZnO-H_2O nanofluid.

The viscosity of nanofluid with smaller sized nanoparticles (14 nm) is found to be less than that of larger sized nanoparticles (25 nm). From Figure 4.6, it is clear that the larger size nanoparticles are agglomerating to a greater extent which leads to increase in the viscosity of nanofluid.

Variation of viscosity is measured for 4 sonication times. These four sonication durations are:

1) 0 hour sonication.
2) 2 hour sonication
3) 4 hour sonication
4) 6 hour sonication

Four samples of nanofluid are prepared. Viscosity of first sample is measured directly without sonicating it. This sample will give the viscosity of sample with zero hour sonication. Then

other samples are sonicated for 2, 4 and 6 hours so that the viscosity of nanofluid with sonication time can be measured. In order to evaluate the viscosity of nanofluid, firstly the variation of shear stress with shear rate is evaluated. This variation is used to evaluate the behavior of nanofluid. Figure 4.7 shows the variation of shear stress with shear rate for 14 nm size at a volume fraction of 0.01%, for the above mentioned sonication time.

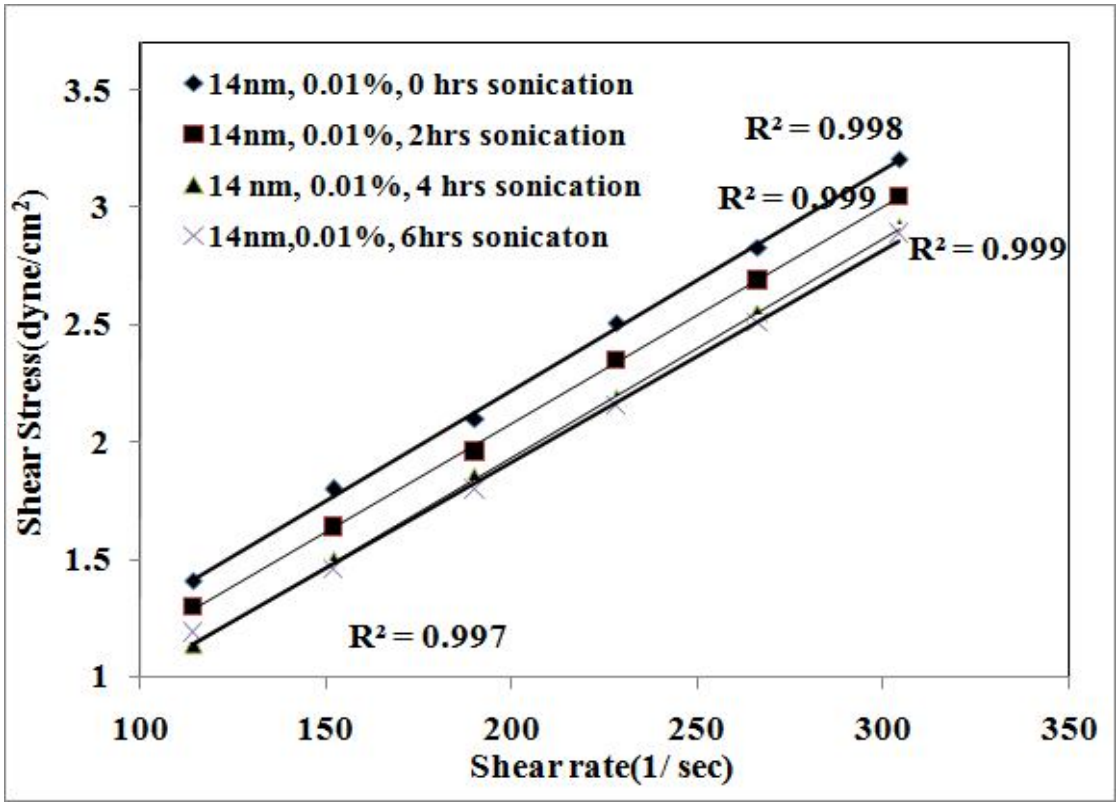

Figure 4.7: Shear stress versus shear rate for 14 nm, 0.01% volume fraction at different sonication time.

Linear trend line is plotted for each sonication time with R^2 more than 0.99. Figure 4.7 shows a linear relation between shear stress and shear rate. Thus nanofluid is showing Newtonian behavior. With the increase in sonication time of nanofluid, shear stress is decreasing for corresponding values of shear rate.

Figure 4.8 shows the variation between shear stress and shear rate for 25 nm size ZnO- water nanofluid at 0.01% volume fraction for all the sonication times.

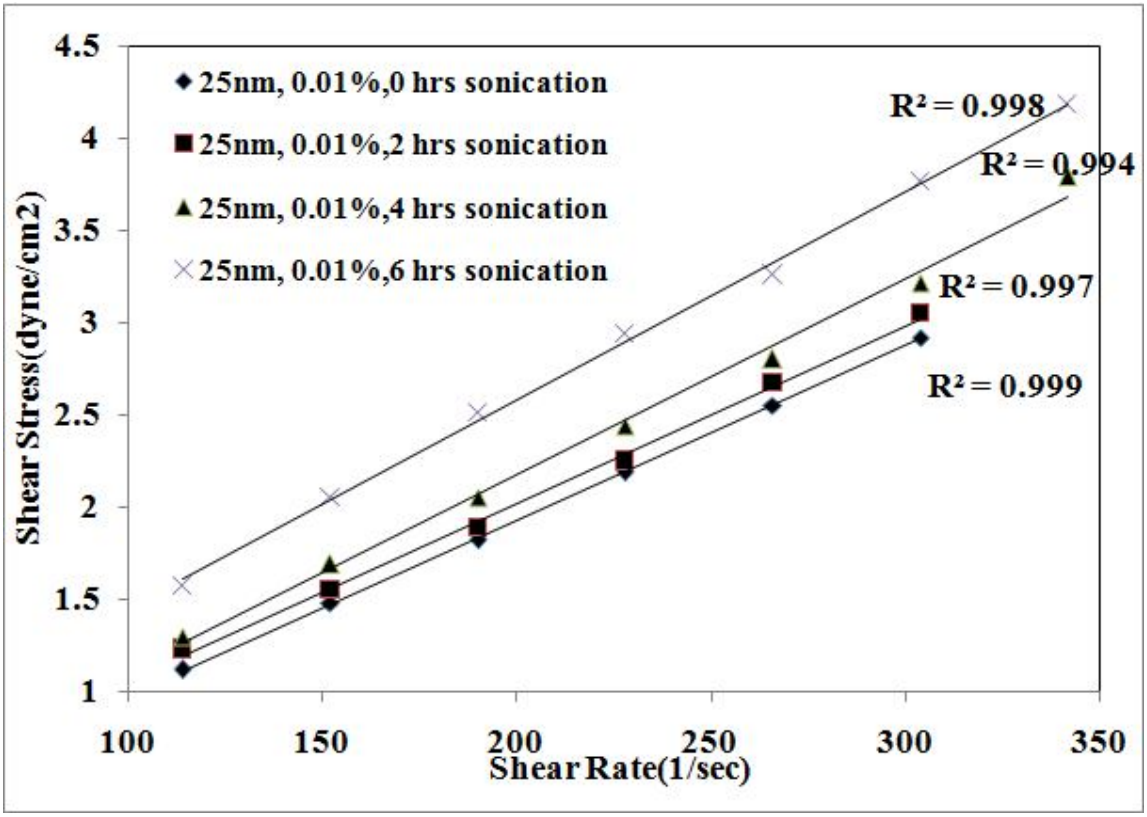

Figure 4.8: Variation of shear stress with shear rate for 25 nm size ZnO-water at 0.01% volume fraction for various sonication times.

Again a linear relation is noted between shear stress and shear rate. This linear trend indicates that the nanofluid is behaving like a Newtonian fluid. Similar trends are noted for 14 nm, 25 nm sizes ZnO- water nanofluid for 0.05% volume fraction and are shown in Appendix A5 and A6.

Figure 4.9 shows the variation in viscosity of water based ZnO nanofluid with sonication time for nanoparticles size of 14 nm and 25 nm at a volume fraction of 0.01% and 0.05%.

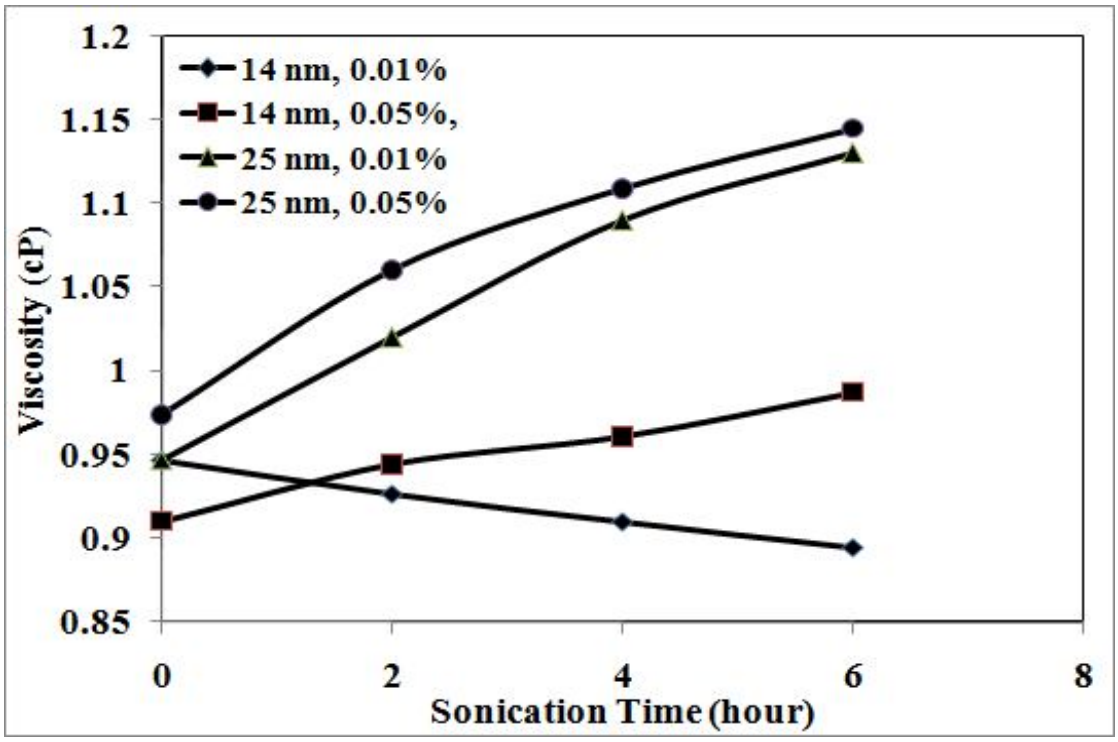

Figure 4.9: Viscosity versus sonication time for ZnO-water nanofluid for various sonication timings.

In Figure 4.9, it is evaluated that for 14 nm ZnO nanofluid, at a volume fraction of 0.01%, viscosity decreases with increase in sonication time. Viscosity of 14 nm ZnO nanofluid, at a volume fraction of 0.05%, increases with increase in sonication time. Similar pattern is obtained for 25 nm ZnO nanofluid at volume fraction of 0.01% and 0.05%. It is also evaluated that with the increase in size and volume fraction of nanofluid, viscosity of nanofluid is increasing. With the increase in size and volume fraction, the particles are not getting dispersed with the increase in sonication time and hence the viscosity of nanofluid is increasing.

Variation of viscosity is evaluated for four settling times. These timing are as follows:

1) 0 hour settling

2) 2 hour settling

3) 4 hour settling

4) 6 hour settling

In order to evaluate viscosity of nanofluid, sample is sonicated for 8 hours. Shear stress and shear rate is noted for each settling time and graph is drawn between shear stress and shear rate to evaluate the viscosity behavior of nanofluid.

Figure 4.10 shows the variation of shear stress with shear rate for 14 nm ZnO nanofluid at a volume fraction of 0.01% at various settling time.

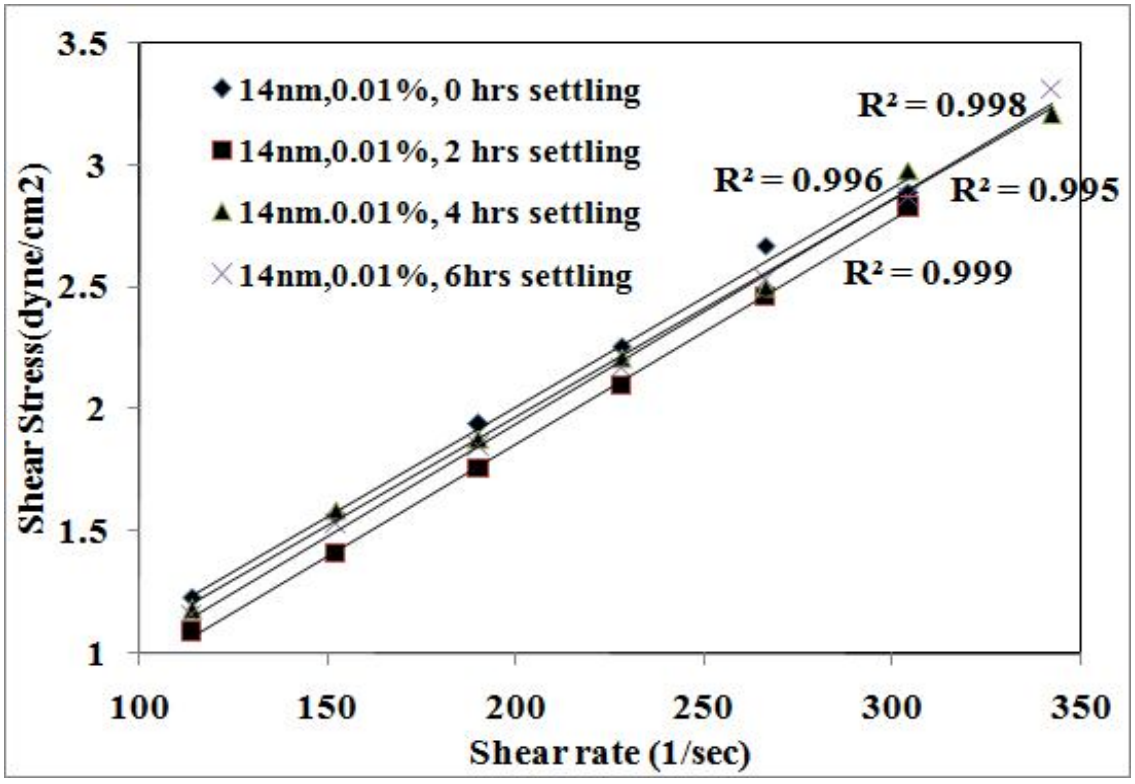

Figure 4.10: Shear stress versus shear rate for 14 nm ZnO - water nanofluid, at volume fraction of 0.01% for various settling times.

It is found that shear stress is varying linearly with shear rate that is the nanofluid is showing Newtonian behavior. Thus viscosity for various settling time can also be evaluated by calculating the slope of the line. Similar trends are noted for 14 nm ZnO-water at 0.05% volume fraction and 25 nm ZnO-water at 0.01% and 0.05% volume fractions and are shown in Appendix A7, A8 and A9.

Figure 4.11 shows the variation of viscosity of water based ZnO nanofluid with sonication time for the nanoparticles size of 14nm and 25nm and for a volume fraction of 0.01 and 0.05%

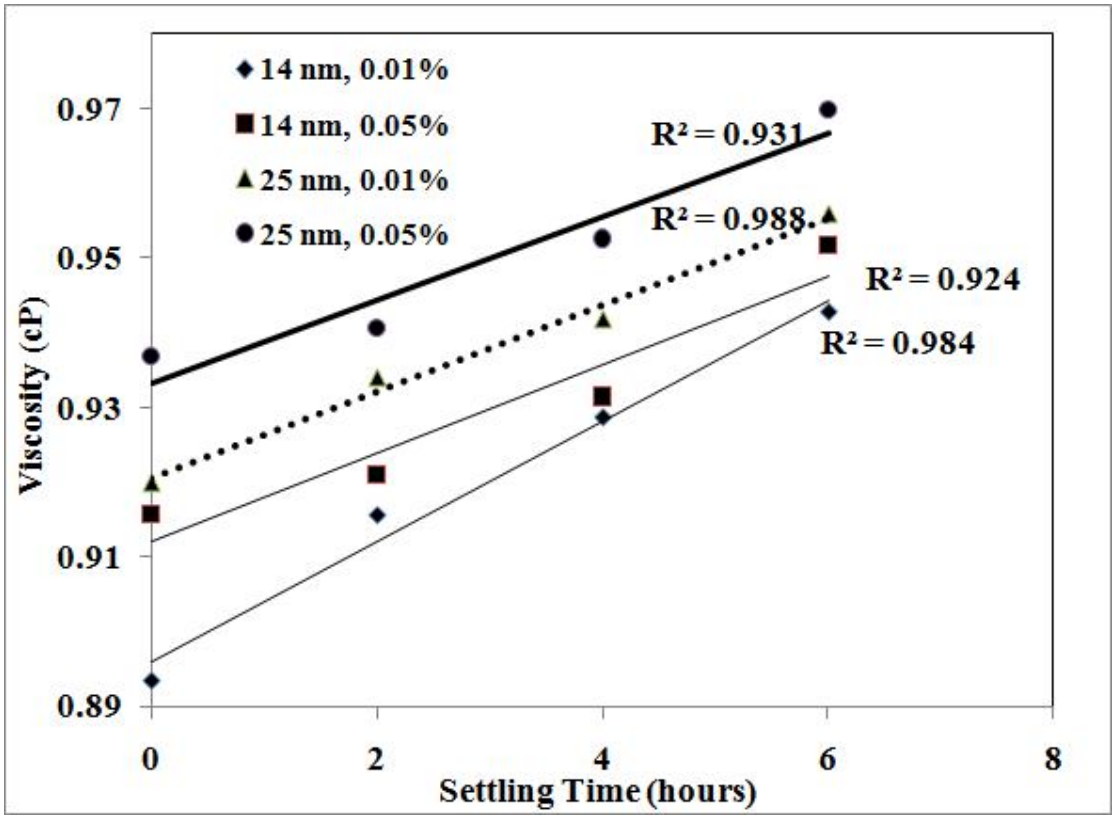

Figure 4.11: Variation of viscosity with settling time for ZnO-H_2O nanofluid

From Figure 4.11, it is found that with the increase in settling time, viscosity of nanofluid increases. As the nanoparticles in the base fluid is allowed to settle down, the nanoparticles

starts agglomerating. This agglomeration leads to the formation of clusters of nanoparticles in nanofluid. This clustering increases the viscosity of nanofluid. There is an increase in viscosity with the increase in volume fraction and size of nanoparticles. Increase in volume fraction leads to the increase in the amount of particles in the given volume of fluid. This makes the particles to come close to each other and after that the cohesive force comes in to play and the particles starts agglomerating. Maximum viscosity is evaluated at 0.05% volume fraction for 25 nm nanofluid.

2) ZnO-EG Nanofluid

Figure 4.12 shows the variation of viscosity of ethylene glycol based ZnO nanofluid with temperature for nanoparticles size of 14 nm and 25 nm and a volume fraction of 0.01% of nanoparticles.

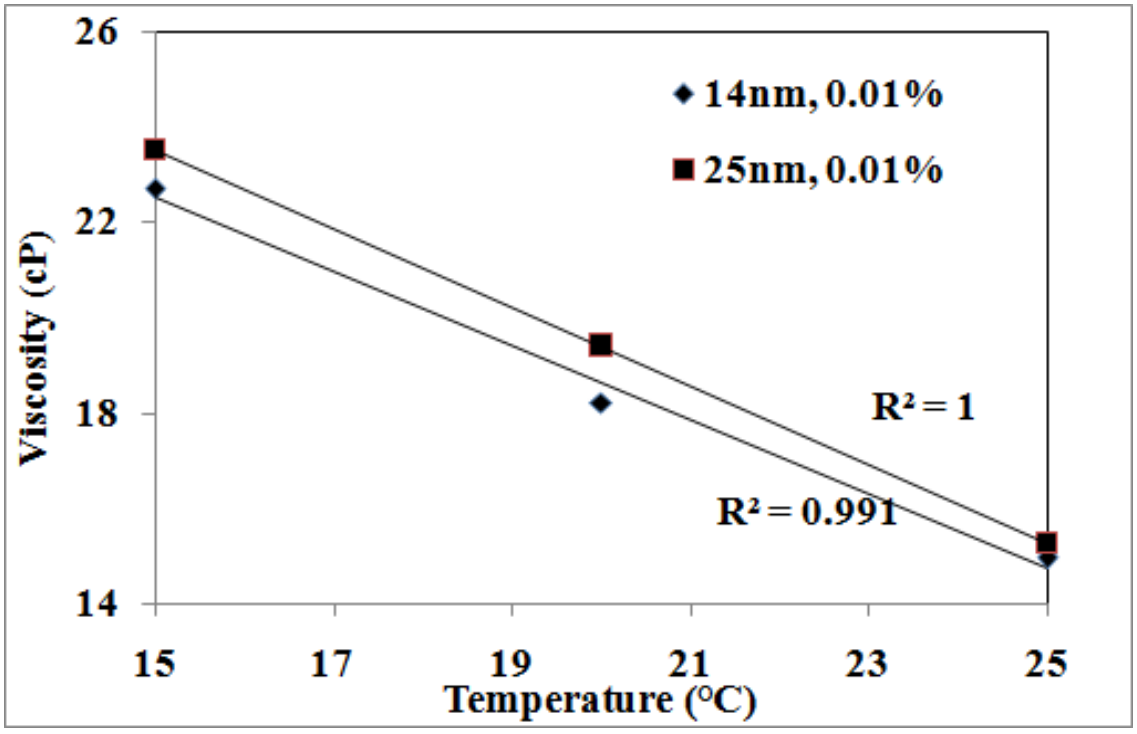

Figure 4.12: Variation of viscosity of ethylene glycol based ZnO nanofluid with temperature.

The temperature of the nanofluid is varied from 15 to 25˚C and the behavior of the nanofluid is noted. It is found that with the increase in temperature, the viscosity of nanofluid decreases continuously. Increase in temperature makes the molecules of fluids loosely bonded. These loosely bonded molecules have less cohesive forces, which decreases the viscosity of fluid. The viscosity of nanofluid of 25 nm sized nanoparticles is found to be greater than the viscosity of 14 nm sized nanofluid. Increase in size of nanoparticles makes the particles to stay close to each other which again make the particles to agglomerate and increase the viscosity of nanofluid. Figure 4.13 shows the variation of shear stress with shear rate for ethylene glycol based ZnO nanofluid for a volume fraction of 0.01% for different hours of sonication.

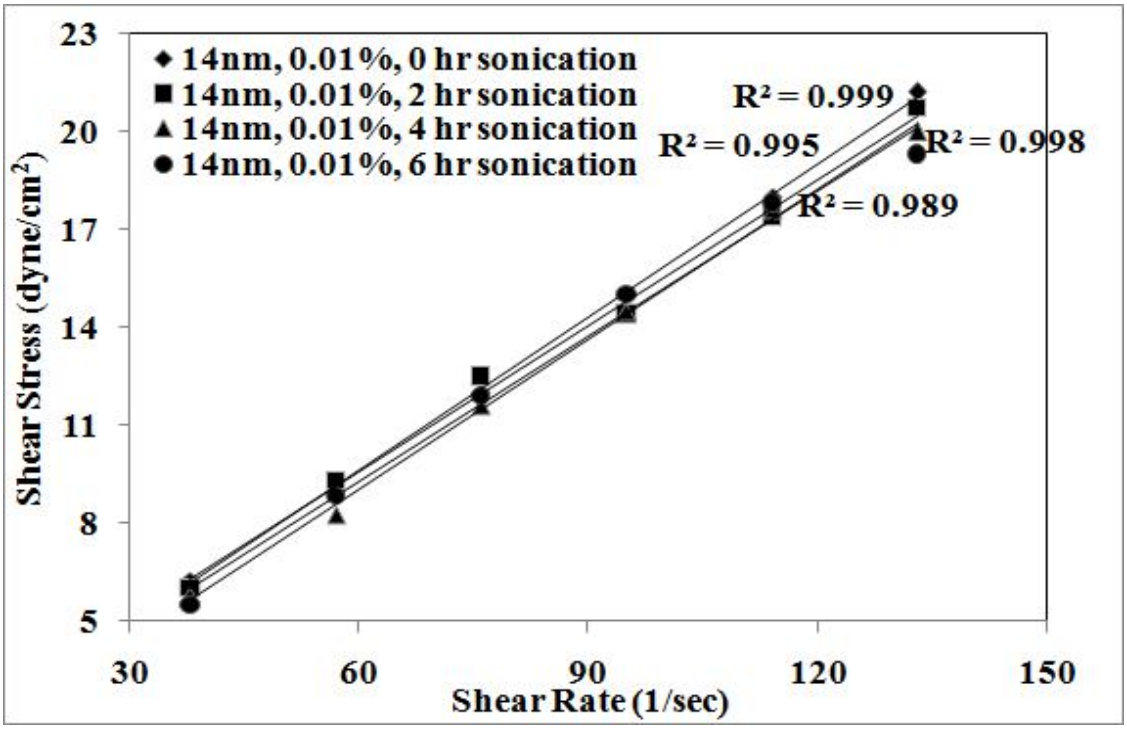

Figure 4.13: Shear stress versus shear rate for 14 nm sized ZnO based ethylene glycol nanofluid for different sonication times.

In order to notify the behavior of nanofluid, a curve is plotted between shear stress and shear

rate. From Figure 4.13, it is found that the shear stress is varying linearly with shear rate. A linear trend line is plotted for all the sonication timings. The linear trend line shows that the nanofluid is behaving like Newtonian fluid. Similar curves are obtained for different nanofluids and are shown in Figure 4.14, 4.15 and 4.16.

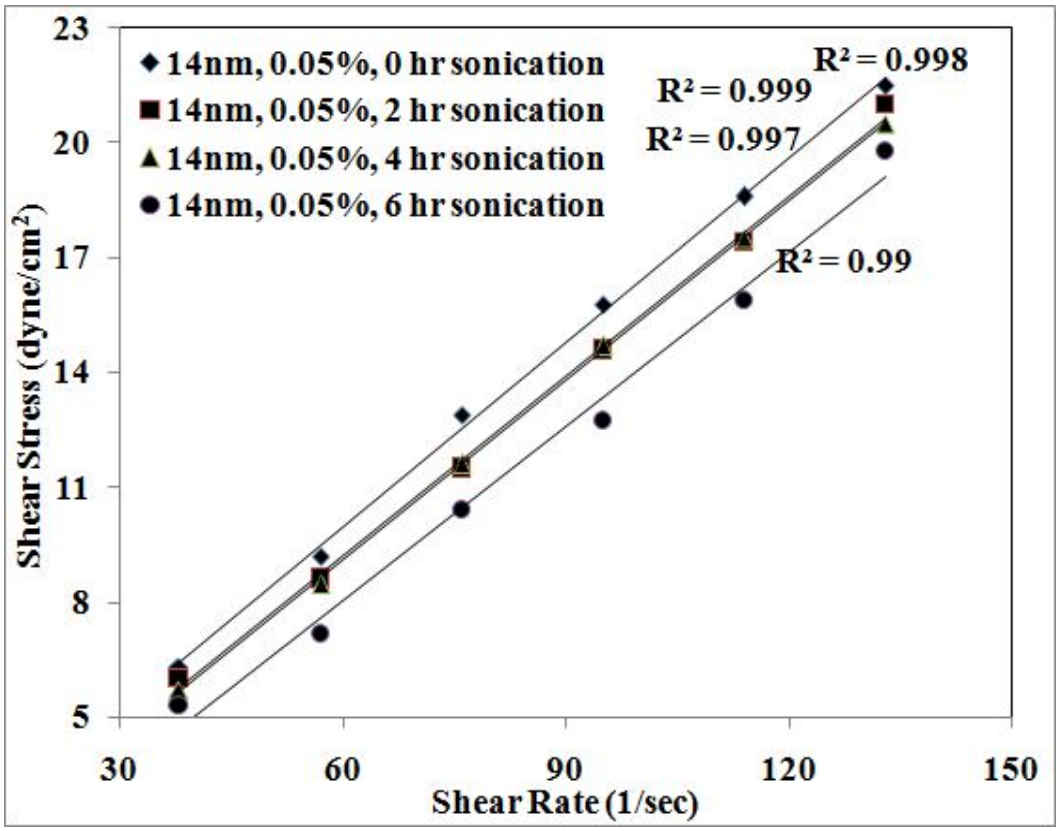

Figure 4.14: Shear stress versus shear rate for 14 nm sized ZnO based ethylene glycol nanofluid at a volume fraction of 0.05% for different sonication timings.

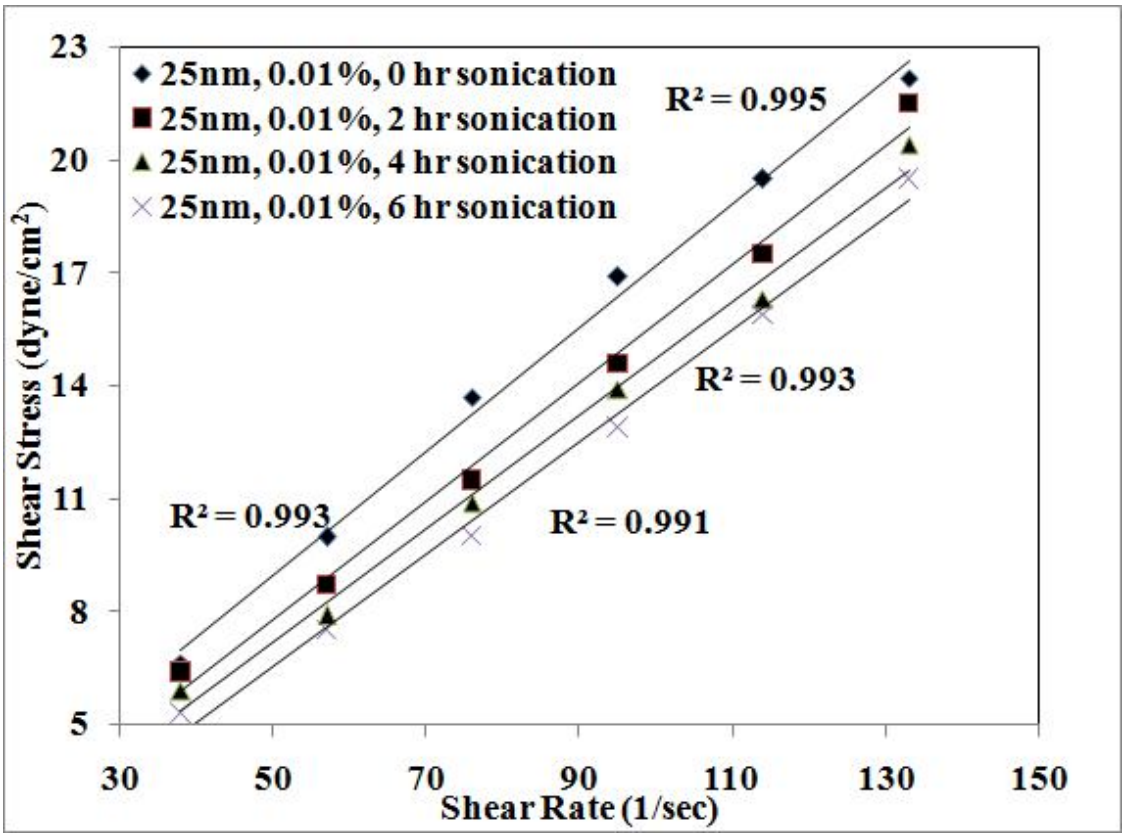

Figure 4.15: Shear stress versus shear rate for 25 nm sized ZnO based ethylene glycol nanofluid at a volume fraction of 0.01%.

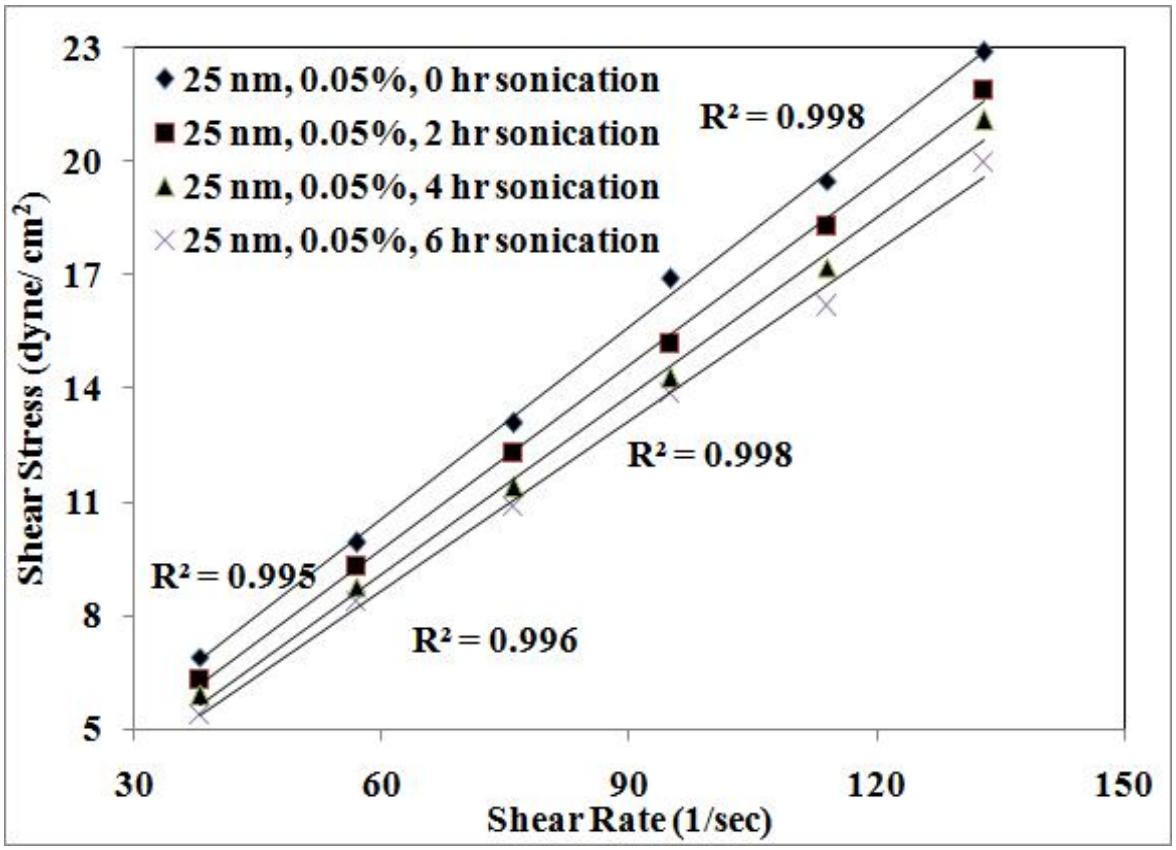

Figure 4.16: Shear stress versus shear rate for 25 nm sized ZnO based ethylene glycol nanofluid at a volume fraction of 0.05% for different sonication timings.

Figure 4.17 shows the variation of viscosity of ethylene glycol based ZnO nanofluid with sonication time for the nanoparticles size of 14nm and 25nm and for a volume fraction of 0.01 and 0.05%

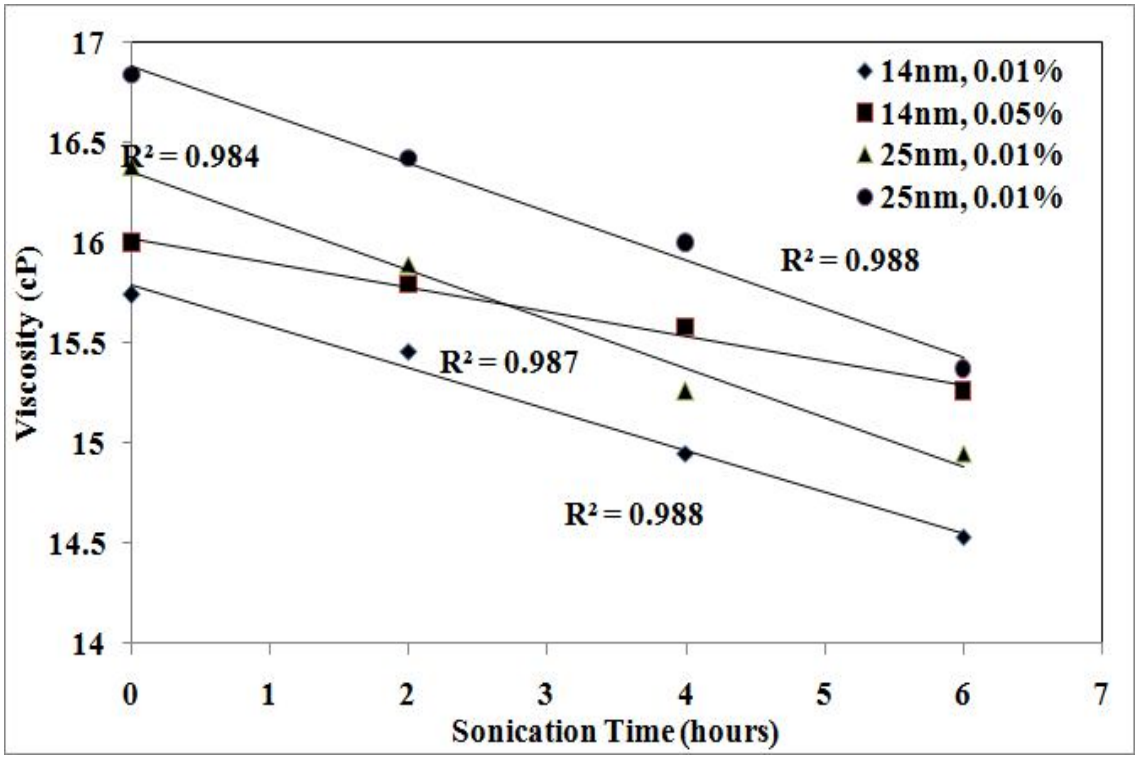

Figure 4.17: Variation of viscosity of ethylene glycol based ZnO nanofluid with sonication time.

In Figure 4.17, it is found that there is a decrease in viscosity of nanofluid with the increase in the sonication time. The decrease in viscosity with the sonication time is because of the reason that the nanoparticles disperse in the basefluid to a better extent as the sonication time increases. Also it is found that with the increase in the size of nanoparticles, there is an increase in the viscosity of nanofluid. Moreover, the increase in volume fraction of nanofluid also increases the viscosity of nanofluid. The minimum viscosity of nanofluid is obtained for 6 hours of sonication. There is a very small decrement in viscosity of nanofluid for a particle size of 14 nm and volume fraction of 0.05% whereas the nanofluid with 25 nm size particles and volume fraction of 0.01% has a very sharp decrease in viscosity.

Figure 4.18 shows the variation of shear stress with shear rate for 14 nm sized ZnO based

ethylene glycol nanofluid at a volume fraction of 0.01% for different settling hours.

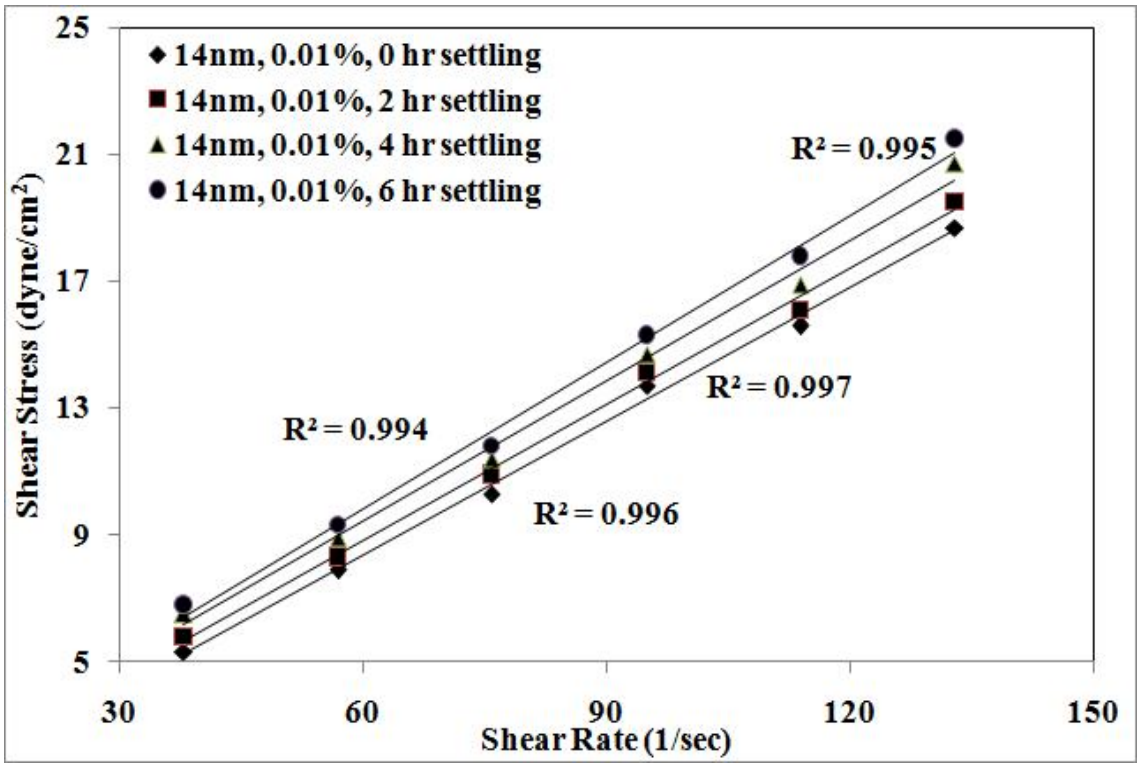

Figure 4.18: Shear stress versus shear rate for 14 nm sized ZnO based ethylene glycol nanofluid at a volume fraction of 0.01% for different hours of settling.

In order to measure the behavior of nanofluid with setting time, a curve is plotted between shear stress and shear rate. It is found that for the shear rate given to nanofluid, the shear stress is varying linearly. This linear behavior shows the Newtonian behavior of nanofluid even after 6 hours of settling. Similar curves are plotted for different nanofluids and are shown in Figure 4.19, 4.20 and 4.21.

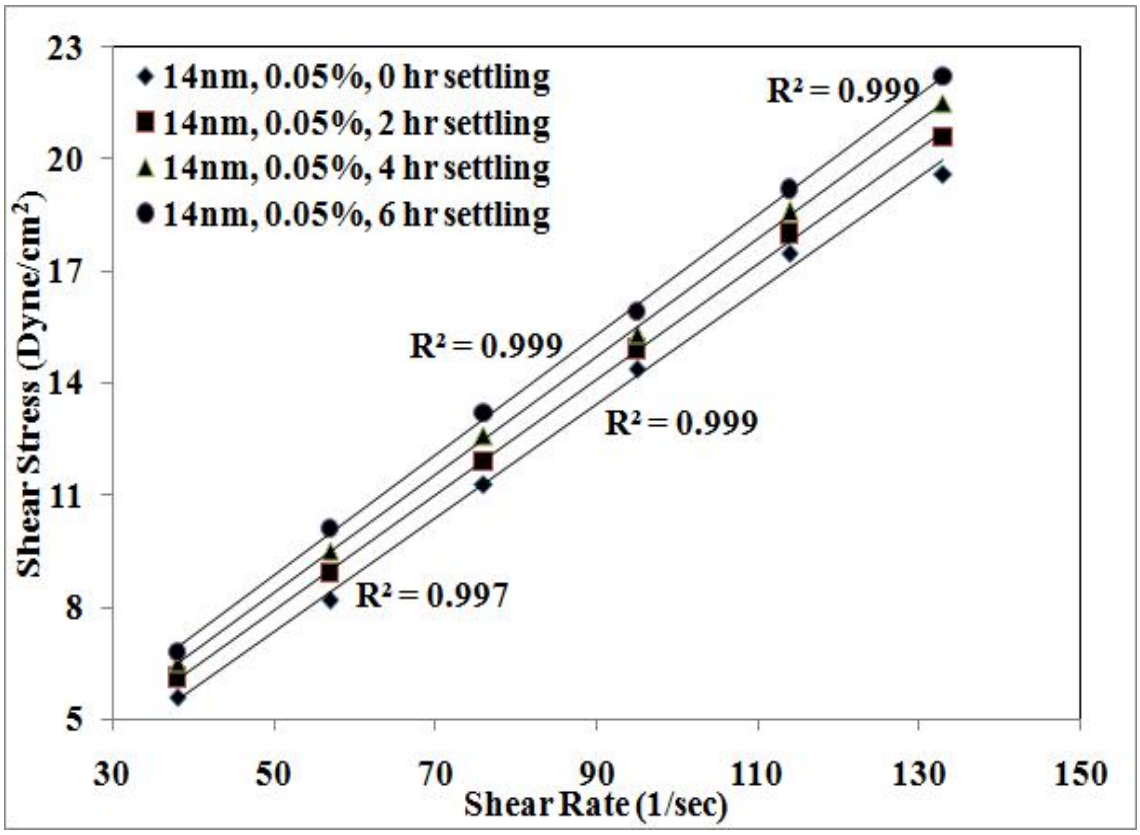

Figure 4.19: Shear stress versus shear rate for 14 nm sized ZnO based ethylene glycol nanofluid at a volume fraction of 0.05% for different hours of settling.

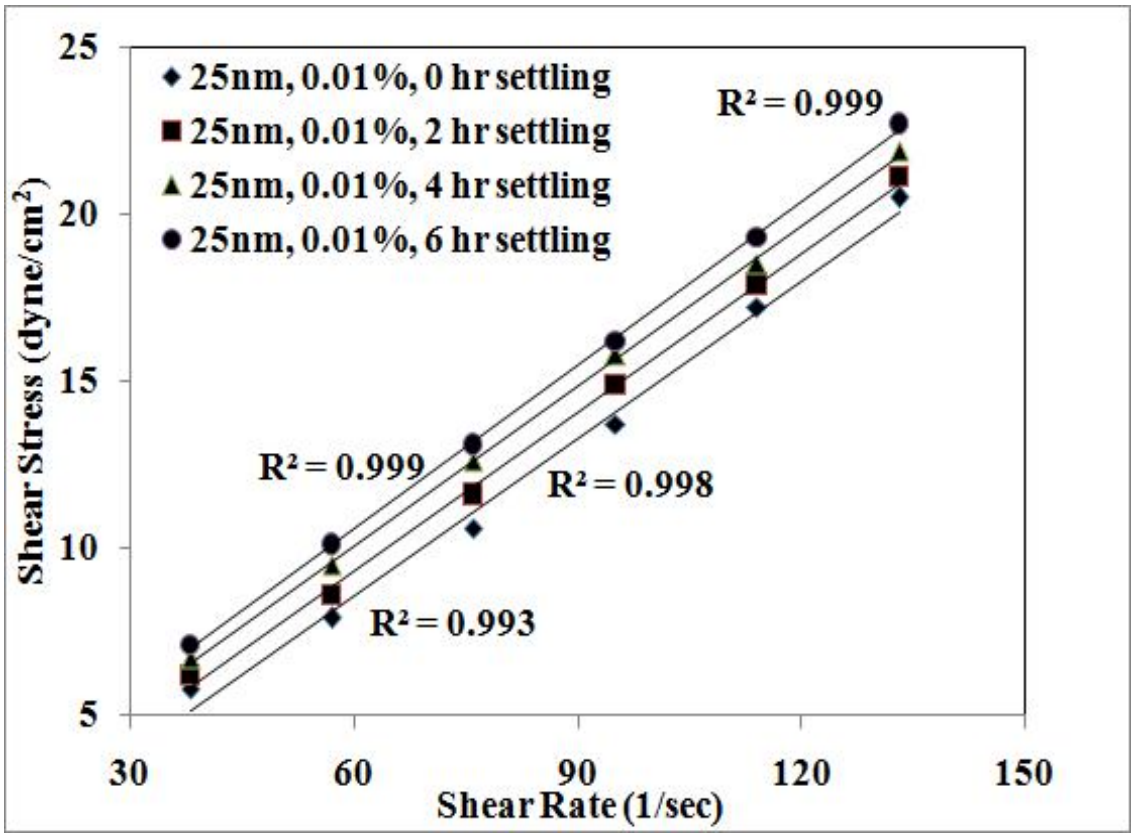

Figure 4.20: Shear stress versus shear rate for 25 nm sized ZnO based ethylene glycol nanofluid, at a volume fraction of 0.01% for different hours of settling.

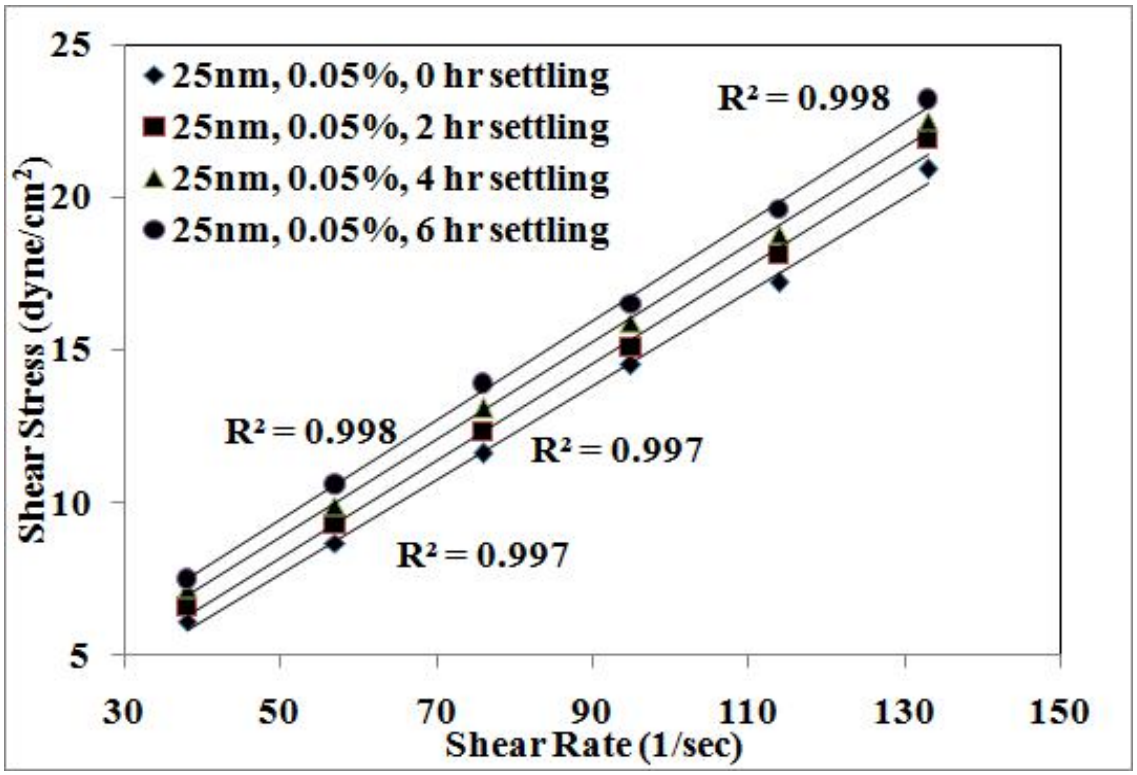

Figure 4.21: Shear stress versus shear rate for 25nm sized ZnO based ethylene glycol nanofluid at a volume fraction of 0.05% for different hours of settling.

Figure 4.22 shows the variation of viscosity of ethylene glycol based ZnO nanofluid with settling time for a particle size of 14 and 25 nm and a volume fraction of 0.01 and 0.05%.

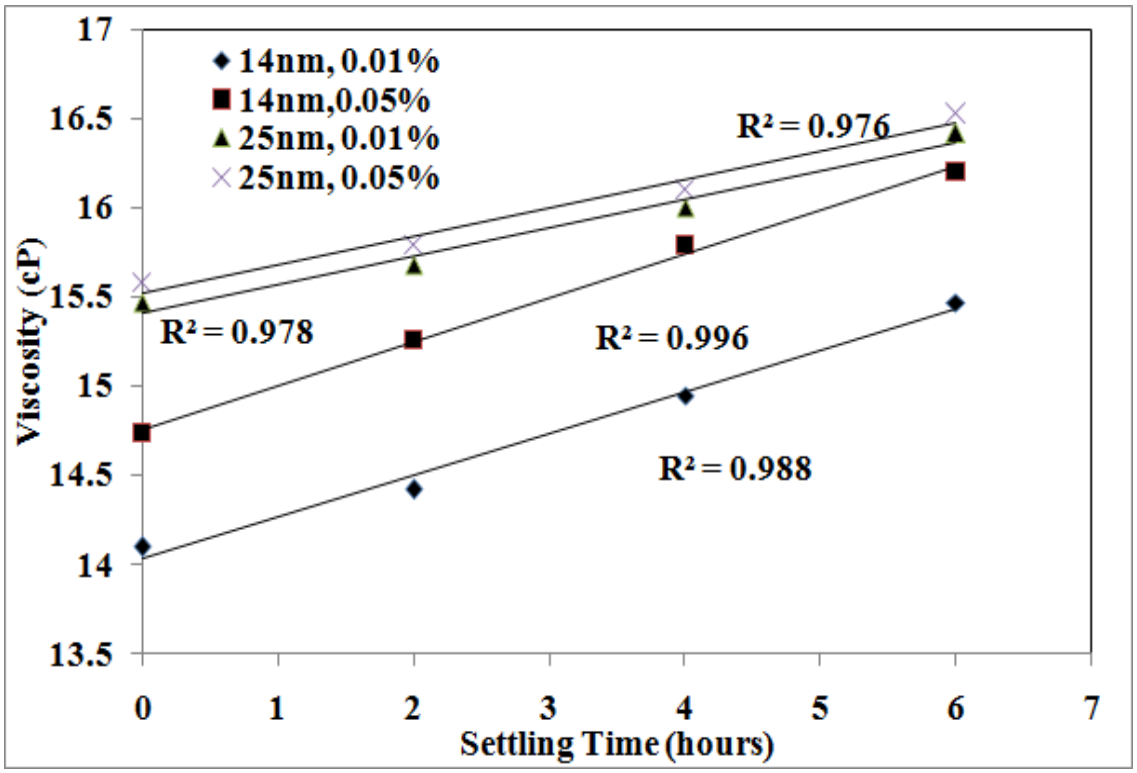

Figure 4.22: Variation of viscosity of ethylene glycol based ZnO nanofluid with settling time.

In order to check the behavior of viscosity of nanofluid with settling time, the nanofluid is sonicated for 8 hours first and then the particles of nanofluid is allowed to settle down. From Figure 4.22, it is found that the viscosity of nanofluid increases with the settling time. Also with the increase in size and volume fraction of nanofluid, there is an increase in the viscosity of nanofluid. The results obtained from Figure 4.22 shows that the particles in the nanofluid start agglomerating as the nanofluid is allowed to settle down. This agglomeration increases the viscosity of nanofluid.

3) SWCNT-H_2O Nanofluid

Figure 4.23 shows the variation of viscosity of water based single walled carbon nanotube

nanofluid for a volume fraction of 1% of nanoparticles with temperature.

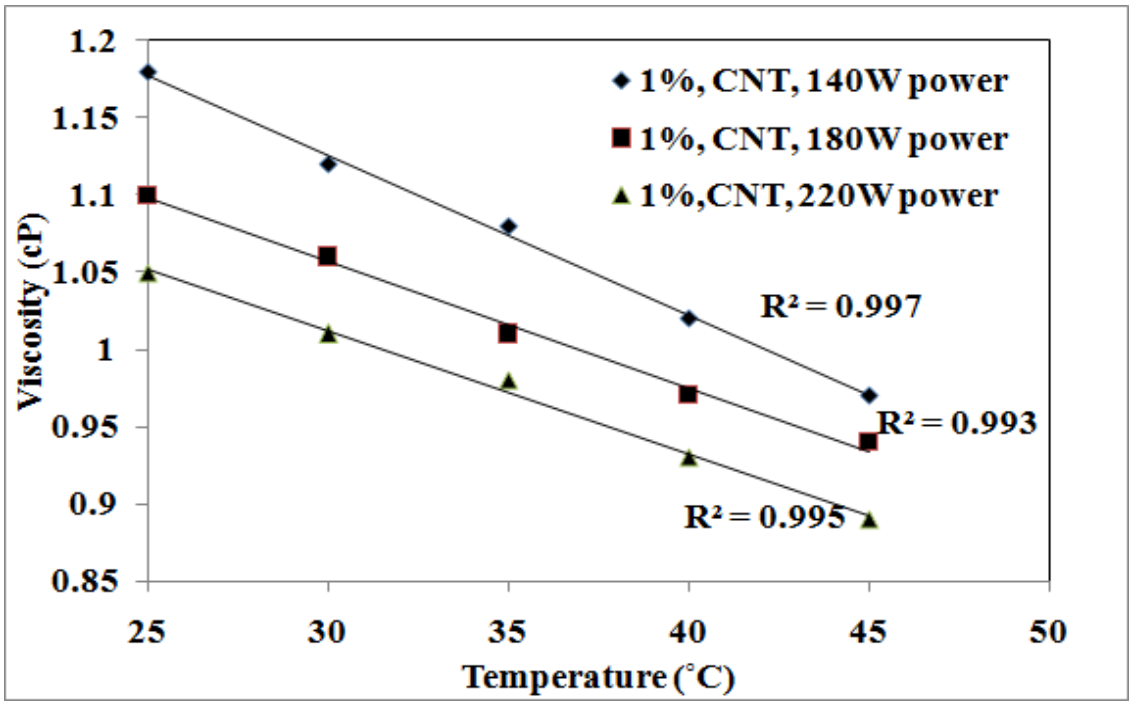

Figure 4.23: Variation of viscosity of water based single walled carbon nanotube nanofluid with temperature.

In Figure 4.23, it is found that the viscosity of the nanofluid decreases with the increase in the temperature of nanofluid. Viscosity of nanofluid is measured for a temperature range of 25 to 45˚C. Nanofluids are found to have higher viscosity at 25˚C and less viscosity at 45˚C because of the decrease in the cohesive forces of fluid. It is found that the nanofluid sample which is sonicated for higher power has lesser viscosity in comparison with the sample sonicated with lesser power. In Figure 4.23, there are 3 samples of nanofluid sonicated with 140 W, 180 W and 220 W. The sample sonicated with 220 W of power has least viscosity and the sample sonicated with 140 W of power. The higher power of sonication makes the particles disperse in the fluid to a greater extent than that of lesser power of sonication.

Figure 4.24 shows the variation of viscosity of single walled carbon nanotube based water nanofluid for 1% volume fraction of nanoparticles at a temperature of 25˚C with the sonication time for different powers of sonication.

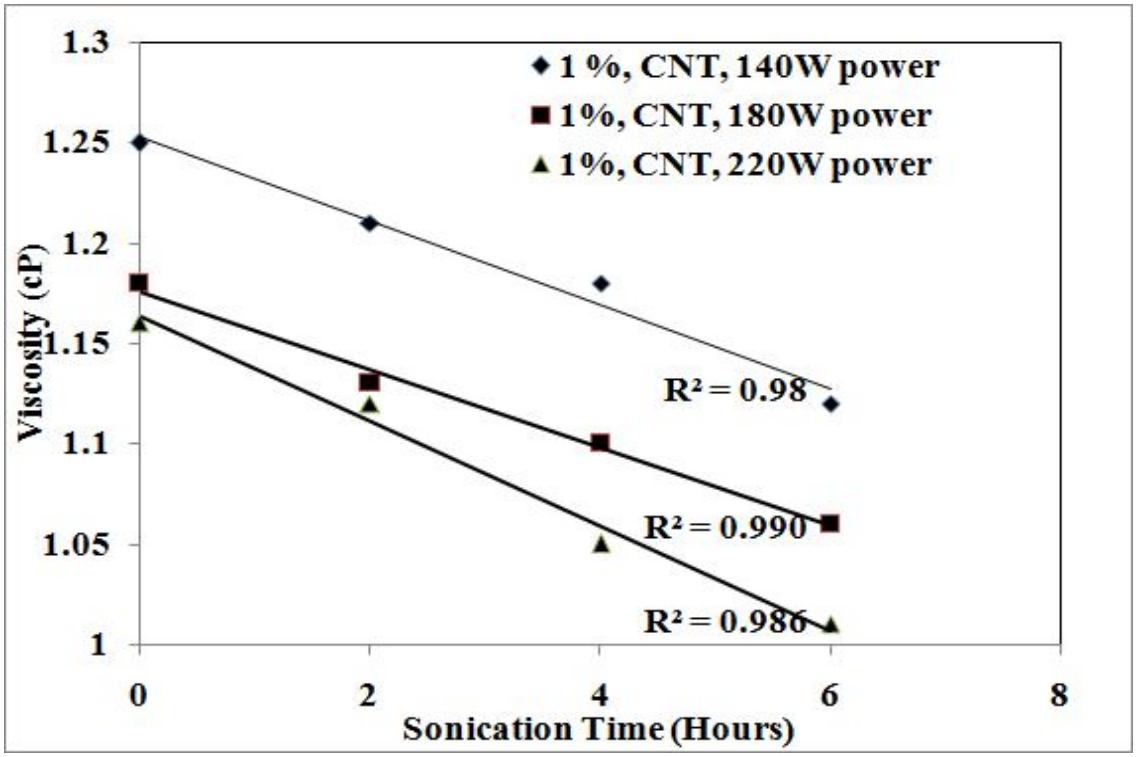

Figure 4.24: Variation of viscosity of water based single walled carbon nanotube nanofluids with sonication time.

In Figure 4.24, it is found that with the increase in sonication time, there is a gradual decrease in the viscosity of SWCNT based nanofluid. As the sonication time increases, the particles start separating from each other and avoid the clustering effect and decrease the viscosity of nanofluid. There is a decrease in the viscosity of nanofluid with the increase in power of sonication. The minimum viscosity of nanofluid is obtained for the power of 220 W and for a sonication time of 6 hours.

Figure 4.25 shows the variation of viscosity of SWCNT based water nanofluid for a volume fraction of 1 % of nanoparticles with settling time.

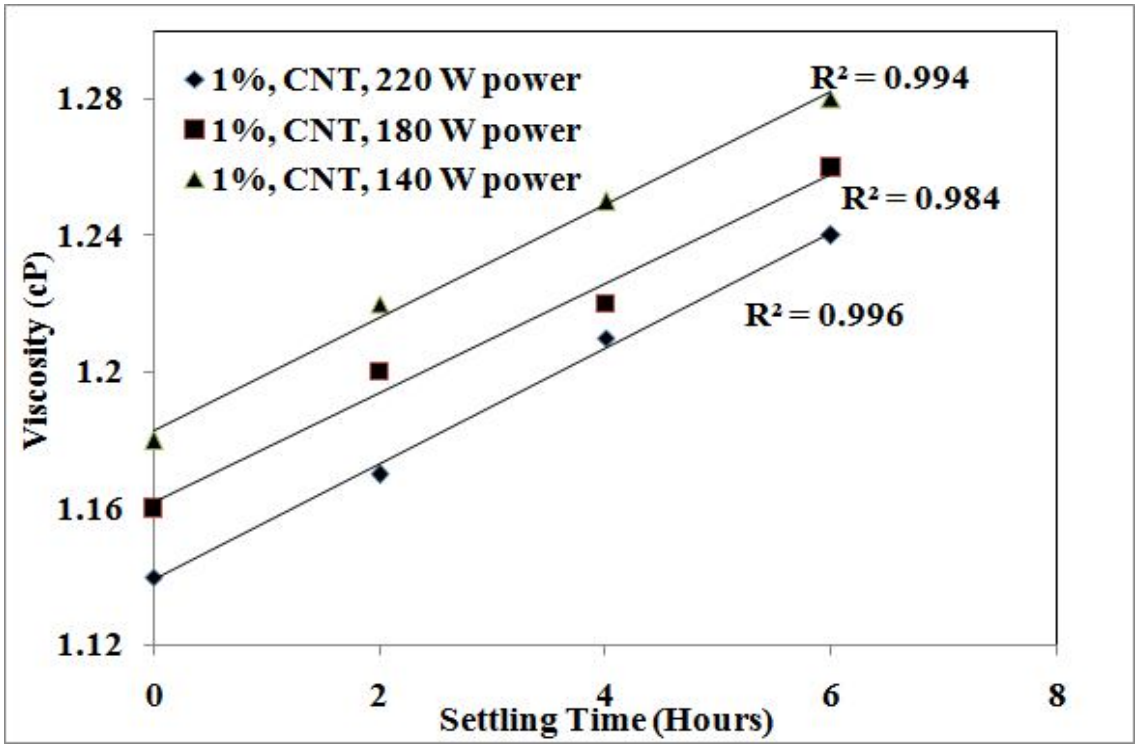

Figure 4.25: Variation of viscosity of water based single walled carbon nanotube nanofluid with settling time.

Before checking the behavior of nanofluid with settling time, the nanofluid is sonicated for 8 hours and then nanoparticles in the nanofluid are allowed to settle down. The same procedure is done for three different powers of sonication. From Figure 4.25, it is found that as the settling time of the nanofluid is increased, there is an increase in the viscosity of nanofluids. This indicates that the particles in the nanofluid start to agglomerate as they are allowed to settle down. Also for the nanofluids sonicated with larger power, there is comparatively less increase in its viscosity.

4) Aqueous Silver- H_2O Nanofluid

Figure 4.26 shows the variation of viscosity of water based aqueous silver nanofluid with the temperature at a volume fraction of 4%.

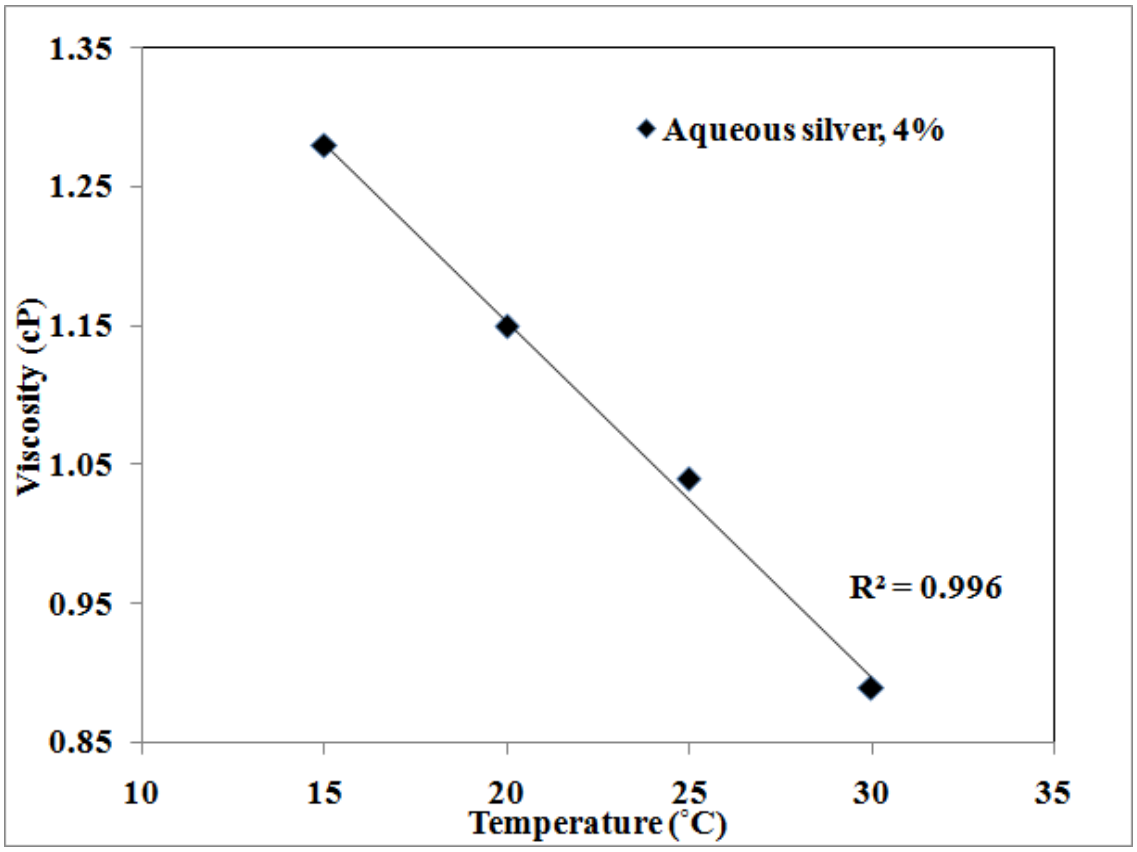

Figure 4.26: Variation of viscosity of water based aqueous silver nanofluid with temperature.

From Figure 4.26, it is found that the viscosity of nanofluid decreases with the increase in temperature. The viscosity of nanofluid is measured in a range of 15 to 30˚C. The viscosity of nanofluid is found to be higher at a temperature of 15˚C and less at a temperature of 30˚C. This decrease in viscosity of nanofluid follows the similar trend as was obtained for all the other nanofluids.

Figure 4.27 shows the variation of viscosity of water based aqueous silver nanofluid with sonication time at a volume fraction of 4%.

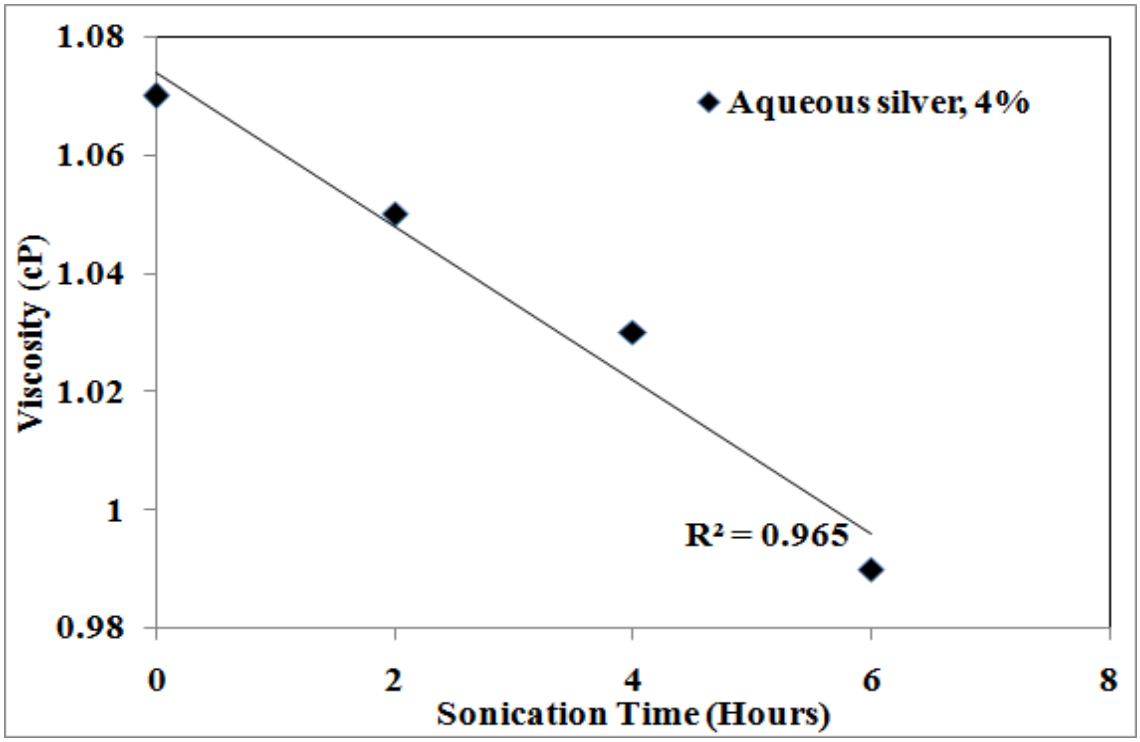

Figure 4.27: Variation of viscosity of water based aqueous silver nanofluid with sonication time.

In Figure 4.27, it is found that the viscosity of nanofluid decreases with the sonication time. Viscosity of nanofluid decreases only 7% for 6 hours of sonication. This little decrease in the viscosity of nanofluid is because of the reason that the nanoparticles are already in liquid state. These liquid state nanoparticles disperse in the basefluid easily without forming clusters. So there is a little effect of sonication time on viscosity of nanofluid. A linear trend is obtained with the coefficient of regression R^2 equal to 0.965.

Figure 4.28 shows the variation of viscosity of water based aqueous silver nanofluid with

settling time at a volume fraction of 4%.

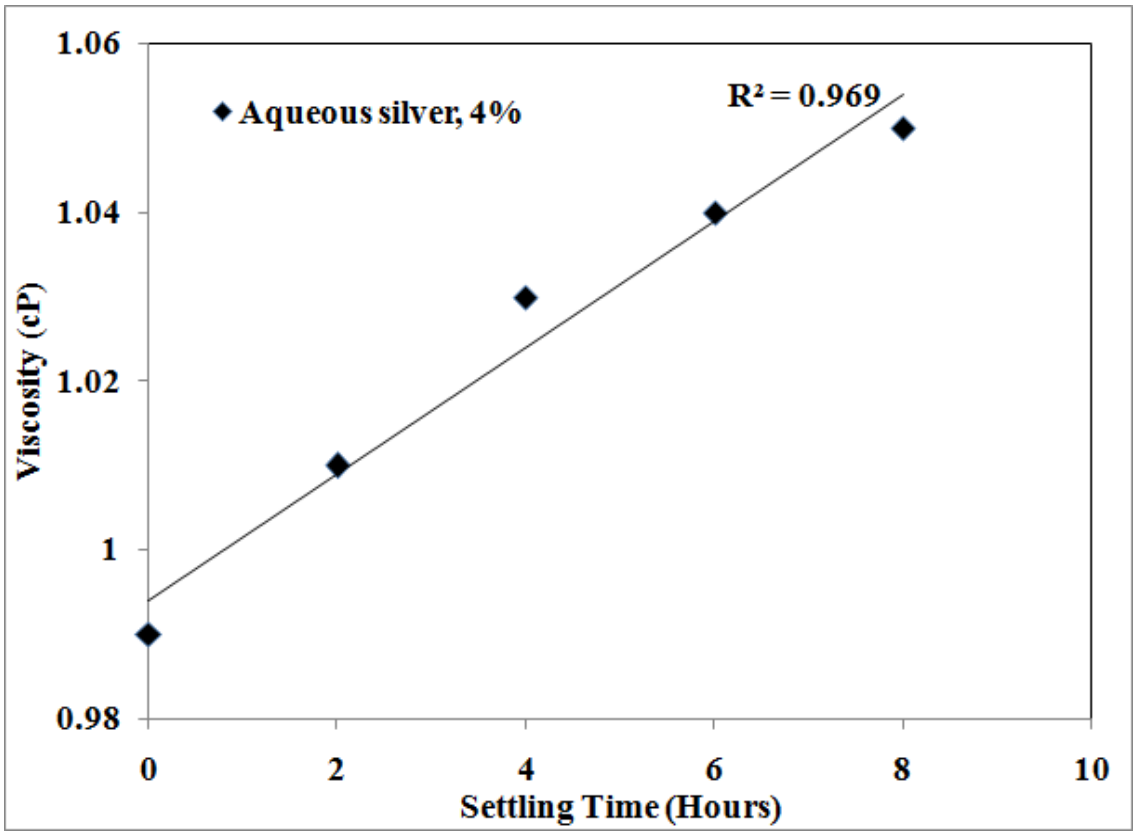

Figure 4.28: Variation of viscosity of water based aqueous silver nanofluid with settling time.

In Figure 4.28, it is found that the viscosity of nanofluid starts increasing with the increase in settling time. As the nanofluid is allowed to settle, the nanoparticles in the fluid starts to agglomerate that leads to increase in viscosity of nanofluid, although the increase in the viscosity of aqueous silver nanofluid is comparatively less than the increase in viscosity of other nanofluids. There is only 6% increase in the viscosity of nanofluid with the increase in settling time. This is because of the reason that the nanoparticles are well dispersed in the basefluid as the nanoparticles are also in aqueous form.

4.7 Comparison of Results for ZnO- EG and ZnO-H_2O Nanofluid

Relative viscosity of ZnO-EG and ZnO-H_2O has been compared with each other for the following three parameters:

1) Temperature
2) Sonication time
3) Settling time

The results of comparison are as follows:

Figure 4.29 shows the variation of relative viscosity of ethylene glycol based and water based ZnO nanofluids.

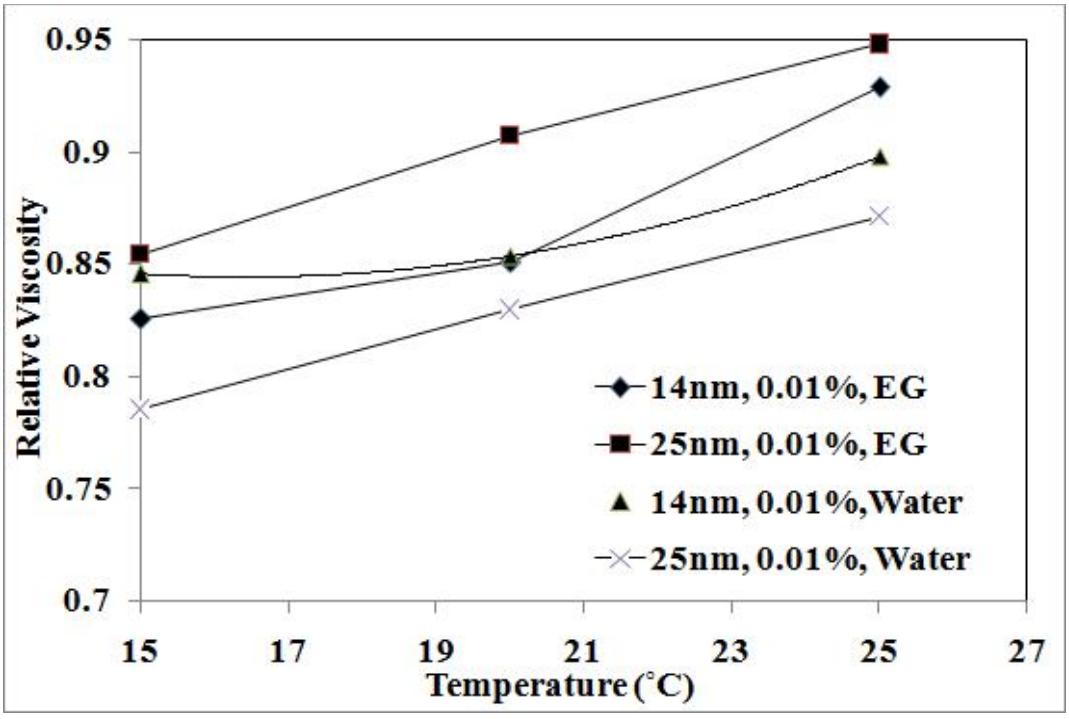

Figure 4.29: Relative viscosity versus temperature for EG - ZnO and water - ZnO nanofluids.

The relative viscosity of nanofluids is found to be increasing with the increase in temperature

of nanofluids. The value of relative viscosity remains less than 1. This indicates that the viscosity of nanofluids remain less than the viscosity of base fluid as temperature of nanofluid increases, but the viscosity of base fluid decreases at a faster rate than that of nanofluid which makes the relative viscosity to increase with temperature.

Figure 4.30 shows the variation of relative viscosity of ethylene glycol based and water based ZnO nanofluid with sonication time.

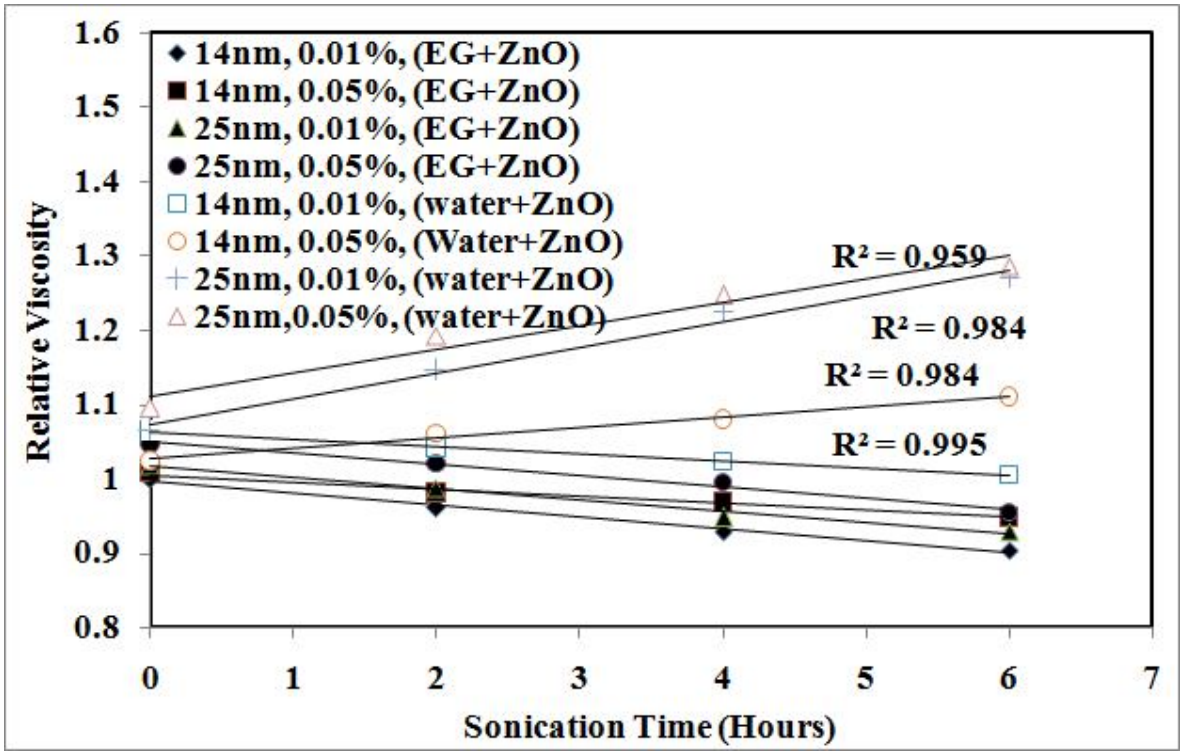

Figure 4.30: Relative viscosity versus sonication time for EG-ZnO and water-ZnO nanofluids.

From Figure 4.30, it is found that Relative viscosity of ethylene glycol based ZnO nanofluid decreases with the increase in sonication time. But the relative viscosity of water based ZnO nanofluid increases with the increase in sonication timing. The relative viscosity of water

based nanofluid is more than that of ethylene glycol based nanofluid. This indicates that the viscosity of water increases to a greater extent than that of ethylene glycol, when nanoparticles are added. The relative viscosity of nanofluid increases continuously, with the increase in size and volume fraction of nanoparticles in base fluid. The relative viscosity of ethylene glycol based nanofluid comes very close to 1 at zero hours of sonication. This shows that there is almost no change in the viscosity of ethylene glycol with the addition of nanoparticles to it because ethylene glycol is highly viscous than water. The viscosity of ethylene glycol is 15 times more than the viscosity of water (section 4.6.1 and 4.6.2). But the relative viscosity of water increases up to a considerably higher value with the addition of nanoparticles in it.

Figure 4.31 shows the variation of relative viscosity of ethylene glycol based and water based ZnO nanofluid with settling time.

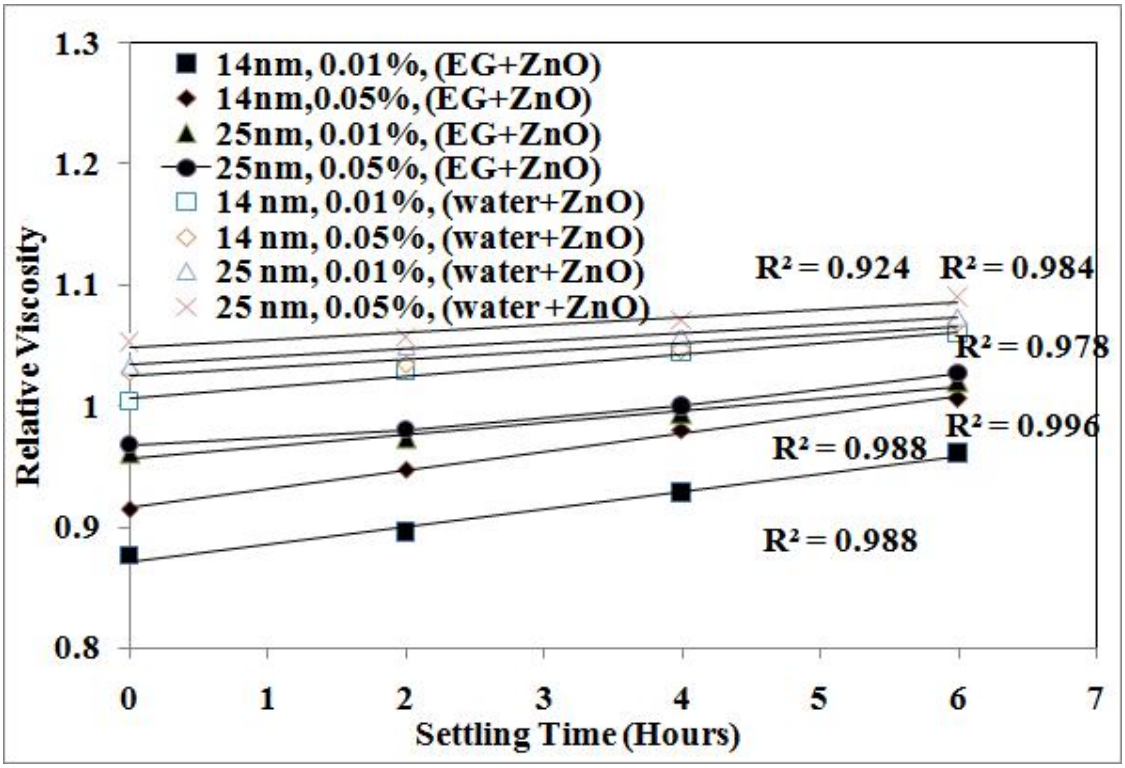

Figure 4.31: Relative viscosity versus settling time for EG-ZnO and water-ZnO nanofluids.

The relative viscosity of the nanofluids is found to be increasing with the increase in settling time. This increase in the relative viscosity of nanofluids is because of the reason that the particles in nanofluid start to settle down and agglomerate as the sonication of nanofluid is stopped. The obtained result shows that the relative viscosity of ethylene glycol based nanofluid is less than the relative viscosity of water based nanofluid because the viscosity of water is comparatively vary less than the viscosity of ethylene glycol and because of higher viscosity of ethylene glycol, particles remain suspended for a comparatively longer time and there is less increase in the viscosity of ethylene glycol based nanofluid.

Chapter 5: Development of New Model for Viscosity of Nanofluids

In this chapter, new model has been developed to measure viscosity of nanofluids. Model has been developed by considering the fact that the viscosity of nanofluid depends on many parameters.

5.1 Development of Model for Viscosity of Nanofluid

From literature review and experimentation, it is found that the viscosity of nanofluid depends on following parameters like:

- Viscosity of basefluid
- Volume fraction of nanoparticles in basefluid
- Density of nanoparticles
- Density of basefluid
- Diameter of nanoparticles
- Shape factor of nanoparticles
- Shear velocity
- Temperature

Viscosity of nanofluid depends on the viscosity of basefluid. For example, the viscosity of ethylene glycol is higher than the viscosity of water so is the viscosity of ethylene glycol based nanofluid (section 4.7). Viscosity of nanofluid depends on the volume fraction of nanoparticles. The viscosity of nanofluid increases with the increase in the volume fraction of nanoparticles in basefluid (section 4.6). Similarly viscosity of nanofluid depends on the density of nanoparticles and basefluid. The viscosity of nanofluid depends on the size of nanoparticles. The viscosity of nanofluid increases with the increase in diameter of nanoparticles. The viscosity of nanofluid depends on the shear velocity and shape factor also. The viscosity of nanofluid decreases with the increase in shear velocity. Shear velocity has

not been considered by any of the researcher. The effect of shear velocity is noted in the experimentation. The viscosity of nanofluid is found to be decreasing with the increase in shear velocity of fluid. Viscosity of nanofluid is affected by temperature also. Viscosity of a fluid depends on temperature also. But temperature is not considered directly for the calculation of viscosity. Direct consideration of temperature for the modeling of viscosity makes it a dimensionless parameter, which cannot be used for any calculation of viscosity. The density of a fluid ρ_f is believed to be dependent on temperature.

$$\rho_f = f(T) \tag{5.1}$$

It is found that the density of water decreases with the increase in temperature (Kestin et al. 1978). A curve is plotted between the relative density of water and temperature as shown in Figure 5.1. Relative density is ratio of density at various temperatures to the density at 20˚C. The relation between density and temperature for water basefluid is presented in equation 5.2.

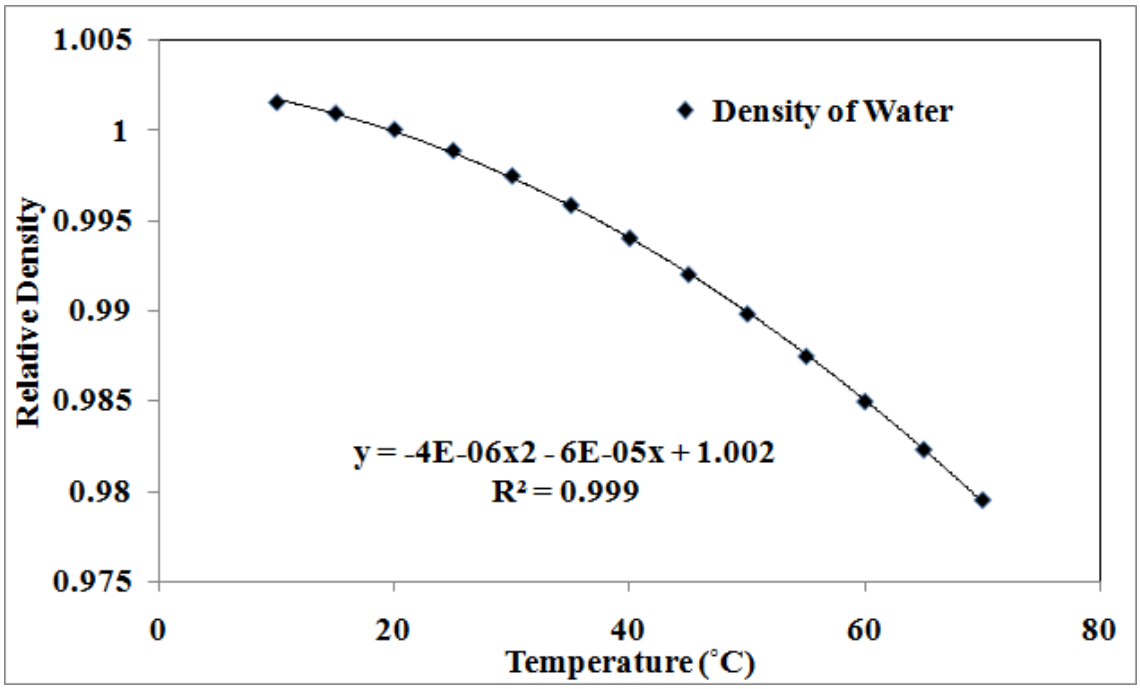

Figure 5.1: Density versus Temperature for water basefluid.

So, relative density of water ρ_r is:

$$\rho_{r\,(water)} = (-4*10^{-06})\,T^2 - (6*10^{-5})\,T + 1.002 \qquad (5.2)$$

In the similar way, a curve is plotted for the relative density of ethylene glycol (Li et al. 1993) and temperature in Figure 5.2. For Ethylene Glycol basefluid, the relation between relative density and temperature is shown in equation 5.3.

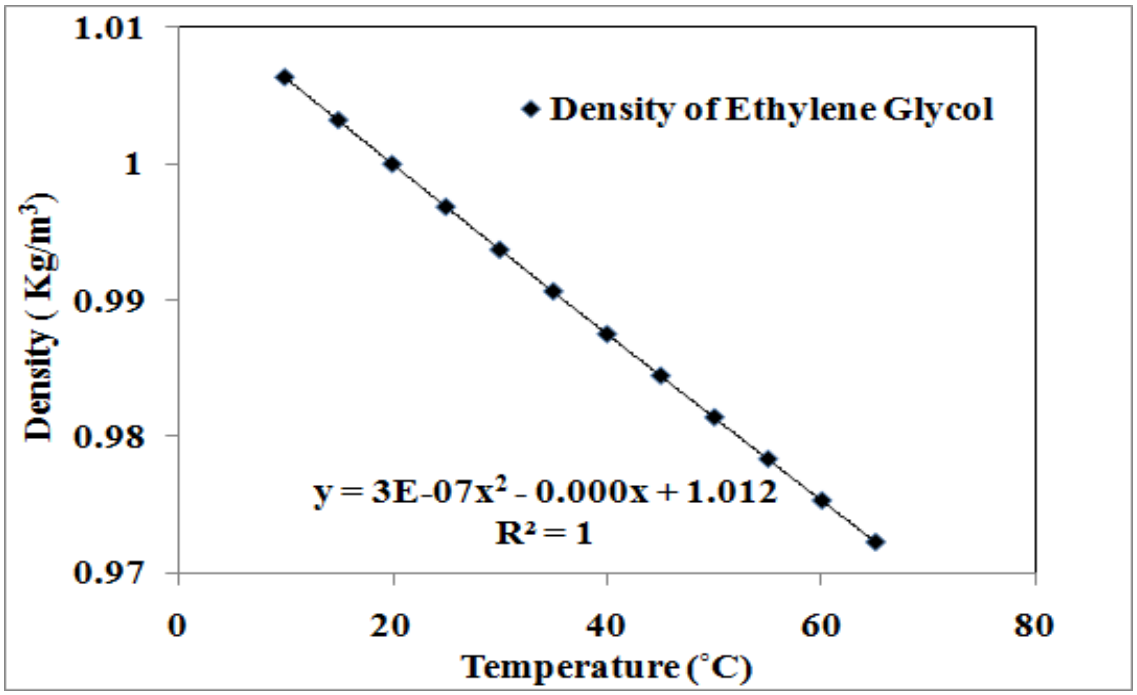

Figure 5.2: Density versus Temperature for Ethylene Glycol basefluid.

So, relative density of ethylene glycol is:

$$\rho_{r\,(EG)} = (3*10^{-07})\,T^2 + 1.012 \qquad (5.3)$$

Thus the viscosity of nanofluid is believed to be dependent on various particle and basefluid properties as given by:

$$\mu_{nf} = f(\mu_{bf}, \square, \rho_p, \rho_f, V, d, \chi)$$

(5.4)

Buckingham Pi theorem is used on the parameters affecting the viscosity of nanofluid (Streeter 1962). The following dimensionless groups have been obtained, using Buckingham Pi theorem:

$$\Pi_1 = \mu_{nf}, \Pi_2 = \ , \ \Pi_3 = \frac{\rho_p V d}{\mu_f}, \Pi_4 = \frac{\rho_f V d}{\mu_f}, \Pi_5 = \chi$$

Π_3 and Π_4 represents the Reynolds number (Re) for particle and fluid.

Using experimental data for ZnO-water nanofluid and ZnO-ethylene glycol nanofluid for a wide range of volume fraction, particle size and temperature, the following model has been derived using regression analysis.

$$\mu_{nf} = 10^{-4.61 \ \ 0.0395} \left(\frac{\rho_p V d}{\mu_f}\right)^{-0.765} \left(\frac{\rho_f V d}{\mu_f}\right)^{-0.11} \quad (5.5)$$

The coefficient of regression R^2 for the equation comes out to be 0.976.

The values exponents of Π_5 have come equal to zero as ZnO particles have been assumed to be spherical (with aspect ratio=1). The value of this exponent is expected to be non-zero if the model was developed using nanoparticles of different shapes.

5.2 Validation of New Developed Model

The above model (equation 5.5) has been further evaluated by using it to predict the nanofluid viscosity for a range of experimental conditions and by comparing the predicted versus experimental values.

In Figure 5.3, the experimental values of viscosity obtained for Yu et al. (2009) for ZnO nanoparticles of diameter 10 to 20 nm for a volume fraction of 2% are compared with the new developed model for ZnO based nanofluid (equation 5.5).

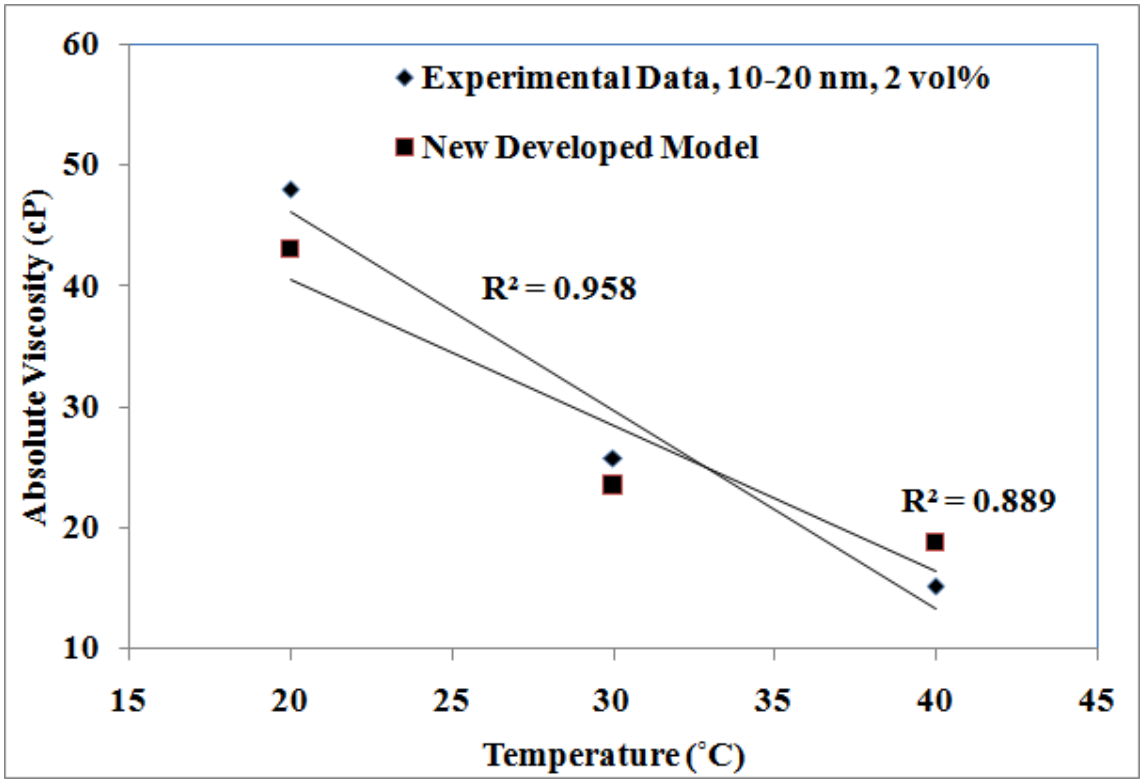

Figure 5.3: Experimental versus predicted values (present model) of Viscosity with increase in temperature, d: 10-20 nm.

Figure 5.3 shows that the new developed model predicts the experimental values. The trend of prediction comes very close to the experimental data. Although the new model under predicts the experimental values up to a temperature of 33˚C and after this temperature the

model over predicts the experimental values.

In Figure 5.4, the experimental values of viscosity obtained for Yu et al. (2009) for ZnO nanoparticles of diameter 10 to 20 nm for a volume fraction of 3% are compared with the new developed model for ZnO based nanofluid (equation 5.3).

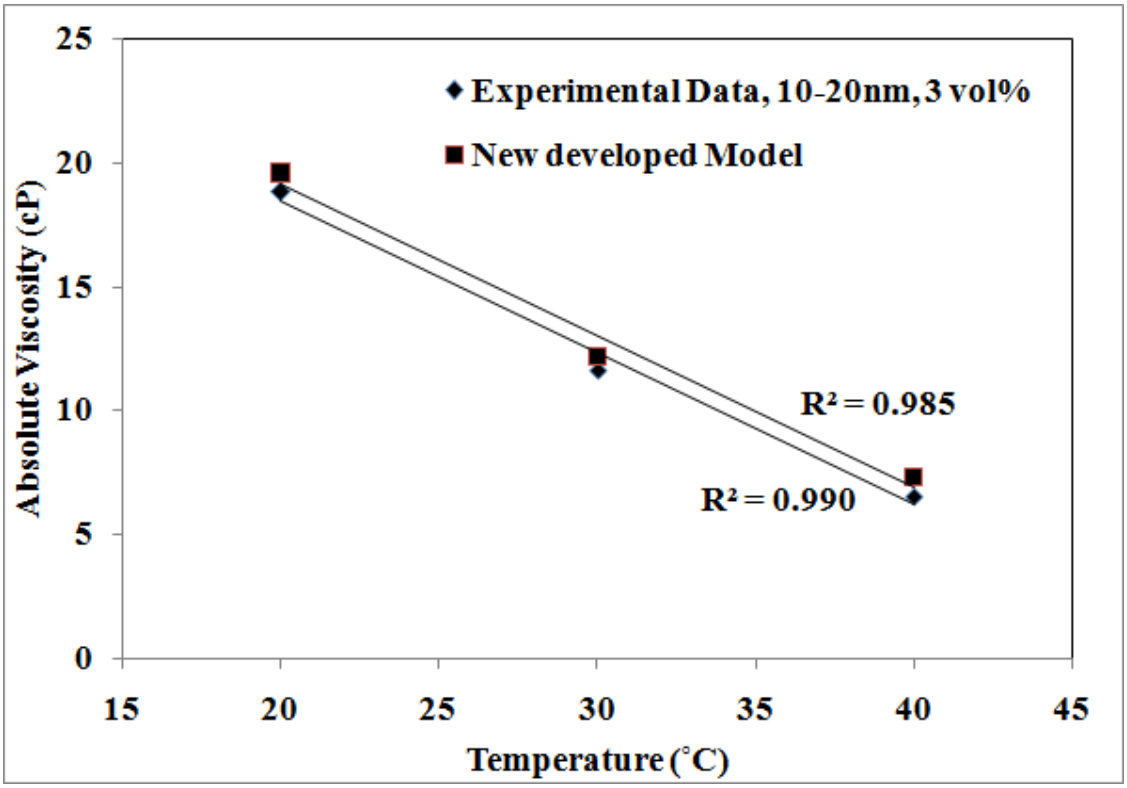

Figure 5.4: Experimental versus predicted values (present model) of Viscosity with increase in temperature, d: 10-20 nm, 3 vol%.

Figure 5.4 shows that the new developed model predicts the experimental data of viscosity very closely. The trend line obtained from the predicted values comes parallel to the experimental values although the predicted values over predicts the experimental values.

In Figure 5.5, the viscosity data for aqueous silver nanoparticles dispersed in water basefluid (Figure 4.30) is compared with the viscosity values predicted from the newly developed model.

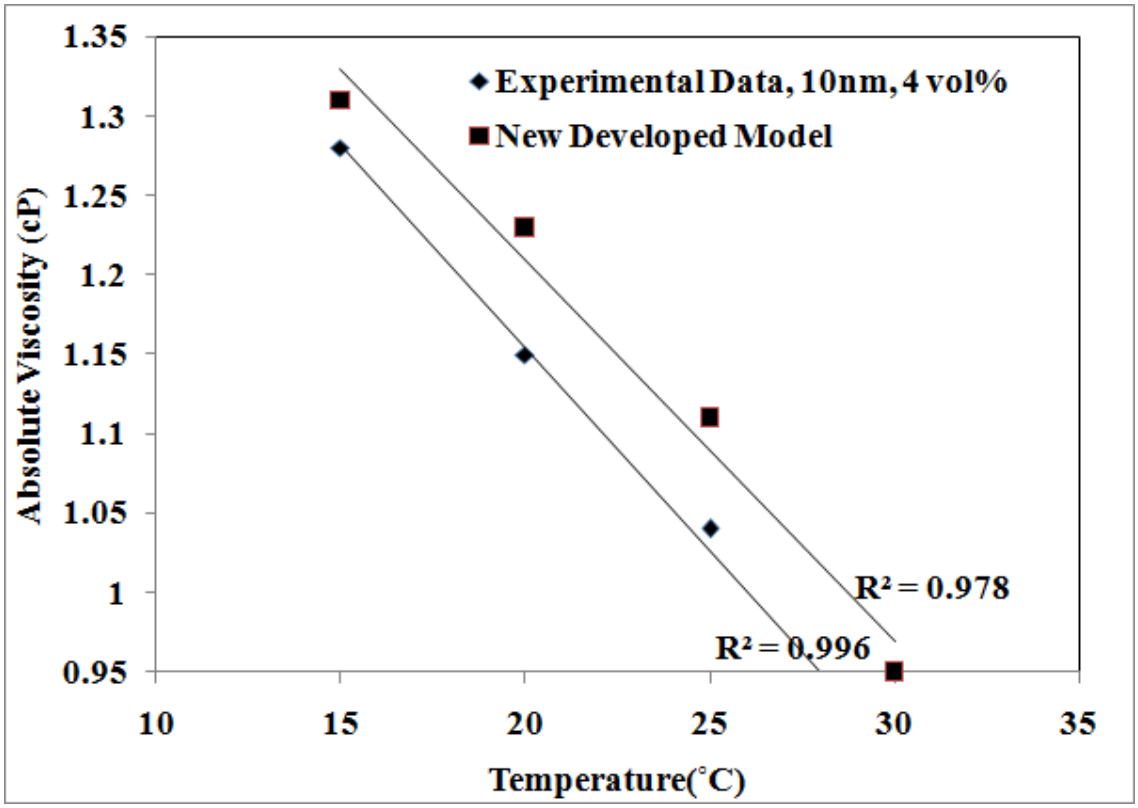

Figure 5.5: Experimental versus predicted values (present model) of Viscosity for aqueous silver nanofluid with increase in temperature.

Figure 5.5 shows that the newly developed model predicts the experimental data very closely. The predicted viscosity values decreases with the increase in temperature. The trend line obtained from the prediction data comes almost parallel to the experimental data.

Table 5.1 provides average of sum of absolute values of relative error for thermal conductivity ratio (using the formula given below) to indicate the prediction accuracies of the new developed model (Figure 5.3 to 5.5)

$$\text{Relative error} = \sum_{n} \left| \frac{\text{experimental value - predicted value}}{\text{experimental value}} \right| \times 100\%$$

Table 5.1: Relative Errors of New Developed Model Predictions (%)

Figures	**New Developed Model (equation 5.5)**
5.3	1.561
5.4	8.28
5.5	7.379

.

From the error analysis, it is clear that the existing new model for nanofluids provides inaccuracies (over/under-predictions) in the range of 1.56 - 8.28% where as the error in predicting the experimental values from the theoretical and empirical model, discussed in Chapter 3, is in the range of 33.53 – 71.25% and 8.27 – 53.48% respectively (Table 3.2). Thus the model presented in equation 5.5 is much efficient than the other models although this model needs to be validated for more experimental data.

Chapter 6: Conclusion and Future Scope of Work

6.1 Conclusion

- Accuracy of existing theoretical and empirical model has been evaluated by comparing the predicted values of viscosity with experimental values of CuO- water and CuO- EG nanofluid. It has been found that the nanofluid viscosity could not be predicted by any of the model. The inaccuracy in predicting the viscosity by existing model is in the range of 8 - 71%.

- Variation in viscosity with volume fraction and size has been measured for ZnO-water and ZnO-EG nanofluid. It has been found that the viscosity of nanofluid increases with the increase in volume fraction of nanoparticles in basefluid and decreases with the increase in the temperature of nanofluid.

- Variation in viscosity with sonication time and settling time has been measured for ZnO-water, ZnO-EG, SWCNT-water and aqueous silver – water nanofluid. It has been found that the viscosity of nanofluid decreases with the increase in the sonication time and increases with the increase in the settling time.

- A new viscosity model has been developed by using dimensionless analysis which includes Reynolds number as one of the dimensionless number and volume fraction as other dimensionless number. This newly developed model has been found to generally predict the viscosity with in ± 6% for ZnO-water, ZnO-EG and aqueous Ag-water nanofluid.

6.2 Future Scope of Work

- Testing of viscosity is required for a high temperature range. Nanofluid has to be used at a very high temperature. This may change the viscosity behavior of nanofluid. Thus it is essential to evaluate the viscosity behavior of nanofluid at high temperature range .
- Further studies are required to better understand the mechanism of viscosity in nanofluid and the influence of different experimental conditions on the viscosity of nanofluids for more accurate modelling.

- A standard theoretical model for nanofluid viscosity has to be developed for a wide range of volume fraction by taking consideration of all the possible mechanisms and effect of all the factors such as size, shape, temperature, volume fraction, ultrasonication time, settling time and pH.

List of Symbols

V = Shear velocity

d = Diameter of particle

T = Temperature (˚C)

P = Pressure

W = Watt

h = Heat transfer coefficient

k = Thermal conductivity

l = Characteristic length

R^2 = Coefficient of regression

O = Higher order terms

c_p = Specific heat

mV = Millivolt

cP = Centipoise

 = Intrinsic viscosity

Greek Symbols

μ = Dynamic viscosity

 = Volume fraction of particles

ρ = Density

Π = Buckingham term

χ = Shape factor

Subscripts

P = Particle

f = Fluid

r = Relative

nf = Nanofluid

bf = Basefluid

m = Maximum packing fraction

Abbreviations

DI = De ionized

EG = Ethylene glycol

Re = Reynolds number

Ra = Rayleigh number

Pr = Prandtl number

Nu = Nusselt number

Wt. = Weight fraction

SWCNT = Single walled carbon nanotube

References

Akoh, H., Tsukasaki, Y., S. Yatsuya, and Tasaki, A., 1978: Magnetic properties of ferromagnetic ultrafine particles prepared by vacuum evaporation on running oil substrate. *Journal of Crystal Growth*, 45, 495–500.

Abu-Nada Eiyad, 2010: Effects of Variable Viscosity and Thermal Conductivity of CuO-Water Nanofluid on Heat Transfer Enhancement in Natural Convection: Mathematical Model and Simulation, *Journal ofHeat Transfer,* Vol. 132 / 052401-1.

Brinkman H.C., 1952: The viscosity of concentrated suspensions and solution, *J. Chem. Phys.* 20, 571–581.

Batchelor G.K., 1977: The effect of Brownian motion on the bulk stress in a suspension of spherical particles, *J. Fluid Mech*. 83, 97–117.

Chandrasekar M., Suresh S. and Bose A.C., 2010: Experimental investigations and theoretical determination of thermal conductivity and viscosity of Al_2O_3/water nanofluid, *Experimental Thermal and Fluid Science*, 34, 210-216

Choi, S.U.S., Rogers C. S. and Mills D. M., 1992: High-performance microchannel heat exchanger for cooling high-heat-load x-ray optical elements, in *Micromechanical Systems,*

Choi, S.U.S., 1995: Enhancing thermal conductivity of fluids with nanoparticles ,in *Developments and Applications of Non-Newtonian Flows*, D. A. Singer and H. P.Wang,

Eds., American Society of Mechanical Engineers, New York, FED–231/MD-66: 99–105.

Choi, S.U.S., Zhang Z. G., and Keblinski P., 2004: Nanofluids. In *Encyclopedia of Nanoscience and Nanotechnology*, vol. 6, H. S. Nalwa; Ed., American Scientific Publishers, city, pp. 757– 773.

Cullity B.D. and Stock S.R., 2001: Elements of X-Ray Diffraction, Third Edition, Pub. Prentice Hall.

Das, S. K., Putra N., Thiesen P. and Roetzel W., 2003: Temperature dependence of thermal conductivity enhancement for nanofluids, *J. Heat Transfer*, 125: 567–574.

Das S. K., Choi S.U.S., Yu W., Pradeep T., 2008: Nanofluids Science and Technology. Wiley Publication.

Duan Fei, Kwek D. and Crivoi A., 2011: Viscosity affected by nanoparticle aggregation in Al_2O_3-water nanofluids, *Nanoscale Research Letters*, 6:248.

Einstein A. 1906: Eine neue Bestimmung der Moleküldimensionen, Annalender Physik 19, 289–306.

Fedele L., Colla L. and Bobbo S., 2012: Viscosity and thermal conductivity measurements of water-based nanofluids containing titanium oxide nanoparticles, *International Journal of Refrigeration*, 35, 1359-1362.

Garg J., Poudel B., Chiesa M., Gordon J.B., Ma J.J., Wang J.B., Ren Z.F., Kang Y.T., Ohtani H., Nanda J., McKinley G.H. and Chen G., 2008: Enhanced thermal conductivity and viscosity of copper nanoparticles in ethylene glycol nanofluid, *Journal of Applied Physics*, 103, 074301.

Ghadimi A., Saidur R., Metselaar H.S.C., 2011: A review of nanofluid stability properties and characterization in stationary conditions, *International Journal of Heat and Mass Transfer*, 54, 4051-4068.

Incropera F.P., Dewitt D.P., 2012: Fundamentals of Heat and Mass Transfer, Wiley Publication.

Jang S.P., Hwang K.S., Lee J.H., Kim J.H., Lee B.H. and Choi S.U.S., 2007: Effective Thermal Conductivities and Viscosities of Water-based Nanofluids Containing Al2O3 with Low Concentration, *International Conference on Nanotechnology*, August 2 - 5,, Hong Kong.

Kestin J., Sokolov M. and Wakeham W.A., 1978: Viscosity of Liquid Water in the Range -8˚C to 150˚C, *J. Phys. Chem.* Vol. 7, 0047-2689 /78/3121-0941.

Krieger I.M.and Dougherty T.J., 1959: A mechanism for non-Newtonian flow in suspensions of rigid spheres, Trans. Soc. Rheol. 3 137–152.

Kulkarni Devdatta P., Das Debendre K. and Vajjha Ravikanth S., 2009: Application of nanofluid in heating buildings and reducing pollution, *Applied Energy* 86,2566-2573.

Kwak K. and Kim C,, 2005: Viscosity and thermal conductivity of copper oxide nanofluid dispersed in ethylene glycol, *Korea-Australia Rheology Journal*, Vol. 17, No. 2, pp. 35-40.

Lundgren T.S. 1972: Slow flow through stationary random beds and suspensions of spheres, *J. Fluid Mech.* 51 (1972) 273–299.

Lee Ji-Hwan, Hwang K. S., Jang S. P., Lee B. H., Kim J. H., Choi S.U.S. and Choi C. J., 2008: Effective viscosities and thermal conductivities of aqueous nanofluids containing low volume concentrations of Al2O3 nanoparticles, *International Journal of Heat and Mass Transfer* 51, 2651–2656.

Maiga E.B., Nguyen C.T., Galanis N. and Roy G., 2004: "Heat transfer behaviors of nanofluids in a uniformly heated tube", *Super lattices and Microstructures*, vol.35,pp., pp. 543 -557.

Muller R.H., 1996: Zetapotential und Partikelladung in der Laborpraxis, first ed., Wissenschaftliche Verlagsgesellschaft, Stuttgart.

Murshed S.M.S., Leong K.C and Yang C., 2008: Investigations of thermal conductivity and viscosity of nanofluids, *International Journal of Thermal Sciences*, 47, 560–568.

Saito N. (1950): Concentration dependence of the viscosity of high polymer solutions, *J. Phys. Soc.* Jpn. 5, 4–8.

Streeter V.L., 1962: Fluid Mechanics, Mcgraw-Hill Book Company Inc.

Namburu P. K., Kulkarni D. P., Misra Debasmita and Das Debendra K., 2007: Viscosity of copper oxide nanoparticles dispersed in ethylene glycol and water mixture, *Experimental Thermal and Fluid Science,* 32, 397–402.

Nguyen C.T., Destranges F., Galanis N., Roy G., Galanis N., Mare T., Boucher S. and Mintsa H. Angue, 2007: Temperature and particle-size dependent viscosity data for water-based nanofluids – Hysteresis phenomenon, *International Journal ofHeat and Fluid Flow*, 28, 1492–1506.

Nguyen C.T., Destranges F., Galanis N., Roy G., Mare T., Boucher S. and Mintsa A. H. 2008: Viscosity data for Al_2O_3–water nanofluid—hysteresis : is heat transfer enhancement using nanofluids reliable?, *International Journal of Thermal Sciences* 47, 103–111.

Nielsen L.E., 1970: Generalized equation for the elastic moduli of composite materials, *J. Appl. Phys.* 41, 4626–4627.

Prasher R., Song D. and Wang J., 2006: Measurements of nanofluid viscosity and its implications for thermal applications, *Applied Physics Letters*, 89, 133108.

Pastoriza-Gallego M.J., Lugo L., Legido J.L. and Piñeiro M.M., 2011: Thermal conductivity and viscosity measurements of ethylene glycol-based $_{Al2O3}$ nanofluids, *Nanoscale Research Letters*, 6:221.

Schmidt A.J., Chiesa M., Torchinsky D.H., Johnson J.A., Boustani A., McKinley G.H, Nelson K. A. and Chen G., 2008: Experimental investigation of nanofluid shear and

longitudinal viscosities, *Applied Physics Letters*, 92, 244107.

Shah M.A. and Ahmed T. 2010: Principles of Nanoscience and Nanotechnology, Narosa Publications.

Wong K.V. and Leon O.D., 2009: Applications of Nanofluids: Current and Future.

Yu W., Xie H., Chen L. and Li Y., 2009: Investigation of thermal conductivity and viscosity of ethylene glycol based ZnO nanofluid, *Thermochimica Acta*, 491, 92-96

Yu W. and Xie H., 2011: A Review on Nanofluids: Preparation, Stability Mechanisms and Applications, *Journal of Nanomaterials*, Volume 2012, Article ID 435873, 17 pages, doi:10.1155/2012/435873

Zhu, H., Lin, Y., and Yin, Y., 2004: A novel one-step chemical method for preparation of copper nanofluids. *Journal of Colloid and Interface Science*, 227, 100–103.

Appendix

Appendix A

Figure A1: Digital Magnetic Stirrer with hot plate.

Figure A2: Ultrasonicator for the sonication of nanofluid for required time.

Figure A3: Brookfield DV III Rheometer with circulating bath.

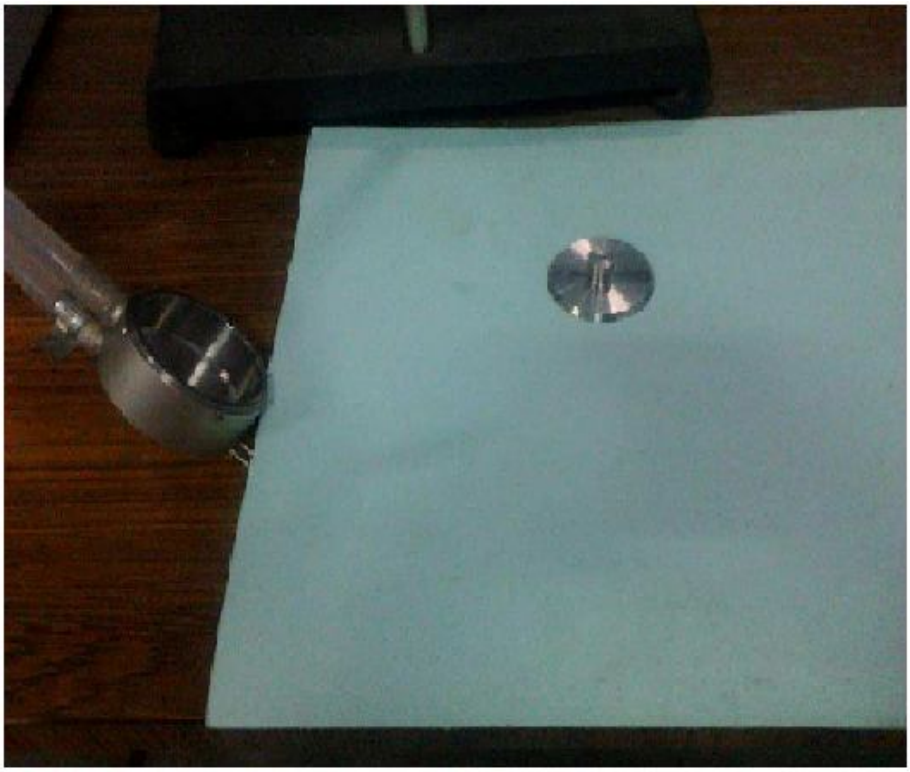

Figure A4: Cup and Cone arrangement of Rheometer.

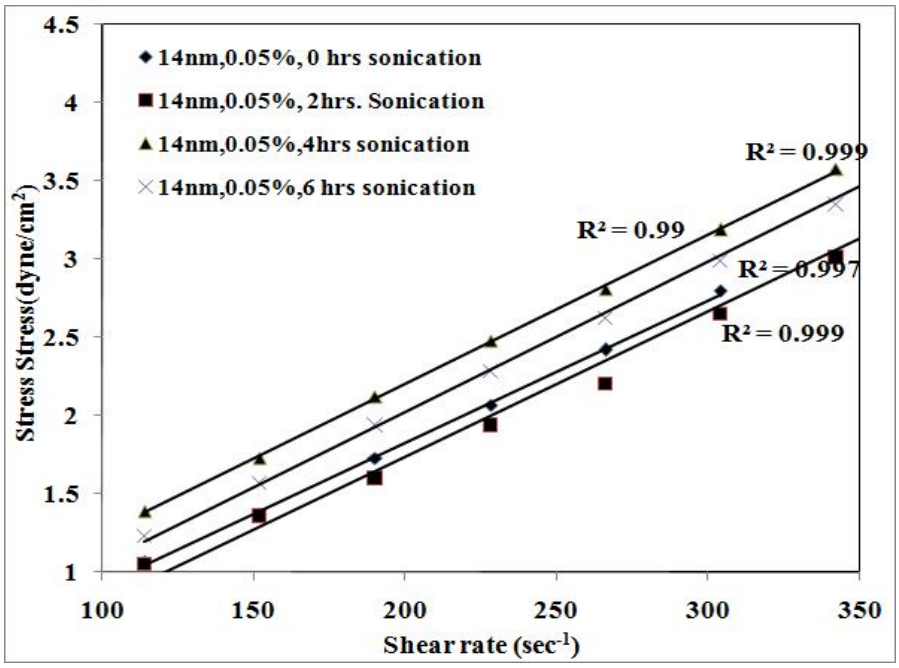

Figure A5: Shear stress versus shear rate for ZnO-water nanofluid for different sonication timings, d = 14 nm; 0.05 vol%.

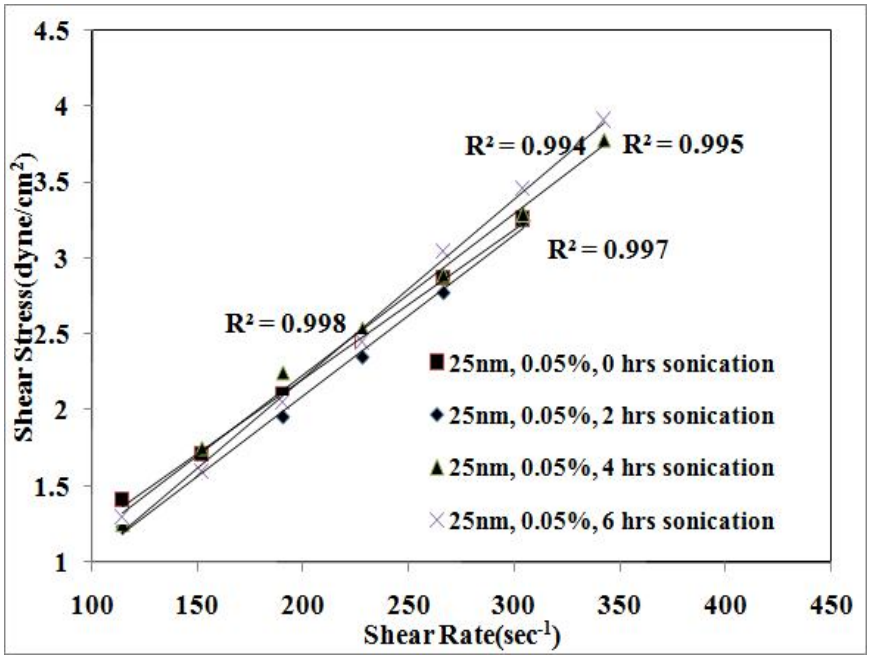

Figure A6: Shear stress versus shear rate for ZnO-water nanofluid for different sonication timings = 0.05%, d = 25 nm.

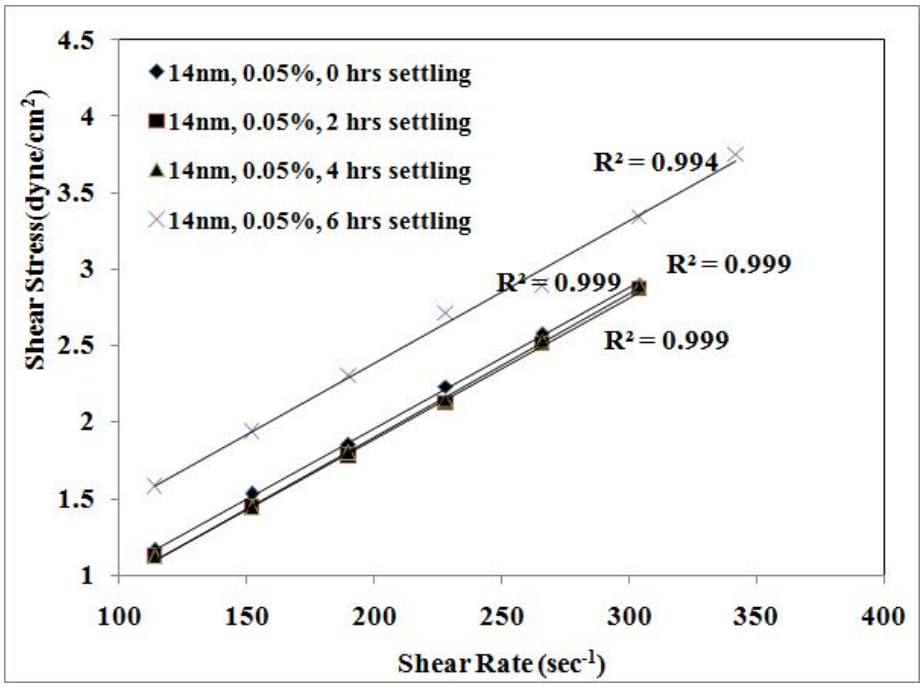

Figure A7: Shear stress versus shear rate for ZnO-water nanofluid for various settling timings, d = 14 nm, □ = 0.05%.

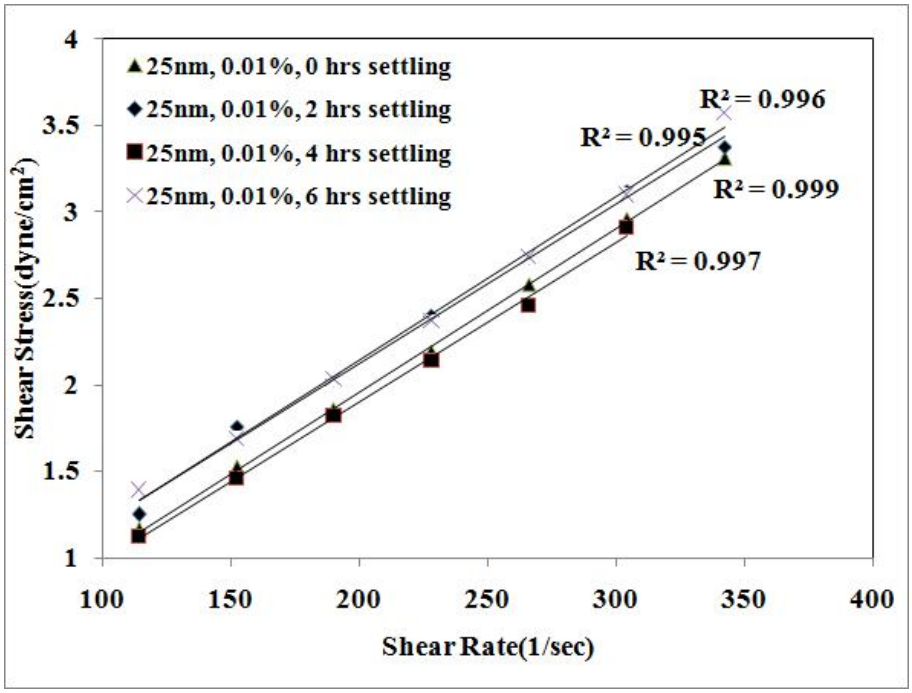

Figure A8: Shear stress versus shear rate for ZnO-water nanofluid for various settling timing, d = 25 nm, □ = 0.01%.

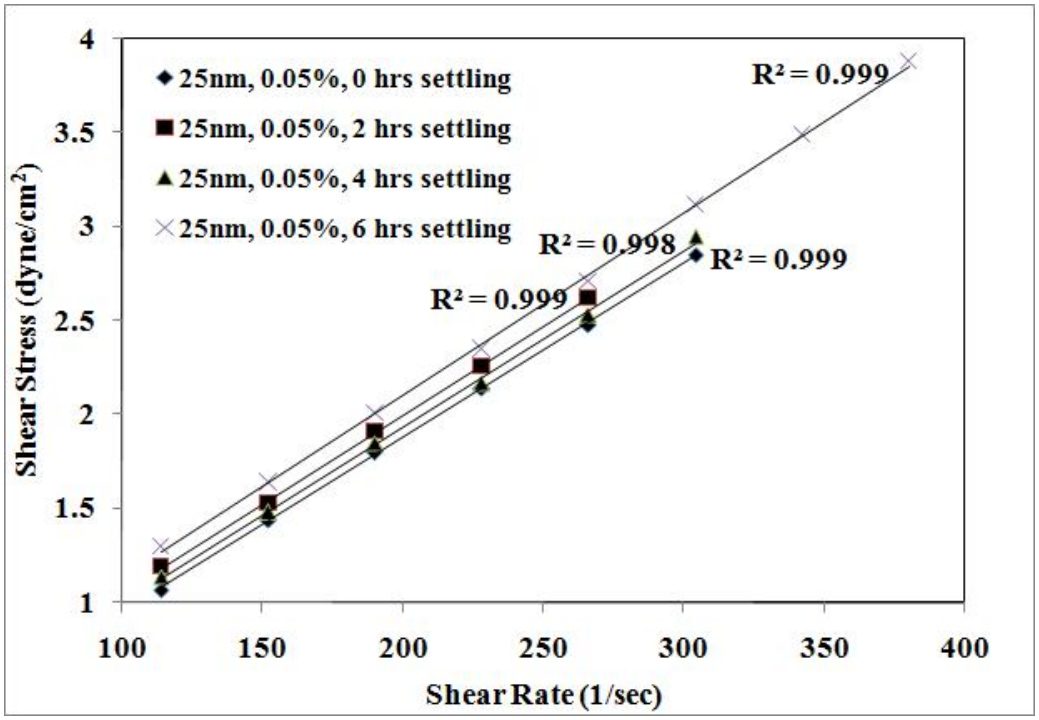

Figure A9: Shear stress versus shear rate for ZnO-water nanofluid for various settling times, d = 25nm, □ = 0.05%.